

ศิลาเคมีของหินภูเขาไฟในบริเวณควี-พรอสเปกต์ของแหล่งแร่ทองคำชาติรี จังหวัดพิจิตร



นางสาวเจนศรินทร์ วิวัฒน์ภิญโญ

ศูนย์วิทยพัทยากร
จุฬาลงกรณ์มหาวิทยาลัย

วิทยานิพนธ์นี้เป็นส่วนหนึ่งของการศึกษาตามหลักสูตรปริญญาวิทยาศาสตรมหาบัณฑิต

สาขาวิชาธรณีวิทยา ภาควิชาธรณีวิทยา

คณะวิทยาศาสตร์ จุฬาลงกรณ์มหาวิทยาลัย

ปีการศึกษา 2553

ลิขสิทธิ์ของจุฬาลงกรณ์มหาวิทยาลัย

PETROCHEMISTRY OF VOLCANIC ROCKS IN Q-PROSPECT OF THE CHATREE
GOLD DEPOSIT, CHANGWAT PHICHIT



Miss Jensarin Vivatpinyo

ศูนย์วิทยทรัพยากร
จุฬาลงกรณ์มหาวิทยาลัย
A Thesis Submitted in Partial Fulfillment of the Requirements
for the Degree of Master of Science Program in Geology

Department of Geology

Faculty of Science

Chulalongkorn University

Academic Year 2010

Copyright of Chulalongkorn University

เจนศรินทร์ วิวัฒน์ภิญโญ : ศิลปินของหินภูเขาไฟในบริเวณคิว-พรอสเปกต์ของแหล่ง
แร่ทองคำชาติ จังหวัดพิจิตร. (PETROCHEMISTRY OF VOLCANIC ROCKS IN
Q-PROSPECT OF THE CHATREE GOLD DEPOSIT, CHANGWAT PHICHIT)
อ. ที่ปรึกษาวิทยานิพนธ์หลัก : ผศ. ดร. จักรพันธ์ สุทธิรัตน์, อ. ที่ปรึกษาวิทยานิพนธ์
ร่วม : รศ. ดร. ปัญญา จารุศิริ, 108 หน้า.

คิว-พรอสเปกต์วางตัวอยู่ทางตอนเหนือของแหล่งแร่ทองคำชาติ ซึ่งประกอบด้วย หิน
แอนดีไซต์เนื้อดอก แอนดีซิติคทัฟฟ์ และไรโอไลติกทัฟฟ์ หินตะกอนขนาดเล็ก ที่ถูกตัดแทรก
โดยผนังหินแอนดีไซต์ จากการศึกษาศิลาบรรณานาในหินแอนดีไซต์เนื้อดอกมักจะแสดง
ลักษณะผลึกขนาดเล็กมาก และเนื้อดอกขนาดเล็กถึงเนื้อดอก วางตัวอยู่ในเนื้อหินซึ่งได้แก่ แร่
แพลจิโอเคลส และเนื้อแก้ว หินแอนดีซิติคทัฟฟ์มีชิ้นส่วนภูเขาไฟขนาด 0.05 - 2 มม.
ประมาณ 20% ผังอยู่ในถ้ำภูเขาไฟและวัสดุเหมือนแก้ว หินไรโอไลต์ประกอบด้วยแร่ควอตซ์
ขนาด 0.5 - 2 มม. และลิมเศษหิน ซึ่งส่วนใหญ่ถูกแทนที่โดยแร่คลอไรต์ ผลึกเหล่านี้และเศษ
หินตั้งอยู่ในแร่ ควอตซ์ขนาดเล็กมากและเนื้อแก้ว นอกจากนี้ผนังหินแอนดีไซต์ยังแสดง
ตัวอย่างลักษณะซัปไอฟิติกนั้นคือลักษณะที่แร่แพลจิโอเคลสขนาดเล็กถูกปิดล้อมด้วย
บางส่วนของแร่ไพรอกซีน

จากการศึกษาธรณีเคมีจากตัวอย่างหิน 25 ตัวอย่าง โดยทำการวิเคราะห์หาปริมาณ
ธาตุออกไซด์หลัก ธาตุร่องรอย และธาตุหายาก โดยใช้วิธี XRF และ ICP-MS ตามลำดับ
แผนภาพของ Zr/TiO_2-SiO_2 ให้เทียบผลทางเคมีของตัวอย่างหินแสดงให้เห็นว่ากลุ่มตัวอย่าง
หินเหล่านี้เทียบเท่ากับ หินแอนดีไซต์ หินซัลฟาไลน์ บะซอลต์ หินไรโอเดไซต์/เดไซต์ และหิน
ไรโอไรท์ นอกจากนี้ตัวอย่างหินส่วนใหญ่ยังปรากฏว่าได้มาจากโพลีติกแมกมา ยกเว้นผนัง
หินแอนดีไซต์ซึ่งได้มาจากแคลอัลคาไลน์แมกมา แผนภาพเกี่ยวกับเทคนิค เช่น Th-Zr-Nb,
La-Y-Nb, Zr-Ti, La/Yb-Sc/Ni และ Th/Yb-Nb/Yb ปรากฏว่าหินเหล่านี้ได้มาจาก
ความสัมพันธ์กับแนวเกาะภูเขาไฟ นอกจากนี้ไดอะแกรม MORB แสดงการเพิ่มมากขึ้นของ
ธาตุ Sr, K, Rb, Ba และ Th พร้อมกับการลดลงของธาตุ HFS ซึ่งระบุว่าเกิดในสภาพแวดล้อม
แบบแนวภูเขาไฟ

ภาควิชา..... ธรณีวิทยา..... ลายมือชื่อนิสิต เจนศรินทร์ วิวัฒน์ภิญโญ.....
สาขาวิชา..... ธรณีวิทยา..... ลายมือชื่อ อ.ที่ปรึกษาวิทยานิพนธ์หลัก.....
ปีการศึกษา..... 2553..... ลายมือชื่อ อ.ที่ปรึกษาวิทยานิพนธ์ร่วม.....

507 22457 23 : MAJOR GEOLOGY

KEYWORDS : PETROGRAPHY / GEOCHEMISTRY / TECTONIC / VOLCANIC / ARC

JENSARIN VIVATPINYO : PETROCHEMISTRY OF VOLCANIC ROCKS IN Q-PROSPECT OF THE CHATREE GOLD DEPOSIT, CHANGWAT PHICHIT
 THESIS ADVISOR : ASST. PROF. CHAKKAPHAN SUTTHIRAT, Ph.D., THESIS
 CO-ADVISOR : ASSOC. PROF. PUNYA CHARUSIRI, Ph.D., 108 pp.

Q-prospect area is situated in the northern Chatree gold deposit in which is generally composed of porphyritic andesite, andesitic tuff, rhyolitic tuff that are cross cut by andesite dike. Petrographically, the porphyritic andesite samples usually show hypocrySTALLINE and microporphyritic to porphyritic textures. Their groundmass usually contains plagioclase microlite and glass. Andesitic tuff contains 0.05-2 mm up to 20 % volcanic fragments embedded in volcanic ash and glassy materials. Rhyolitic tuff usually present 0.5-2 mm quartz grains and wedge-shaped rock fragments, mainly replaced by chlorites; these crystals and rock fragments are set in microcrystalline quartz and glass. Andesite dike samples normally show subophitic texture, which represented by the occurrence of small plagioclase enclosed partly by pyroxene crystals.

Geochemically, twenty-five rock samples were analyzed for major oxides and some trace elements using XRF and ICP-MS techniques, respectively. Plots of Zr/TiO_2 versus SiO_2 diagram indicate that these rock samples are equivalent to andesite, sub-alkaline basalt to rhyodacite/dacite and rhyorite. They appear to have derived from tholeiitic magma for host porphyritic andesite, andesitic tuff and rhyolitic tuff, and calc-alkaline magmas for late stage andesite dike, based on $Zr-P_2O_5$ and $Zr-Y$ diagrams. Regarding tectono-diagrams, such as Th-Zr-Nb, La-Y-Nb, Zr-Ti, La/Yb-Sc/Ni and Th/Yb-Nb/Yb, suggest that these rocks appear to have originated in relation to island arc. MORB normalized patterns show enrichments of Sr, K, Rb, Ba and Th with depleted of HFS elements indicating volcanic arc environment.

Department : Geology Student's Signature Jensarin
 Field of Study : Geology Advisor's Signature C.S. Thir
 Academic Year : 2010 Co-advisor's Signature Punya Charusiri

ACKNOWLEDGMENTS

The author would like to express deeply sincere gratitude to her thesis advisor and co-advisor, Assistant Professor Dr. Chakkaphan Sutthirat and Associate Professor Dr. Punya Charusiri, Department of Geology, Faculty of Science, Chulalongkorn University, for their invaluable supervisions, suggestions, encouragements and contributions, especially their kind-heartedness to make this research well achieved.

This research project is financially supported by the 90th Anniversary of Chulalongkorn University Fund (Ratchadaphiseksomphot Endowment Fund), Graduate School, Chulalongkorn University for financial support.

The author is grateful to Miss Ladda Tangwattananukul and Miss Sasikan Janplook for their help during sample collection at Akara mine. Professor Dr. Toshio Mizuta, Professor Dr. Daizo Ishiyama, Dr. Takeyuki Ogata and Dr. Hinako Sato at Department of Earth Science and Technology, Akita University gave valuable suggest and support during sample preparation and XRF/ICP-MS whole-rock analyses. Financial support for the author during staying at Akita City, Japan was from EATGRU Unit, Department of Geology, Chulalongkorn University. Several persons, whose names cannot be entirely listed, are also deeply thanked.

ศูนย์วิทยทรัพยากร
จุฬาลงกรณ์มหาวิทยาลัย

CONTENTS

	Page
ABSTRACT IN THAI.....	IV
ABSTRACT IN ENGLISH.....	V
ACKNOWLEDGEMENTS.....	VI
CONTENTS.....	VII
LIST OF TABLE.....	IX
LIST OF FIGURES.....	X
CHAPTER I INTRODUCTION.....	1
1.1 General statement.....	1
1.2 Location and Accessibility.....	3
1.3 Physiography.....	3
1.4 Objective.....	5
1.5 Previous works.....	5
1.6 Scope of Work.....	6
1.7 Methodology.....	6
CHAPTER II GEOLOGIC SETTING.....	12
2.1 Tectonic Evolution of Thailand.....	12
2.2 Pre-Jurassic Volcanic Rocks in Thailand.....	16
2.3 Regional Geology.....	21
2.4 District Geology.....	26
2.5 Chatree Geology and Mineralization.....	28
CHAPTER III PETROGRAPHY.....	35
3.1 Introduction.....	35
3.2 Petrographic Description.....	36
3.2.1 Porphyritic Andesite.....	36
3.2.2 Andesitic Tuff Unit.....	41
3.2.3 Rhyolitic Tuff Unit.....	44
3.2.4 Andesite Dike.....	47

	Page
CHAPTER IV GEOCHEMISTRY.....	49
4.1 Introduction.....	49
4.2 Geochemical Analysis.....	50
4.2.1 Major Compositions.....	50
4.2.2 Trace Elements and Rare Earth Elements.....	56
<i>Trace elements</i>	56
<i>Rare earth elements</i>	66
4.3 Rock Classification.....	71
CHAPTER V DISCUSSIONS.....	73
5.1 Petrogenesis.....	73
5.2 Tectonic Setting.....	76
CHAPTER VI CONCLUSIONS.....	87
REFERENCES.....	88
APPENDICES.....	100
APPENDIX A.....	101
APPENDIX B.....	103
APPENDIX C.....	105
APPENDIX D.....	107
BIOGRAPHY.....	108

ศูนย์วิทยทรัพยากร
จุฬาลงกรณ์มหาวิทยาลัย

LIST OF TABLE

Table		Page
4.1	Major oxide (in wt.%), trace and rare earth elements (in ppm) for Q-prospect volcanic rocks.....	52



ศูนย์วิทยทรัพยากร
จุฬาลงกรณ์มหาวิทยาลัย

LIST OF FIGURES

Figure	Page
1.1 Index map of Thailand showing location of the study area (Siamanswer, 2011 online).....	2
1.2 Topographic map of the study area and adjacency along Wang Pong District of Phetchabun Province and Thap Klo District of Pichit Province, north central Thailand showing land forms, routes and location of Q-prospect.....	4
1.3 Locations of fourteen drill holes for sample collection at Q-prospect area, northern part of Khao Mo, Chatree gold deposit.....	7
1.4 Schematic diagram showing sequences of work under this study.....	11
2.1 Tectonic map of Thailand showing regional tectonic features and exposures of some rock types related to the main collisions herein the country (modified from Charusiri et al., 2001 by Sutthirat, 2009).....	15
2.2 Distribution of Pre-Jurassic volcanic rocks in Thailand (modified from Panjasawatwong et al., 1997).....	20
2.3 Regional geologic map of the Thap Klo - Wang Pong - Chon Daen areas and study area (modified from Chonglakmani and Satayalak, 1979).....	22
2.4 Detailed geologic map of Chatree gold deposit and its vicinity (modified after Crossing, 2006; updated to include the observations of Comming et al., 2004).....	27
2.5 Surface and subsurface geologic map of the study and surrounding areas, Chatree gold deposit, boundary between Pichit and Phetchabun Provinces, north central Thailand (modified from Comming et al., 2006).....	34
3.1 Simplified stratigraphic correlation of Chatree gold deposit, using geological survey and drill hole data (modified from Salam, 2008).....	36

Figure	Page
3.2 A slab specimen of porphyritic andesite (sample no.Q7 of RD2327) showing aphanitic rock with porphyritic texture. Black and white spots are phenocrysts, probably plagioclase, K-feldspar and relic hornblende.....	38
3.3 Photomicrograph (under cross-polarized light) of porphyritic andesite (sample no. Q1 of RD2270) showing porphyritic texture. The phenocrysts are subhedral to euhedral plagioclase (Pl) and K-feldspar (Kfs) sit in glass and fine-grained quartz (Qtz).....	38
3.4 Photomicrograph (under cross-polarized light) of porphyritic andesite (sample no. Q1 of RD2270) showing euhedral K-feldspar (Kfs) phenocrysts with replacement of sericite (Src). Euhedral opaque (Opq) minerals (pyrite) disseminated in groundmass and in K-feldspar phenocryst.....	39
3.5 Photomicrograph (under cross-polarized light) of porphyritic andesite (sample no. Q1 of RD2270) showing relic hornblende (Hbd) grain fully replaced by sericite (Src). This relic hornblende shows rhombohedral shape with two-direction cleavages with intersection angle of 60 and 120 degree. Opaque (Opq) minerals are also found in groundmass.....	39
3.6 Photomicrograph (cross-polarized light) of porphyritic andesite (sample no. Q7 of RD2327) showing phenocrysts sit in microlite and glassy groundmass. Trachytic texture (see yellowed-lines) is also recognized. Plagioclase (Pl) and K-feldspar (Kfs) phenocrysts are partly replaced by sericite. Relic hornblende (Hbd) altered fully to calcite (Cc).....	40
3.7 Classification diagram of pyroclastic rocks (Fisher, 1966) and compositional plots of andesitic tuff and rhyolitic tuff samples under this study.....	42
3.8 A slab specimen of andesitic tuff (sample no. A28 of RD7155) showing various sizes (mostly < 1 cm) of volcanic casts.....	43

Figure	Page
3.9 Photomicrograph (under cross-polarized light) of andesitic tuff (sample no. A28 of RD7155) showing quartz (Qtz), plagioclase (Pl), K-feldspar (Kfs) and rock fragments (Rf) ranging in size mostly < 0.5 mm of andesite consisting of plagioclase phenocryst surrounded by glassy material.....	43
3.10 A slab specimen of rhyolitic tuff (sample no. Q17 of RD2884) showing volcanic fragments (maybe rhyolite) and angular quartz grains. Fiamme texture, lenticular chlorite and welded materials, is generally found.....	45
3.11 Photomicrograph (under cross-polarized light) of rhyolitic tuff (sample no. Q17 of RD2884) shows angular to subrounded quartz (Qtz) grains and rock fragments (Rf) sit in fine-grained quartz. Some quartz grains show embay outline. The rock fragments are mostly rhyolite.....	45
3.12 Photomicrograph (under cross-polarized light) of rhyolitic tuff (sample no. Q19 of RD2884) showing volcanic rock fragments (Rf) that appear to be porphyritic andesite with size of about 1 to 2 mm. K-feldspar (Kfs) and rounded quartz (Qtz) grains sit in groundmass. Sericite (Src) is generally found in this rock.....	46
3.13 Photomicrograph (under cross-polarized light) of rhyolitic tuff (sample no. Q19 of RD2884) showing lenticular sericite (Src) surrounded by chlorite (Chl). Rock fragment (Rf), quartz (Qtz), calcite (Cc) is commonly found.....	46
3.14 A slab specimen of andesite dike (sample no. Q6 of RD2327) shows aphanitic groundmass and porphyritic texture. Black and white spots indicate phenocrysts which may be plagioclase and pyroxene.....	47
3.15 Photomicrograph (under cross-polarized light) of andesite dike (sample no. Q6 of RD2327) showing subophitic texture, euhedral plagioclase (Pl) enclosed partly by clinopyroxene (Cpx), quartz (Qtz) and chlorite (Chl) surrounded by glassy material and plagioclase.....	48

Figure	Page
3.16 Photomicrograph (under cross-polarized light) of andesite dike (sample no. Q6 of RD2327) shows clinopyroxene (Cpx), plagioclase (Pl) and quartz (Qtz). Epidote (Ep) and chlorite (Chl) are also found in this rock...	48
4.1 Harker-type variation diagrams of major and minor oxides (wt%) versus SiO ₂ (wt%) of rock samples from Q-prospect.....	54
4.2 Harker-type variation diagrams of major oxides (wt%) versus MgO (wt%) of rock samples in the study area.....	55
4.3 Variation diagrams plotting SiO ₂ (wt. %) against some trace elements (ppm).....	60
4.4 MORB normalized incompatible element patterns of porphyritic andesites from Q-prospect. The MORB values are from Pearce (1983)...	62
4.5 MORB normalized incompatible element patterns of andesitic tuffs from Q-prospect. The MORB values are from Pearce (1983).....	62
4.6 MORB normalized incompatible element patterns of rhyolitic tuffs from Q-prospect. The MORB values are from Pearce (1983).....	63
4.7 MORB normalized incompatible element patterns of andesite dikes from Q-prospect area. The MORB values are from Pearce (1983).....	63
4.8 Primitive mantle (McDonough et al., 1992) normalized incompatible element patterns of porphyritic andesites from Q-prospect area.....	64
4.9 Primitive mantle (McDonough et al., 1992) normalized incompatible element patterns of andesitic tuff from Q-prospect area.....	64
4.10 Primitive mantle (McDonough et al., 1992) normalized incompatible element patterns for rhyolitic tuff from Q-prospect area.....	65
4.11 Primitive mantle (McDonough et al., 1992) normalized incompatible element patterns for andesite dike from Q-prospect area.....	65
4.12 Chondrite normalized REE patterns of samples from porphyritic andesite rocks. The chondrite compositions are from Boynton (1984).....	69
4.13 Chondrite normalized REE patterns of samples from andesitic tuff. The chondrite compositions are from Boynton (1984).....	69

Figure	Page
4.14 Chondrite normalized REE patterns of samples from rhyoritic tuff. The chondrite compositions are from Boynton (1984).....	70
4.15 Chondrite normalized REE patterns of samples from andesite dike. The chondrite compositions are from Boynton (1984).....	70
4.16 Total alkalis silica (TAS) diagram (Le Bas et al., 1986) for volcanic and pyroclastic rocks from Q-prospect area. The subdivision of volcanic rocks into alkaline and subalkaline (tholeiitic) was made from data of Irvine and Baragar (1971).....	71
4.17 Rock classification plots of Zr/TiO_2 versus SiO_2 (Winchester and Floyd, 1977) for volcanic and pyroclastic rocks from Q-prospect.....	72
5.1 AFM diagram with a boundary line separating fields of tholeiitic and calc-alkaline (Irvine and Baragar, 1971). Most volcanic and related rocks from Q-prospect plots fall within the calc-alkaline field.....	74
5.2 Zr versus P_2O_5 variation diagram after Winchester and Floyd (1976) for the discrimination between precursors of alkali basalt and tholeiitic character (sub-alkaline). All volcanic and related rocks of Q-prospect are plotted in tholeiitic basalt.....	75
5.3 Y-Zr discrimination diagram showing volcanic and related rocks from Q-prospect falling within both areas of tholeiitic and calc-alkaline/transitional (fields after MacLean and Barrett, 1993).....	75
5.4 Plots of Th-Zr-Nb in triangular diagram (Wood 1980) for Q-prospect rock samples indicating volcanic arc basalts.....	77
5.5 La-Y-Nb diagram (after Cabanis and Lecolle, 1989) showing the porphyric andesite, andesitic tuff and rhyolitic tuff plotted in volcanic arc tholeiite (VAT) and overlapping area of VAT and calc-alkali; andesite dikes are plotted in volcanic arc calc-alkali.....	77
5.6 Ti-Zr variation diagram (after Pearce and Cann, 1973) indicating Q-prospect rock samples are related to island-arc tholeiites and calc-alkali basalts.....	78

Figure	Page
5.7 La/Yb versus Sc/Ni diagram distinguishing different types of volcanic arc andesite (Bailey, 1981) showing rock samples plotted mostly in oceanic arc except late stage andesite dike in continental arc.....	78
5.8 Th/Yb versus Nb/Yb diagram (after Dunphy and Ludden, 1998) confirming most Q-prospect host rocks are related to oceanic arc whereas andesite dike is related to continental arc.....	79
5.9 Primitive mantle (McDonough et al., 1992) normalized trace element patterns of selective porphyritic andesitic samples compared to that of 25 Ma basaltic andesite from Yap arc, southern Philippine (data from Ohara et al., 2002).....	81
5.10 MORB (Preace, 1983) normalized trace element patterns of the selective porphyritic andesitic samples compared to that of 25 Ma basaltic andesite from Yap arc, southern Philippine (data from Ohara et al., 2002).....	81
5.11 MORB (Preace, 1983) normalized spidergram of the andesite dikes (No. Q-6 and A-26) compared to those of Eocene volcanic rock (KG-1) from the South Shetland arc (Machado et al., 2005) and Island arc calc-alkaline (Sun, 1980).....	82
5.12 Evolution of tectonic setting of Chatree volcanic rocks, Phichit-Phetchabun Provinces.....	83
5.13 Subdivision of pre-Jurassic volcanic rocks along Eastern Volcanic belt; into Western sub-belt and Eastern sub-belt. Detail of cross section lines show in Figure 5.12. (LE = Loei Province, PB = Phetchabun Province, LB = Lop Buri Province, and SB = Saraburi Province).....	85
5.14 Tectonic model of Eastern Volcanic Belt of Thailand during Late Paleozoic to Early Mesozoic.....	86

CHAPTER I

INTRODUCTION

1.1 General Statement

Volcanic rocks found in Thailand appear to have several periods of explosion during Devonian to Quaternary (Jungyusuk and Khositant, 1992). In addition, these volcanisms may also be associated with gold and gem deposits of the country. Permo-Triassic or Pre-Jurassic volcanic rocks, significantly related to gold deposit, can be subdivided into three main belts including Chiang Rai-Chiang Mai belt, Tak-Chiang Khong belt and Loei-Phetchabun-Nakhon Nayok belt in which they appear to have formed in paleo-oceanic terranes or continental plates (e.g., Jungyusuk and Khositant, 1992; Intasopa, 1993; Panjasawatwong, 1999; Charusiri et al., 2002; Phajuy et al., 2005).

Gold occurrences in Thailand have been found in many areas, such as Chiang Rai-Phrae, Loei-Udon Thani-Nong Khai, Phetchabun-Phichit-Lop Buri and several areas in the eastern region. However, the highest potential areas economically suitable for gold mining have been located within two provinces, i.e., Phichit and Loei. Among these deposits, Chatree gold deposit has been proven as the largest deposit which is located about 280 km north of Bangkok. It is situated in the vicinity of Thap Klo District, Phichit Province and Wang Pong District, Phetchabun Province, upper central of Thailand (Figure 1.1).

Geologically, the Chatree deposit is a part of Loei-Phetchabun-Nakhon Nayok volcanic belt lining along the western edge of Khorat plateau. Recently, approximate 19 km² of 7 prospect areas have been pointed out and 7 mining pits, namely A, C, D, H, K, Q and Mar, have been in operation (James and Cumming, 2007). Total production at Chatree in 2009 was about 93,002 ounces of gold and 293,472 ounces of silver from a

total ore reserves 1.5 million ounces of gold in 37 million tons of rocks at grading 1.2 grams/ton Au (Kingsgate, 2009 online).



Figure 1.1 Index map of Thailand showing location of the study area (Siamanswer, 2011 online).

1.2 Location and Accessibility

The Chatree gold deposit is located in a hilly area of Khao Khem, Khao Mo and Khao Pong lining from north to south. These hills have average elevation range from 80-190 meters above mean sea level and situate on the edge of Cenozoic Chao Phraya basin at the boundary between Phetchabun Province and Phichit Province.

Q-prospect, located in the northern part of Chatree mine, is the main focus of this study. It is present on a topographic map (Figure 1.2) scale 1: 50,000 of Royal Thai Survey Department, edition 1-RST, series L 7017, sheet 5141 IV, Amphoe Wang Sai Phun. Its grid reference in UTM system is 676000E-678000E and 1804000N-1806000N or between the latitudes $16^{\circ} 18' 38''$ to $16^{\circ} 19' 43''$ N and the longitudes $100^{\circ} 38' 51''$ to $100^{\circ} 39' 58''$ E.

The study area is about 280 kilometers north of Bangkok, and about 45 kilometers south-east of Phichit town. The area can be accessed using the national highway no. 1 (so-called Paholyothin) from Bangkok to Phichit Province before turning right onto the highway No.11 from Tak Fa District to Thap Klo District passing Khao Sai junction for about 15 km then turning right to road No. 1301 for about 6 km arriving Akara mine at the Chatree gold deposit. It usually takes about 4 hours drive from Bangkok following the route suggested above.

1.3 Physiography

Physiography of the area is mostly occupied by flat plain in which some small hills are situated around. They are Khao Khem, Khao Mo and Khao Pong hills that have average elevation range from 80-190 m above mean sea level. The highest point of Khao Mo in the central area is about 190 m above flat plain. Most of the hills are regionally aligned in the north-south trend (Figure 1.2).

Climate of this area, a part of the north-central Thailand, is classified as tropical savanna with rainy season lasting from May to October, winter season from November to February, and summer season from middle February to April. The minimum temperature

is about 14 °C in winter; on the other hand, the maximum temperature is about 33 °C in summer. The average annual temperature is about 30 °C.

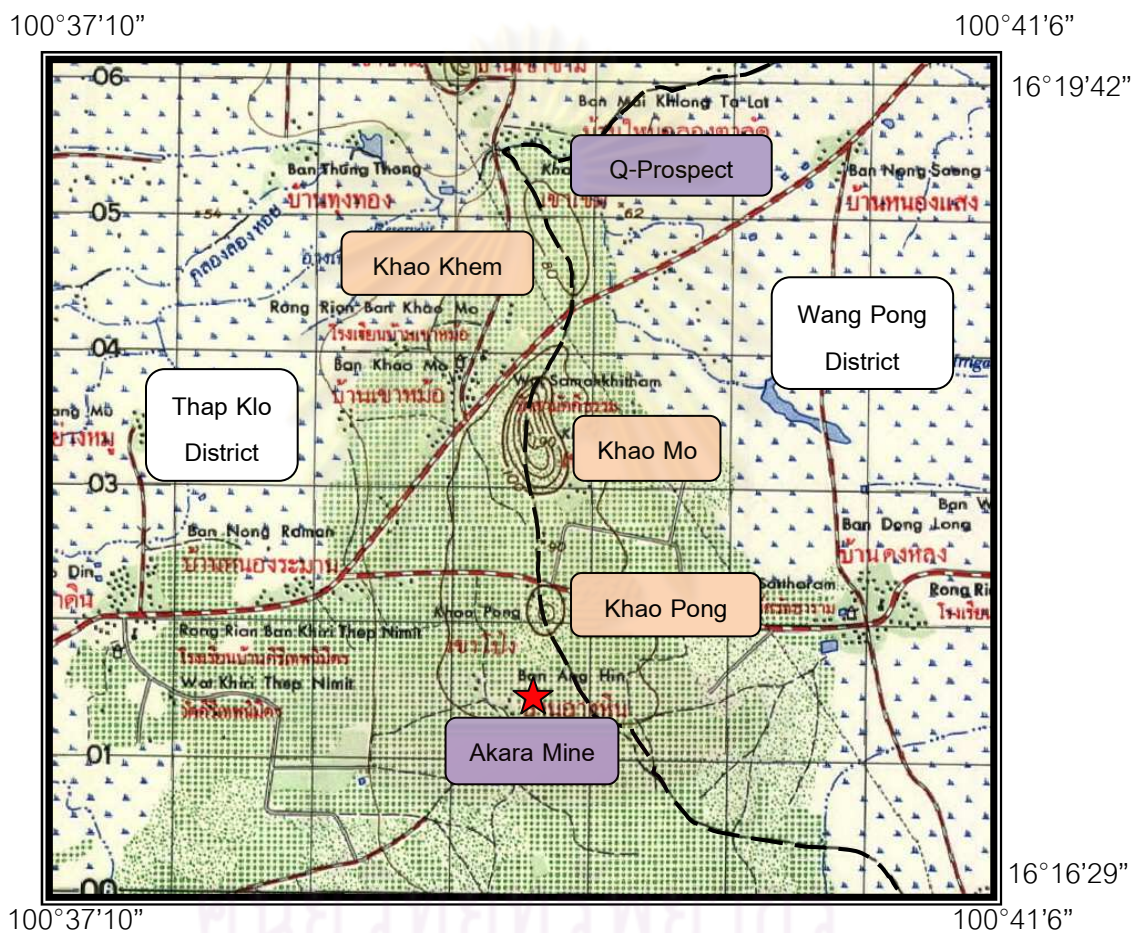


Figure 1.2 Topographic map of the study area and adjacency along Wang Pong District of Phetchabun Province and Thap Klo District of Pichit Province, north central Thailand showing land forms, routes and location of Q-prospect.

1.4 Objective

The objective of this study is to study the petrochemical characteristics of volcanic rocks in Q-prospect and leading to interpretation of tectonic processes.

1.5 Previous works

Permo-Triassic Loei-Phetchabun-Kho Chang volcanic belt is crucially associated with gold deposits. This volcanic belt is exposed along the north-south trend which volcanic rocks along the belt comprise both lavas and their associated pyroclastics ranging in composition from felsic to mafic. Moreover, some dike rocks appear to have subsequently cut into these rocks mostly placing along the northeast-southwest trend of main fault. These dike rocks consist of diorite, dolerite and andesite (Jungyusuk and Khositant, 1992). Diemar et al. (2000) suggested that the Chatree gold deposit and its vicinity are associated with ancient back-arc basin.

In the regional area of Chatree deposit, there are composed of plagioclase phyrific andesite, hornblende phyrific andesite, monomictic andesitic breccia, polymictic andesitic breccia, volcanoclastic sandstone, siltstone, rhyolitic breccia and flame breccia (Comming et al., 2006). Dike rocks in Chatree deposit cross cut most of the host volcanic rocks but they seem to be gold-barren veins. They are mostly characterized by andesitic dikes which lie along the north-south and northeast-southwest directions (Tangwattananugul, 2006). Study of fluid inclusion in gold-bearing quartz vein can reconstruct hydrothermal temperature of this gold deposit which falls within an epithermal range, about 150-220 °C (Marhotorn, 2002).

N and V Prospects in the southern parts of the deposit contain two main types of igneous rocks, porphyritic granodiorite and andesite. The former appears to have intruded into the latter. Geochemically, both rocks belong to the calc-alkaline affinity occurred as volcanic arc granite and island arc tholeiite to volcanic arc basalt, respectively. They may be formed as a result of oceanic subduction between Lampang-Chiang Rai and Nakhon Thai plates during Permo-Triassic period (Marhotorn, 2008).

Results of C- and O-isotope geochemistry reveal that the alteration and associated epithermal gold deposit took place in association with hydrothermal fluids closely related to magmatic and sea-water origins (Nakchaiya, 2008).

Trace elements have become a basic tool or pathfinder of ore exploration and also significant to petrogenetic interpretation. Immobile elements, in particular, are very useful tool for investigation of altered rocks. Rare earth elements, with the exception of Eu, are generally incompatible during igneous fractionation. Heavy REE, i.e., Lu and Yb are essentially immobile whereas light REE may be variably mobile during alteration (MacLean and Barrett, 1993). Europium (Eu) in feldspars can be liberated by hydrothermal alteration leading to present of positive Eu anomaly of chondrite-normalized REE pattern (Gifkins, 2005).

1.6 Scope of Work

The study area is situated in the northern part of Khao Mo, Chatree gold deposit, Phichit province. Forty three selected core samples were taken from fourteen drill cores (i.e., RD2270, RD2327, RD2686, RD2836, RD3039, RD2884, RD2901, RD3888, RD7152, RD7161, RD7165, RD7155, RD7162 and RD7157) along three section lines (see Figure 1.3). These samples were prepared and analyzed by the following methods.

1.7 Methodology

Method of this study is shown as a flow chart (Figure 1.4). It consists of five steps which details are explained below.

1.7.1 Literature review

In this stage, several previous works on regional geology, stratigraphy, alteration, gold mineralization and volcanism of the study area were carried out prior to research planning.

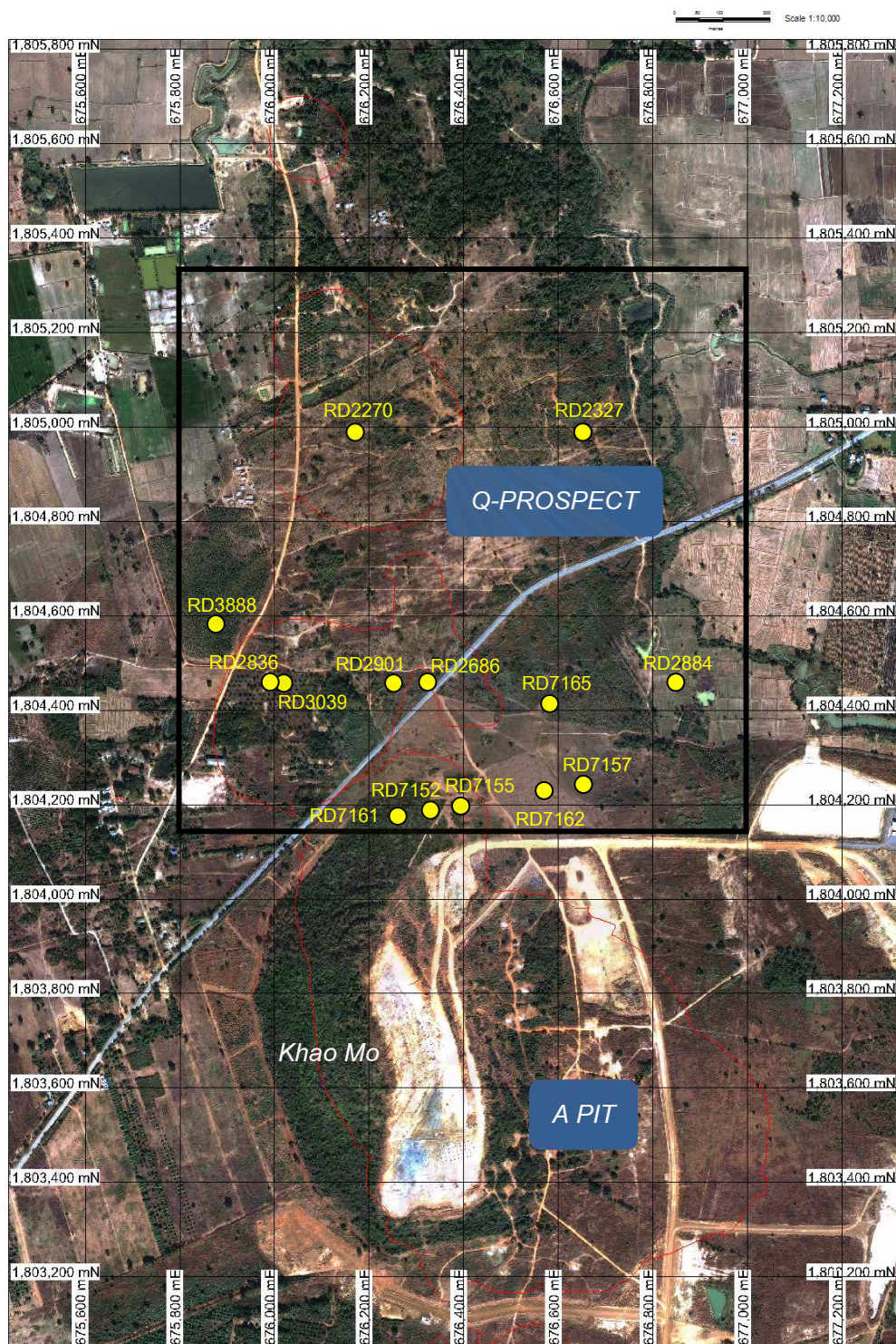


Figure 1.3 Locations of fourteen drill holes for sample collection at Q-prospect area, northern part of Khao Mo, Chatree gold deposit.

1.7.2 Fieldwork and sample collection

The pre-field investigations such as aerial photo interpretation, particularly for geological structures, landforms, rock units and field accessibility were prepared before fieldwork and sample collection were taken place.

1.7.2.1 Field study

Field mapping of rock distribution in the study area was firstly carried out in comparison with the previous work of Corbett (2004). Consequently, local geologic map was modified from Comming et al. (2006). Four groups of rocks, i.e., andesite, andesitic tuff, rhyolitic tuff and andesite dikes, were classified based on field investigation.

1.7.2.2 Sample collection

Geological structure and rock orientation obtained from the fieldwork were used for designation of sample collection from drilled cores. The selected samples were representatives of all rock types in Q-prospect. Forty three samples were taken into laboratory works.

1.7.3 Laboratory study

1.7.3.1 Petrography

All 43 rock samples were slab-cut and then prepared as thin sections. The polished thin sections were usually prepared at about 30 μm thick before polishing with 12, 6, 3, 1 and 3 μm diamond pastes, respectively. After preparation, they were used for petrographic description for mineral assemblage, texture and alteration under a polarizing microscope. Subsequently, representative samples were selected, based on petrographic feature, for further analyses, e.g., whole-rock geochemistry and some mineral chemistry.

1.7.3.2 Whole-rock geochemistry.

Twenty five rock samples were selected and crushed by an iron jaw crusher prior to powdering by an agate mortar. Subsequently, powdered rock samples were fused to glass beads for X-ray Fluorescence (XRF, model Philips PW 2404) based at Department of Earth Science and Technology, Faculty of Engineering and Resource

Science, Akita University. Analyses of 9 major oxides (i.e., SiO_2 , TiO_2 , FeO , MnO , MgO , CaO , Na_2O , K_2O and P_2O_5) and 10 trace elements (i.e., Ba, Zn, Sr, Rb, Zr, Co, Cr, Ni, Y and V) were carried out quantitatively. Rock standards of JA-1, JA-2, JA-3, JB-1, JB-1a, JB-2, JB-3, JG-1, JG-1a, JG-2, JG-3, JGb-1, JP-1, JR-1 and JR-2 provided by Geological Survey of Japan (GSJ) were used for calibration at 40 kV. Moreover, loss on ignition (LOI) was also measured by weighting rock powders before and after ignition at 900° C for 3 hrs in a TMF-200 electric furnace. Trace and rare earth elements were accomplished by an Inductively Coupled Plasma-Mass Spectrometer (ICP-MS, model Agilent technology 7500 series) based at Department of Earth Science and Technology, Faculty of Engineering and Resource Science, Akita University. The 0.1000 g (± 0.0001 g) of powdered samples were taken and then dissolved in a $\text{HF-HNO}_3\text{-HClO}_4$ acid mixture in sealed Teflon beakers. The digested samples were diluted immediately and added mixed standard solution to all samples before ICP-MS analysis, following the method reported by Kimura et al. (1995). This method is a standard addition method. A Japanese rock standard, (JA-1, provided by GSJ) was also analyzed for comparison with recommended values. Detection limits range from 1 ppm - 0.01% for major oxides, 0.01 - 1 ppm for trace elements and 0.01 ppm for rare earth elements.

1.7.3.3 Mineral chemistry

Some crucial minerals were subsequently analyzed using an Electron Probe Micro Analyzer (EPMA, model JXA-810) based at Department of Geology, Faculty of Science, Chulalongkorn University. Selected polished thin sections were coated by thin film carbon prior to analysis. Operation conditions were set at 15 kV with about 24 nA current of focused beam ($< 1 \mu\text{m}$). Pure oxides and mineral standards were used for calibration. Measuring times were set at about 30 seconds for each element before automatic ZAF correction was taken and analyses were reported, accordingly.

1.7.4 Interpretation, Discussion and Conclusion

All results obtained from this study were collected for interpretation before discussions on genesis, alteration, tectonic setting and gold mineralization were carried

out. Subsequently, conclusions in all particular aspects were reported.

1.7.5 Report writing

Finally, thesis report and presentation were made for this defense. Moreover, draft of publication has been prepared for international journals.



ศูนย์วิทยทรัพยากร
จุฬาลงกรณ์มหาวิทยาลัย

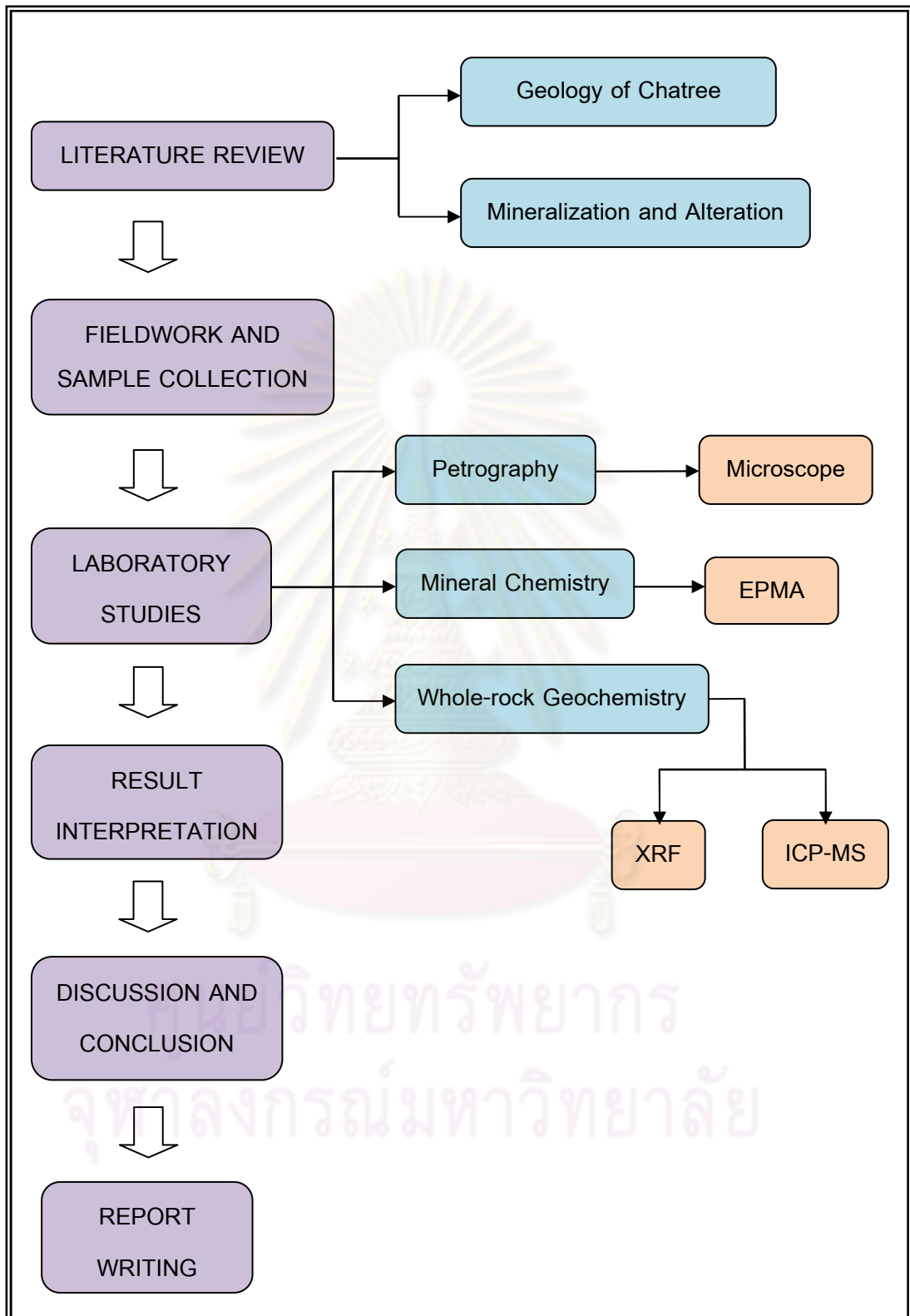


Figure 1.4 Schematic diagram showing sequences of work under this study.

CHAPTER II

GEOLOGIC SETTING

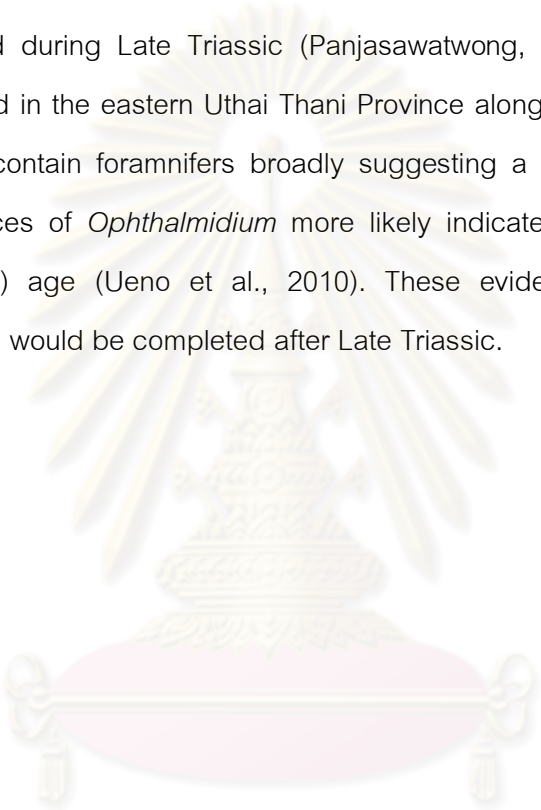
2.1 Tectonic Evolution of Thailand

Tectonic evolution of Thailand was suggested by Bunopas and Vella (1983 and 1992) before a new model was modified by Charusiri et al. (2002). Bunopas and Vella (1983 and 1992) reported that Thailand consists of Shan-Thai and Indochina terranes bound together along Nan suture. The Shan-Thai terrane is located in the western part consisting of eastern Myanmar, western Thailand and some parts of northern Laos. The Indochina terrane occupies parts of eastern Thailand, Laos, Cambodia and Vietnam. In Thailand, the Shan-Thai terrane is underlain by high-grade metamorphic basement which appears to have formed during Precambrian. This basement is overlain by sedimentary and metamorphic sequences of Paleozoic, Mesozoic and Cenozoic, respectively. The Indochina terrane is occupied by Permian platform-carbonate and deep-water clastic rocks which are mainly covered by the Mesozoic sedimentary sequences of Khorat Group. Exposures of Precambrian rocks have never been reported in this terrane. Middle Paleozoic to Triassic sedimentary basin between both terranes formed as parallel volcanic fold-belts, so-called Sukhothai Fold-Belt onto the Shan-Thai, and Loei Fold-Belt onto the Indochina.

Subsequently, Charusiri et al. (2002) proposed two smaller tectonic blocks situated between the Shan-Thai and Indochina terranes. Nakhon Thai block is located on the east whereas Lampang-Chiang Rai block is on the west (Figure 2.1). Both tectonic blocks represent ancient oceanic plates and their associated volcanic terranes. Therefore, the Sukhothai Fold-Belt is parts of the Lampang-Chiang Rai block whereas the Loei Fold-Belt is related to the Nakhon Thai. Charusiri et al. (2002) also suggested four main tectonic stages in Thailand, based on tectonostratigraphic and geochronological data, including Archaeotectonic, Paleotectonic, Mesotectonic and Neotectonic.

During the Archaeotectonic stage, Shan-Thai appears to be parts of the Northwestern Australian continent whereas Indochina may be associated with South China, North China and Kurosegawa-Kitakami terranes located somewhere close to Northern to Northeastern Australia (Bunopas and Villa, 1983; Bunopas, 1992; Metcalfe, 1995; 1997). A major marine transgression (Paleotethys) over both Shan-Thai and Indochina may have been extending from Cambrian to Permian during the Paleotectonic stage as well as their moving northward to the paleoequator. Consequently, oceanic subductions appear to have occurred in Middle Paleozoic leading to new propose of two small tectonic blocks intervening between Shan-Thai and Indochina, namely paleotethyan Nakhon Thai ocean floor to the east and Lampang-Chiang Rai volcanic arc to the west. During Late Paleozoic to Early Mesozoic, all the terranes had already moved northward across the paleoequator and collided with each other resulting termination of the paleotethys without moving further north. It also commenced the Mesotethys in westernmost Thailand. I-type and S-type granites had extruded all over the country. Collision seems to have caused major northeast- and northwest-trending strike-slip fault systems in the country. Landmass had been intensively uplifted then leading to deposition of Late Mesozoic continental red beds, particularly in Indochina, Nakhon Thai, and Lampang Chiang-Rai blocks whereas western Shan-Thai was inundated by Mesotethys until Latest Mesozoic. Subsequently, collision between West Burma block and Shan-Thai may have triggered additionally both I-type and S-type granites in association with mineralization; and also terminated the Mesotethys marking the end of Mesotectonic stage. The interaction of Indian plate to Eurasian plate which in turn closed the Neotethys marked a significant change of tectonic style in Thailand and its adjacency. Reactivation of fault movement with opposite direction may have formed. Rifting appears to have taken place extensively over the region of Southeast Asia, causing development of pull-apart basins in the northern Thailand, opening of the Gulf of Thailand as well as South China and Andaman Sea. Moreover, Neotectonic stage is significantly marked by enormously mantle-derived basaltic volcanism. However, the Neotectonic stage still persists as indicated by hot spring/high-heat flow regions and present-day earthquakes (Kosuwan et al., 1998).

Closures of Paleotethys lying between Shan-Thai and Lampang-Chaing Rai blocks and between Nakhon Thai and Indochina blocks had caused subduction-related volcanism along the Chiang Mai-Chiang Rai suture and the Loei suture (see Figure 2.1); consequently, amalgamations of Shan-Thai, Indochina and their associated blocks during Late Triassic has been confirmed by $^{40}\text{Ar}/^{39}\text{Ar}$ geochronological data (Charusiri, 1989). In addition, Nan-Uttaradit suture appears to have been welded during Late Triassic (Panjasawatwong, 1991). However, Triassic limestones exposed in the eastern Uthai Thani Province along the Chao Phraya Central Plain of Thailand contain foraminifers broadly suggesting a Ladinian or younger age whereas occurrences of *Ophthalmidium* more likely indicates Late Triassic (possibly Carnian or Norian) age (Ueno et al., 2010). These evidences introduce that the Paleotethys closure would be completed after Late Triassic.



ศูนย์วิทยธรณีวิทยา
จุฬาลงกรณ์มหาวิทยาลัย

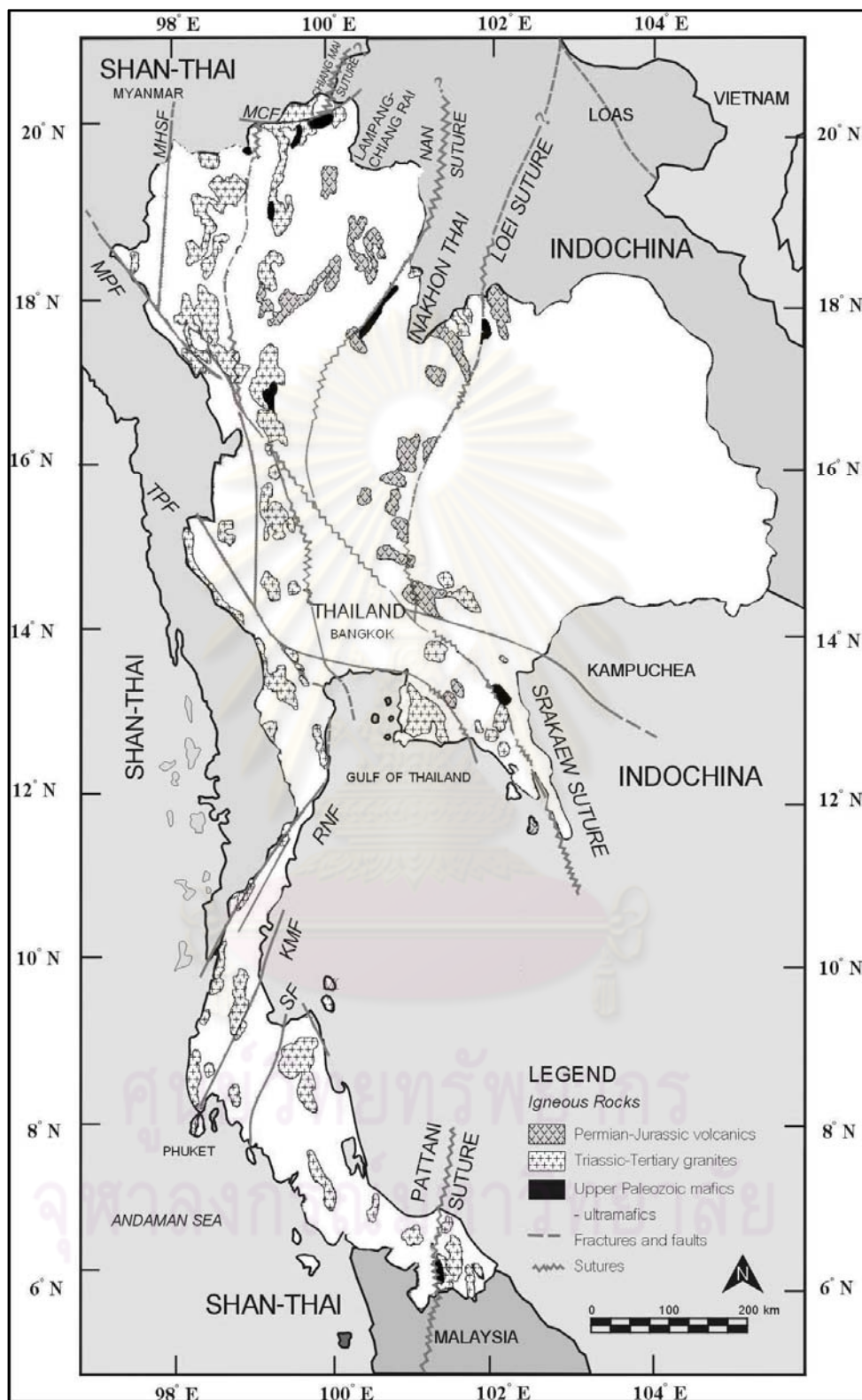


Figure 2.1 Tectonic map of Thailand showing regional tectonic features and exposures of some rock types related to the main collisions herein the country (modified from Charusiri et al., 2001 by Sutthirat, 2009).

2.2 Pre-Jurassic Volcanic Rocks in Thailand

Pre-Jurassic volcanic rocks in Thailand have been discovered extensively and can be separated, base on their distribution and tectonic setting, into three main belts located in the Chiang Rai-Chiang Mai volcanic belt, Chiang Khong-Tak volcanic belt and Loei-Phetchabun-Ko Chang volcanic belt (see Figure 2.1) (e.g., Jungyusuk and Khositanont, 1992; Intasopa, 1993; Charusiri et al., 2002; Phajuy et al., 2005); moreover, these volcanic belts are sometimes associated with epithermal and skarn gold deposits (Jungyusuk and Khositanont, 1992; Potisat, 1996; Diemar and Diemar, 1999 and Khin Zaw et al., 1999). In addition, Charusiri (1989) divided Loei-Phetchabun-Ko Chang volcanic belt into two parts including volcanic rock along Nan - Chanthaburi Suture Zone (NCZ) in the lower part and Loei – Phetchabun - Nakhon Nayok in the upper part (Figure 2.2). All of these volcanic belts are explained below;

Chiang Rai – Chiang Mai volcanic belt: extends along the NNE-SSW direction from the western Chiang Rai Province through the eastern Chiang Mai Province to Li district, Lumphun Province. They are composed of basalt, porphyritic basalt, basalt porphyries, cumulates (wehrlite and clinopyroxenite) and gabbros (Macdonald and Barr, 1978). Moreover, Phajuy et al. (2005) classified this volcanic belt consisting of mafic lava, hyaloclastites, pillow breccias and mafic dikes. Geochemically, these rocks were recognized as tholeiitic and/or transitional alkali basalts. (e.g., Macdonald and Barr, 1978; Barr et al., 1990; Panjasawatwong et al., 1995; Panjasawatwong, 1999; Phajuy et al., 2005). Chiang Rai – Chiang Mai volcanic belt appears to have erupted during Middle Permian to Permo-Triassic (Chuaviroj et al., 1980; Bunopas, 1981; Bunopas and Villa, 1983; Panjasawatwong, 1999; Phajuy et al, 2005). They may have been originally derived from volcanic arc (Hutchison, 1973; Bunopas and Vella, 1978). Moreover, mafic volcanic rocks in the Chiang Rai area appear to have formed in a subduction environment (Macdonald and Barr, 1978; Barr et al., 1990) whereas the volcanic rocks in the Chiang Mai and Lamphun areas may have formed in a continental within-plate environment (Barr et al., 1990); however, Panjasawatwong et al. (1995) and Panjasawatwong (1999) suggested that volcanic rocks from these area would be

erupted in an oceanic within-plate environment as ocean islands and seamounts within either a mature back-arc basin or a major ocean basin. The later model was supported by Metcalfe (2002).

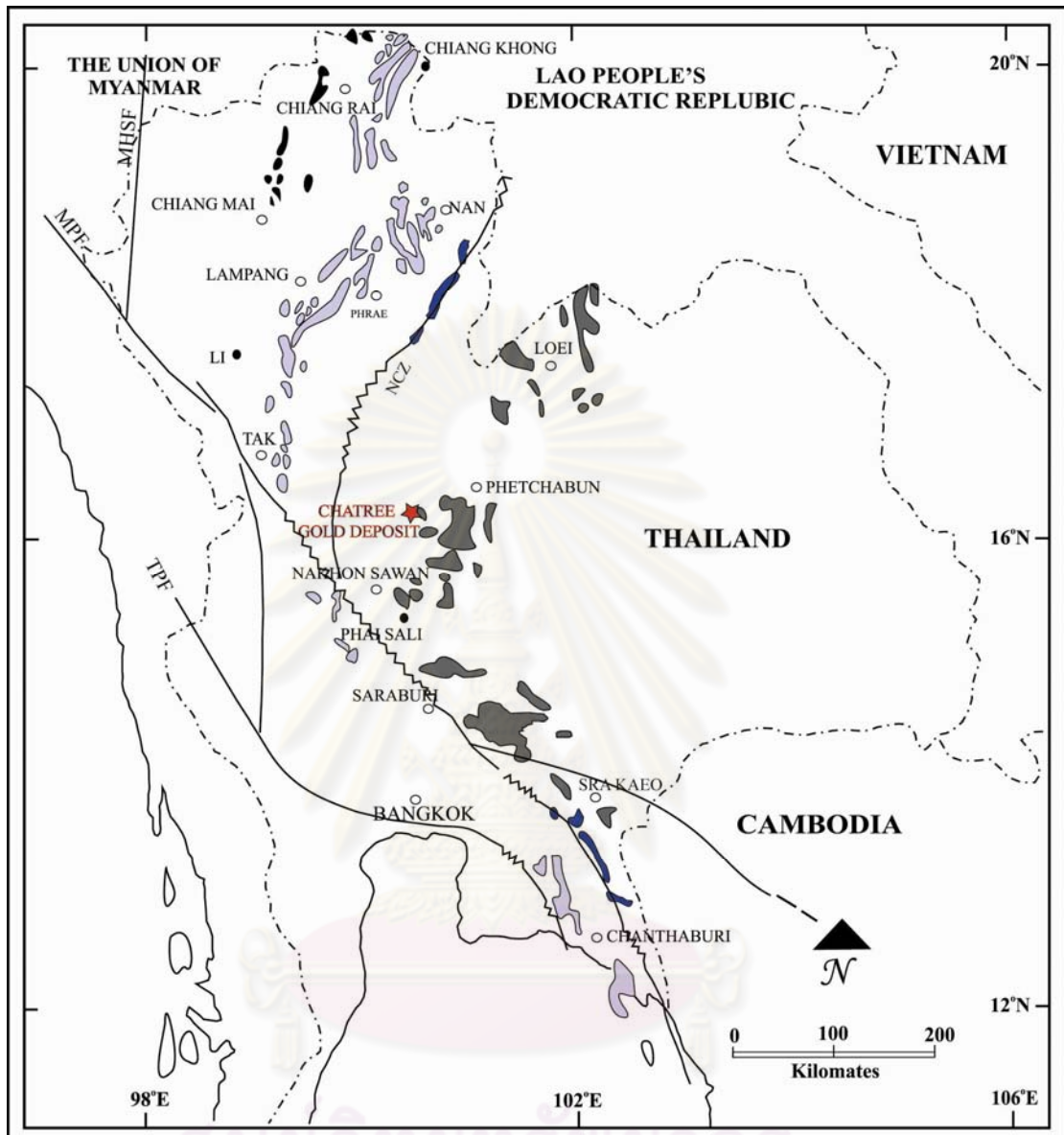
Chiang Khong – Tak volcanic belt: is located on the east of Chiang Rai–Chiang Mai volcanic belt. This volcanic belt extends from Chiang Khong district, Chiang Rai Province toward the western part of Phrae Province and the eastern part of Lampang Province to Tak Province. Volcanic rocks along this belt vary from intermediate to acid compositions including rhyolite, dacite, andesite and pyroclastic rocks. They can be subdivided into two episodes on the basis of stratigraphic correlation, i.e., Permo-Triassic and possibly upper Triassic to lower Jurassic age (Jungyusuk and Khositant, 1992). These volcanic rocks may have been formed by subduction activity as arc environment (Bunopas, 1981; Bunopas and Villa, 1983; Hutchison, 1989; Barr et al., 1990). Panjasawatwong et al. (2003) reported that Permo-Triassic Chiang Khong volcanic rocks have formed in a continental volcanic arc environment. Geochemical characteristics of the Permo-Triassic continental arc Chiang Khong – Tak volcanic belt are related to two magmatic series including tholeiitic series (Panjasawatwong et al., 2003) and calc-alkalic series (Barr et al., 2000). Both series have also been reported in the eastern part of the Lincang-Jinghong volcanic belt in the southwestern China, possible northern extension of the Chiang Khong-Tak volcanic belt (Yang et al., 1994; Yang, 1998).

Loei – Phetchabun – Nakhon Nayok volcanic belt: occurs along NNE-SSW trend from Loei Province toward Phetchabun Province and NW-SE trend from Nakhon Sawan Province to Saraburi Province, Prachinburi Province and Sra Kaeo Province. Volcanic rocks in this belt are composed of lava and pyroclastic those have compositions ranging from felsic to mafic. In Loei area, these volcanic rocks can be subdivided into 3 sub-belts; Eastern, Central and Western sub-belts. The Eastern Loei volcanic rocks locally form N-S along the western margin of the Khorat Plateau. These volcanic rocks are mainly characterized by rhyolitic composition. Based on stratigraphic correlation, the Eastern volcanic rocks are underlain by marine limestone of middle Permian age and they are overlain by the Phu Kradung Formation of early Jurassic age. Therefore, these

volcanic rocks probably occurred in the Permo-Triassic age (Jungyusuk and Khositantont, 1992). However, rhyolitic samples of this sub-belt yielded whole-rock Rb-Sr isochron age of 374 ± 33 Ma (Devonian-Carboniferous) and they may have erupted in continental volcanic arc environment (Intasopa, 1993; Intasopa and Dunn, 1994). The Central Loei volcanic rocks are situated along N-S direction near Pak Chom area (Chairangsee et al., 1990; Jungyusuk and Khositantont, 1992; Pajasawatwong et al., 2006); they are mainly composed of pillow basaltic lava, hyaloclastite and pillow breccias (Pajasawatwong et al., 2006). Fragments of fossiliferous limestone of Devonian age have been locally found in volcanic tuffs (hyaloclastite); this may confirm marine environment in middle Devonian and late Devonian to Carboniferous (Chairangsee et al., 1990). Volcanic rocks of this sub-belt have been interpreted to a mid-oceanic ridge and oceanic island-arc environment (Pajasawatwong et al., 2006); they also yielded a whole-rock Rb-Sr isochron age of 361 ± 11 Ma (Upper Devonian to Lower Carboniferous) (Intasopa and Dunn, 1994). The Western Loei volcanic sub-belt is located along the contact zone of the Permian and Triassic-Jurassic sedimentary rocks. These rocks mainly consist of fine-grained andesite porphyry with subordinate rhyolite, rhyolitic tuff and dacite (Jungyusuk and Khositantont, 1992); they may have formed within Permo-Triassic arc volcanism (Bunopas, 1981). $^{40}\text{Ar}/^{39}\text{Ar}$ age of 242 ± 3 Ma was reported from these rocks (Intasopa et al., 1990). Moreover, volcanic rocks from Phu Chang area at western Loei sub-belt may be related to Permo-Triassic calc-alkaline volcanic arc (cited in Charusiri et al., 1995). South of Loei volcanic is connected to Phetchabun volcanic provinces that located along Sri Thep district in Phetchabun Province toward Phai Sali district in Nakhon Sawan Province. These volcanic rocks mainly consist of basaltic andesite and andesite (Jungyusuk and Khositantont, 1992); they cross-cut and flowed over limestone of the middle Permian age, and they are overlain by Triassic sedimentary rocks (Jungyusuk et al., 1989). In addition, andesite dikes locally cross-cut the upper Triassic sandstone (Jungyusuk, 1985). Therefore, these rocks may have erupted from late Permian to upper Triassic ages. Age of 235 ± 4 Ma was determined using $^{40}\text{Ar}/^{39}\text{Ar}$ method from these rocks (Jungyusuk and Khositantont, 1992). Consequently, Phetchabun volcanic rocks have been suggested as a product of arc subduction-

related activities (Intasopa, 1993; Kamvong et al., 2006). The study area is located within the western part of this volcanic province. (Nakchaiya, 2008; Marhothorn, 2008) that was occurred by subduction-related island arc. In Saraburi-Prachinburi Provinces, the volcanic rocks consist mainly of porphyritic rhyolite, porphyritic dacite, porphyritic andesite, trachyandesite, rhyolitic tuff and andesitic tuff (Hinthong et al., 1985; Junplook, 2006; Vivatpinyo, 2006). These volcanic rocks commonly cross-cut the middle Permian limestone, and are overlain by Phu Kradung Formation; hence, they should have formed in middle Permian or after and prior to Jurassic ages (Hinthong et al., 1985). $^{39}\text{Ar}/^{40}\text{Ar}$ dating of a rhyolite sample from south of Saraburi Province yielded 53 ± 2 Ma (Intasopa et al., 1990). The conflict between stratigraphic correlation and radiometric age determination may have been resulted from complexity of tectonic evolution (Jungyusuk and Khositant, 1992). For chemical data, these volcanic rocks are characterized by calc-alkaline volcanic arc related to subduction environment (Vivatpinyo et al., 2010).

Volcanic Rock along Nan-Chanthaburi Suture Zone (NCZ): is located between the Chiang Khong-Tak volcanic belt and the Loei-Phetchabun-Nakhon Nayok volcanic belt which they extend southward to the Gulf of Thailand. It is widely accepted that this zone represents a Late Triassic continental suture between the Shan-Thai and Indochina terranes (e.g., Bunopas, 1981; Hada et al., 1991; 1999; Chaodumrong, 1992; Singharajwarapan, 1994; Singharajwarapan et al., 2000; Crawford and Panjasawatwong, 1996). Pre-Jurassic volcanic rocks along this suture zone occur as blocks with various sizes embedded in foliated serpentinite matrix (serpentinite mélangé?). Yoshikura (1990) and Crawford and Panjasawatwong (1996) reported that these volcanic rocks are composed of Early to Middle Permian ocean-island basalt, Carboniferous (?) incipient back arc basin basalt and andesite, Permo-Triassic (?) arc basalt and andesite, and mid-ocean ridge basalt.



- Chiang Rai – Chiang Mai volcanic belt
- Chiang Khong – Tak volcanic belt
- Volcanic rocks along the Nan – Chanthaburi suture zone (NCZ)
- Loei – Phetchabun – Nakhon Nayok volcanic belt

Figure 2.2 Distribution of Pre-Jurassic volcanic rocks in Thailand (modified from Panjasawatwong et al., 1997).

2.3 Regional Geology

Base on geologic map modified from Chonglakmani and Satayalak, 1979 (Figure 2.3), the study area lies on boundary between Thap Klo and Wang Pong District, central Thailand. Geology of the regional area mainly includes sedimentary rocks of Permian and Triassic. Unconsolidated Quaternary sediments and igneous rocks are also exposed in this area. The sedimentary rocks are herein described in the order of ages from the oldest to the youngest below.

1. Lower-Middle Permian

Pha Nok Khao Formation: The Lower-Middle Permian rock in this area exposed in eastern region. This formation consists of well bedded to massive limestone with black chert lenses, sandstone and shale.

2. Triassic

Huai Hin Lat Formation: Rocks in this Formation are dominated by yellowish brown conglomerates that are mostly limestone and rhyolite. In addition, Iwai et al. (1964) suggested that this formation consists of yellowish-brown to reddish-brown sandstone, reddish-brown siltstone, and grey shale with leaf fossils. Part of these rocks was metamorphosed by thermal. This Upper Triassic formation was found in the northeastern-eastern part of the regional area.

Nam Phong Formation: This formation overlying on Huai Hin Lat Formation exposes in the northeastern of the regional area. The rocks are brown to reddish-brown sandstone, cross-bedded conglomerate with pebbles (up to 10 cm in diameter) of quartz, chert, red siltstone and sandstone. Moreover, this formation also contains brown to reddish-brown shale and siltstone.

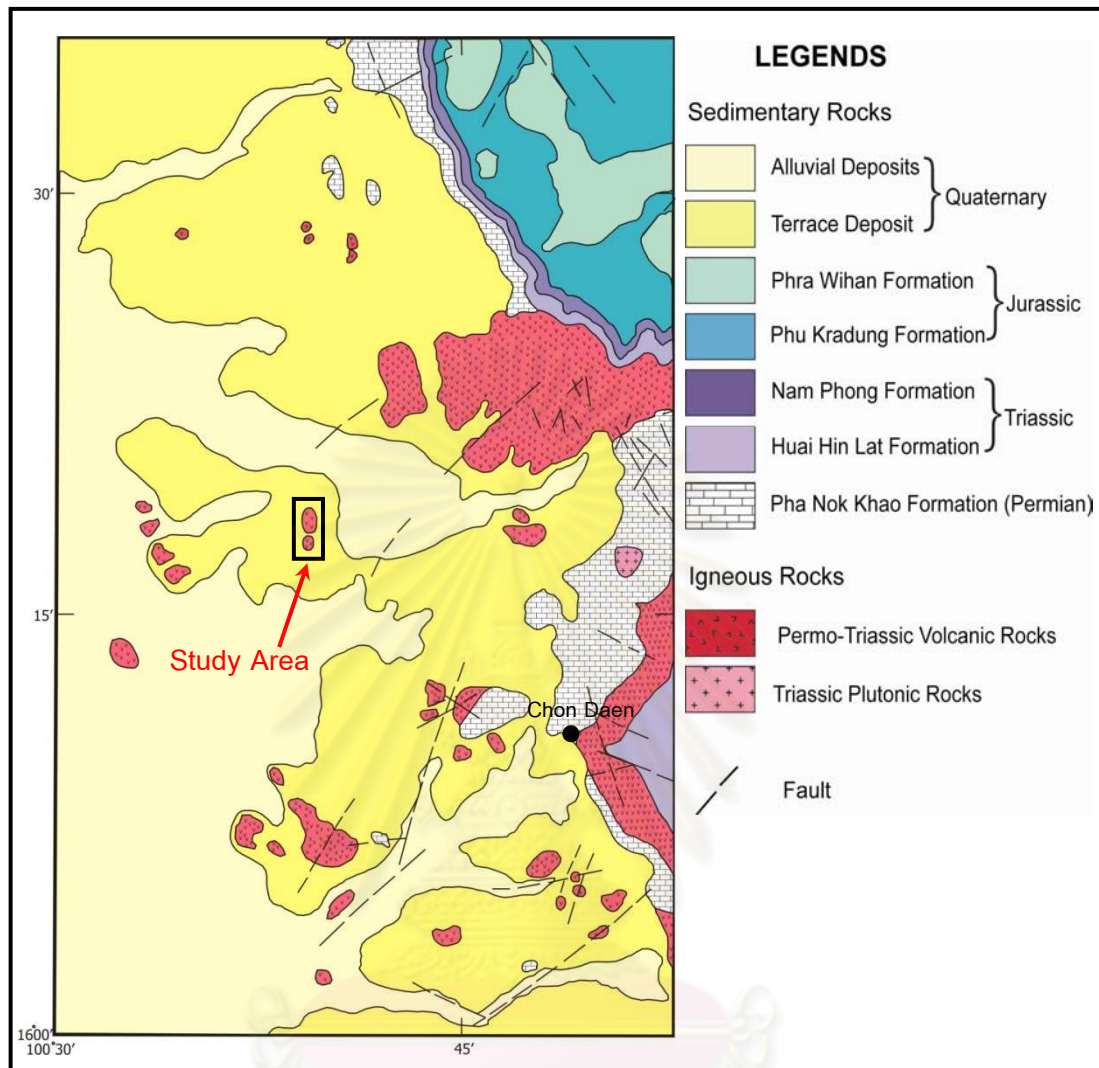


Figure 2.3 Regional geologic map of the Thap Klo - Wang Pong - Chon Daen areas and study area (modified from Chonglakmani and Satayalak, 1979).

จุฬาลงกรณ์มหาวิทยาลัย

3. Jurassic

Phu Kradung Formation: overlies the Nam Phong Formation or Permian rocks. Rocks of this formation expose mostly in the northeastern part of the regional area. They are significantly characterized by brown, reddish-brown, purplish-red, and micaceous shales, brown, gray, micaceous siltstone and sandstone showing small scale cross-bedding, and some limestone-nodule conglomerates. The age of the rock is suggested as lower Jurassic period.

Phra Wihan Formation: The rock is composed of sandstone, white-pink orthoquartzite with cross-bedded to massive layers and with pebbly layers on the upper bed; some intercalations of reddish brown layers are also present. They appear to be Lower-Middle Jurassic period. This rock unit exposes in the northeastern part of the regional geologic map.

4. Quaternary

Unconsolidated deposits: The Quaternary sediments are composed of terrace and alluvial deposits containing gravel, sand, silt and clay. They are found in the western part of the regional area.

5. Igneous Rocks

Plutonic rocks, which have been found in Wong Pong area, can be divided into three types including granite, granodiorite and diorite (Chonglakmani and Satayalak, 1979; Ponprasit et al., 1988). Granite is usually white porphyritic rocks that contain plagioclase phenocrysts. Muscovite is also observed commonly in this granite. Granodiorite is usually dark grey fine grained rocks with porphyritic texture. Phenocrysts, about 1x0.5 cm, are significantly hornblende. Diorite is characterized by dark grey with porphyritic texture; phenocrysts with size of 1x1.5 cm are plagioclase and hornblende. These plutonic rocks are of Triassic age but some of them may be younger. Some of these plutonic rock intruded into the Upper Triassic sediment units. Moreover, plutonic rocks are covered partly by unconsolidated sediments; however,

airborne magnetic data indicate that dikes and stocks of granodiorite intruded in the area, particularly in the southern part of the Chatree gold deposit (Sangsomphong in prep.). Stratigraphic correlation constrains age of these plutonic rocks to a minimum Triassic (Chonglakmani and Satayalak, 1979; DMR, 1999).

Volcanic rocks were found as lava and pyroclastic rocks, consisting of rhyolite, andesite, basaltic andesite, tuff, welded tuff, lapillistone, agglomerate and volcanic breccias (Chonglakmani and Satayalak, 1979; Ponprasit et al., 1988). Andesite commonly showed porphyritic texture with phenocrysts of hornblend, clinopyroxene and plagioclase (Ponprasit et al., 1988). The unit indicates Permo-Triassic in age because it lies in between the Middle-Upper Permian and Lower Triassic units (Chonglakmani and Satayalak, 1979).

Permo-Triassic volcanic rocks in the study area are situated in Loei-Phetchabun-Nakorn Nayok volcanic belt (Jungyusuk and Khositanont, 1992; Panjasawatwong et al., 1997). Jungyusuk and Khositanont (1992) reported that the Permo-Triassic volcanic rocks in Chon Daen-Wang Pong area (Figure 2.3) vary in composition from basalt to rhyolite; however, basaltic andesite and andesite are the most abundance, particularly in the western Loei area to the north. Based on field investigation, these rocks overlie Middle Permian limestone and underlie Triassic sedimentary rocks. However, Jungyusuk and Khositanont (1992) also reported that andesitic tuff and agglomerate are interbedded with Middle Permian sandstone at outcrops along the Phetchabun-Chon Daen road and andesite dikes cross-cut Late Triassic sandstone. That may indicate more than one period of magmatism.

2.4 Detailed Geology

Based on Crossing (2004) study (Figure 2.4), the Chatree region contains several andesitic volcanic centres and a couple of rhyolite centres. Large and well-exposed andesitic volcanic centres are at Ban Mai Wang Takhian, Akkara mine and Khao Phanompha. These andesitic volcanic rocks are intercalated with lavas, pyroclastic and volcanoclastic sedimentary rocks displaying significant lateral facies variation and complex interfingering to the adjacent volcanic centres. Thick andesite lava flows interbedded with andesitic autobreccias and these are also interbedded with lithic tuffs mixed provenance sedimentary rocks. Crystal tuff and ash fall tuff are less volumetrically important. The volcano-sedimentary sequences are mostly gently folded, with dipping lower than 30 degree and rarely exceeding 45 degree except some areas are particularly near faults. In general, bedding becomes shallower dipping in the eastern half toward the edge of Khorat plateau. Steeper dips occur within two zones along NE-SW trending structure. The rhyolitic volcanic centre at Khao Khieo was formed by a very thick rhyolitic crystal tuff with occasional lithic fragments, which distally interbed with andesite units. It contains some thin interbeds of tuffaceous sediments apparently overlaying the adjacent andesitic rocks. At Ban Nikhom, flowed bands of rhyolite and rhyolitic tuff are exposed in several shallow dams. In regional scale, these volcanic units are also related to thick well-bedded sequence of interbedded fine-grained volcanoclastics and epiclastic siltstone and shale, massive tuffaceous mudstone and more distally epiclastic siltstone and shale; these units are well-exposed at Wang Pong. Various intrusive rocks ranging in composition from felsic to mafic intruded these volcanic sequences mostly as small- to medium-sized stocks and dikes. Volumetrically, most important unit is intermediate intrusives, dominated by diorite may be ranging from granodiorite to diorite which their textures vary from fine-grained equigranular to porphyritic rock. Moreover, Crossing (2004) reported that granitic intrusions occur as stocks and dikes, one to the north of the Chatree gold deposit around Ban Wang Phlap, and the other to the south (Ban Lang Du). They appear to be spatially associated with northeast and southeast structural trends. Kamvong (2002); Kamvong et al. (2006)

studied plutonic rock at Wang Pong district (about 50 km from Chatree gold deposit) and consequently described small stocks ranging in composition from granite to diorite. He also classified these intrusive stocks into two types, namely biotite granite and granodiorite. The former is fine-, to medium-grained texture and the later is medium-grained inequigranular texture. Petrochemical characters indicate A-type granite (Kamvong, 2002). Besides, small stocks of granitoid rocks also reported at Khao Ron Thong of Chon Daen District (Rodmanee, 1992). Granodiorite porphyry has also been encountered in some drill holes at N-prospect and V-prospect (Marhotorn, 2008).



ศูนย์วิทยทรัพยากร
จุฬาลงกรณ์มหาวิทยาลัย

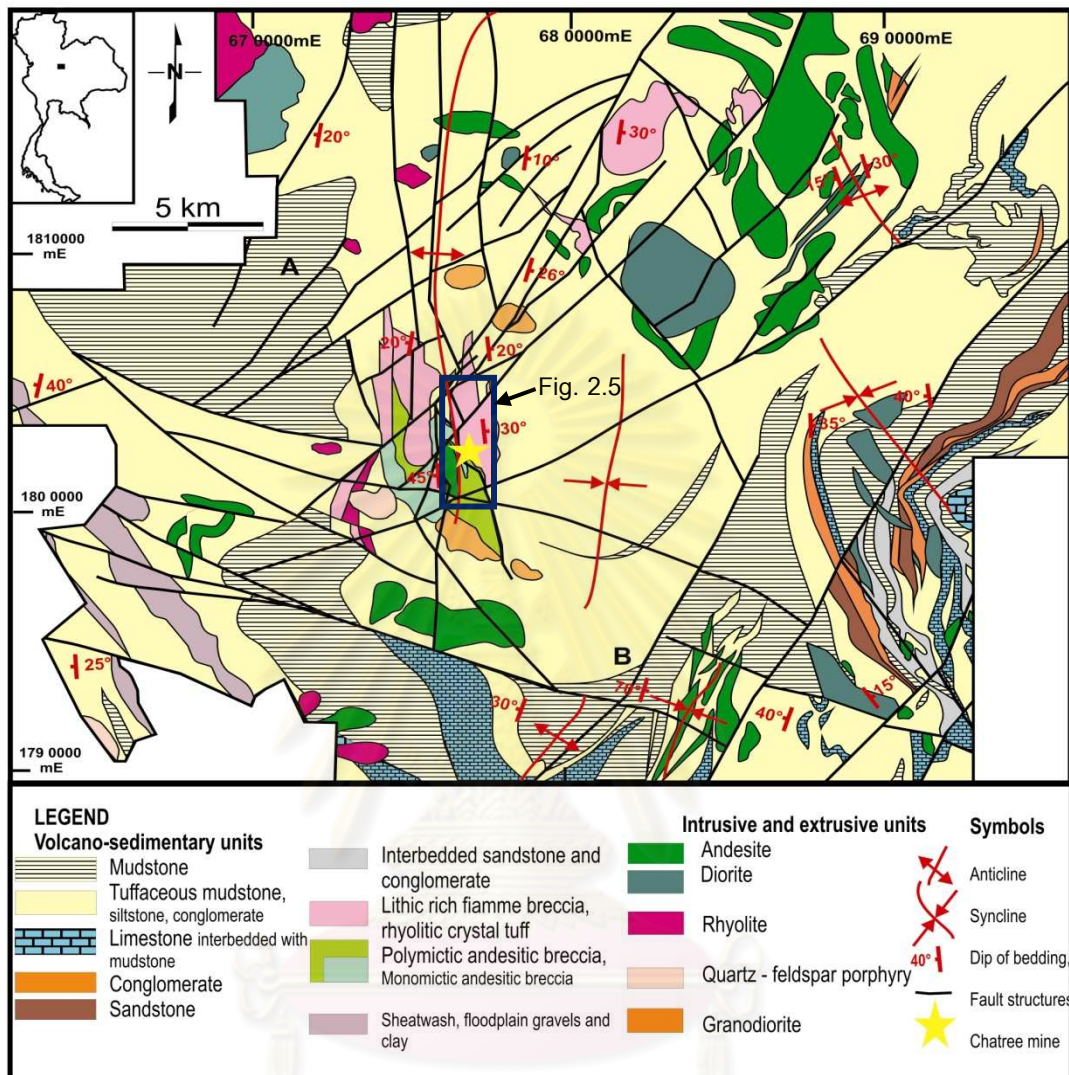


Figure 2.4 Detailed geologic map of Chatree gold deposit and its vicinity (modified after Crossing, 2006; updated to include the observations of Comming et al., 2004).

จุฬาลงกรณ์มหาวิทยาลัย

2.5 Mineralization and Prospecting Areas

This section describes geology and mineralization of C-H pit, K prospect, A pit, Q prospect, N prospect and V prospect of the Akkara mine within the Chatree gold deposit.

1) C-H and H-west Pit

Kromkhun and Zaw (2005) reported that the H zone of the Chatree deposit is a low-sulfidation epithermal deposits consisting of plagioclase-pyroxene phyric andesite, andesite lithic breccias, crystal-rich andesitic pumice breccias, epiclastic and limestone. The depositional environment of host volcanic sequence is mainly subaerial to shallow submarine. Petrographic investigation of C-H and H-west reveals to coherent and non-coherent rocks (Nakchaiya, 2008). The coherent rocks are mainly andesite to basaltic andesite. Compositionally, the non-coherent suite also bears similar characteristics. The non-coherent facies includes three successive breccia units – viz. polymictic, monomictic and fiamme units. The latter is the highest and youngest volcanic unit. Overlying the monomictic unit is the epiclastic unit. This unit is composed mainly of fine-grained clastic unit and was not recognized in the C pits. Only the coherent and monolithic breccia units show strong alteration with associated Au-Ag mineralization.

In the late stage, dike rocks at C-H Zone of Chatree gold deposit form part of the Permo-Triassic Loei-Phetchabun-Nakhon Nayok volcanic belt. Dikes are recognized one in the northeast-southwest direction and the other in the north-south direction. Petrographically, the dike rocks shown porphyritic texture and can be mainly classified as andesite, trachytic andesite and basaltic andesite. Andesite is characterized by plagioclase (oligoclase) and hornblende and shows clearly porphyritic textures (Tangwattananukul et al., 2008).

Ore body at C pit is one of the major ore body of Chatree deposit, it has strike at almost N-S (350°) and dips at an average 40° to the west. The ore body occurs as massive veins at C-south with minor breccia and become stockwork in the northern part (C-central) particularly near surface. At C-north, ore body is massive toward the hanging

wall and become stockwork toward the footwall. At C-south, it has overturned corn-shaped structure at the near surface area, and become thin zone at deeper part. Breccia is predominated particularly by grey silica breccia, mainly confined to the footwall both at C-south and C-north. Multiple stage breccia also has been found and mostly overprinting the grey breccia stage. Grey breccia is generally characterized by angular clasts of mainly porphyritic andesite, minor fine-grained pelagic sedimentary rocks and fiamme breccia. The grey matrix is composed of cryptocrystalline quartz and some fine-grained pyrite. The grey silica material is believed to be barren. However, it is believed to play an important role of ore deposits. The ore body is characterized by crustiform-colloform banding of alternating grey silica, quartz-carbonate-sulphides and quartz-carbonate-chlorite and cream to brown calcite and dolomite bands are common and usually dilute in gold grade. At C-south, the mineralization styles are predominant with quartz-carbonate-pyrite with subordinate quartz-carbonate-chlorite. Gold grade, often diluted by coarse-grained calcite/dolomite, is commonly banded and forming part of the major mineralization stage (Salam, 2006). In the H zone, the mineralization styles are complicated including quartz-sulphide at the H-central and H-south. Quartz-carbonate-pyrite is widely spread through the pit; quartz-carbonate-chlorite and quartz-carbonate-chlorite-sulphide are identified, mainly confined to the area of H-central, H-north. The latter two stages usually carry high gold grade (Salam, 2006).

Marhotorn (2002) mapped the C-H Zone and studied fluid inclusions. The country rock formed silicification and initiation of brecciation by hydraulic fracturing. Hydrothermal fluid enriched in gas phase of magmatic sources ascended along normal faults for many times. The hydraulic fracturing increased permeability within and around the breccia bodies. The gas phased mixed with meteoric fluid, leading to more rapid cooling and dilution of the acidic fluid with temperatures between 178 and 268 °C and salinities less than 5.3 wt.% NaCl equiv. These fluids flowed laterally along the highly permeable rocks of Permo-Triassic volcanic formation where initial acid leaching enhanced the secondary of the host rock formation by the development of vuggy quartz. Late stage meteoric water dominated hydrothermal fluid activity at a lower temperature of around 163 °C. With decreasing temperature, silica-rich fluids deposited and sealed

most of the pore spaces within the hosting rocks (Marhotorn, 2002). The result of overprinting is comb structure presented in milky quartz alteration zone. The latest stage, supergene alteration resulted from post-breccia wall rock alteration fracturing/jointing and accompanying Cenozoic weathering and oxidation.

2) K Prospect

At K prospect, rocks contain lower-fiamme breccia, polymictic andesitic lithic breccia and matrix rich polymictic andesitic lithic breccias. The mineralizations in K-west are similar to C-north in term of style and alteration but they mainly occur as small veins/veinlets and stockworks. Gold is believed to associate with quartz-carbonate-sulfide veins and minor quartz-carbonate-chlorite. Banded texture is also present and characterized by fine-grained white to pale grey quartz, fine-grained chlorite and coarse-grained sulfide bands (Salam, 2006).

3) A Pit

At the A pit and A-east prospect, rocks consist of polymictic andesitic breccia and matrix rich lithic breccia interbedded/intercalated with volcanic mudstone and sandstone with minor limestone. The fiamme breccia occurs at the top part of the sequence and it is known as quartz-rich rhyolitic fiamme breccias (Salam, 2006). The study of Sangsiri and Pisutha- Arnond (2008) at the A prospect, the host rocks are proximal to the mineralized zones, and are dominated by silicification, quartz-adularia alteration, followed by carbonates and finally Fe-sulfide, Fe-Ti oxide, sphene/leucoxene assemblages. The host rocks distal from the mineralized zones are dominated by altered propylitic assemblage such as chlorite/serpentine and/or Fe-Ti oxides.

4) Q Prospect

Q prospect is occupied mainly by fiamme rhyolitic breccias (rhyolitic tuff in this study), epiclastic, polymictic andesitic breccias and porphyritic andesite. Mineralization of Q prospect can be found along veins of quartz-marcasite vein, marcasite (pyrite)-quartz veinlet and quartz fine-grained sulphide±calcite, and particularly appear in the

alteration zones such as sulphide disseminated in strongly silicified host rock. The characteristic of ore veins are small with uncertain direction. Moreover, clay mineral and porous (vuggy) silica can be found on top of the system that indicates process of volatile which is style of top of the hydrothermal system.

5) N Prospect

Marhotorn et al. (2008) studied igneous rocks and reported that felsic porphyry and aphanitic mafic rocks were cross cut by subsequent alteration and mineralization. Petrographically, felsic rocks in the N zone bear similar microporphyritic to porphyritic and phaneritic textures. They were classified as porphyritic fine-grained granodiorite. The granodiorite is mainly composed of plagioclase, quartz and relict hornblende. The groundmass is characterized by fine-grained quartz, apatite and incipient sphene. Quartz and K-feldspar replaced rims of plagioclase phenocrysts. The aphanitic intermediate-mafic rocks bear similar porphyritic andesite. It is characterized by altered plagioclase and glassy groundmass.

N prospect in Chatree gold deposits displays many typical features of porphyry Mo-Cu-Au deposits such as multiphase intrusions, alteration and vein deposition, low grade Cu mineralization and no significant Au. These were identified (Marhotorn, 2008). Alteration formed early K-feldspar halos, indicative of emplacement during early potassic alteration, and later halos of silica-sericite-pyrite (phyllic) alteration. Although two potassic altered diorite intrusions, as well as post-mineral dikes, are recognized at N prospect, they appear to be only one event of Cu mineralization, associated with quartz veins. Two weak events of molybdenite may be present; Au grades are very low, and Cu is consistently in the order of 0.16% in the RC and diamond drilling (Corbett, 2004).

6) V Prospect

Marhotorn (2008) suggested that the rocks of V prospect are mainly porphyritic aphanitic, intermediate to mafic, rocks with abundant green minerals and minor vein systems. The rock in the V zone is dominated by altered porphyritic andesite containing relic plagioclase and hornblende, clearly presenting porphyritic texture. The altered

porphyritic andesite is characterized by replacements of epidote, sericite and chlorite in feldspar glassy groundmass.

Surface and subsurface map were modified from Comming et al., 2006 (Figure 2.5). Geological map shows large zones of lithic rich fiamme breccia on the western and eastern zones of the Chatree gold deposit, large zones of polymictic andesitic breccias, coherent andesite and monomictic andesitic breccias towards the south and western zones and more abundant fine-grained epiclastic and volcanoclastic sediments towards the north. The large zone to the south is the N prospect granodiorite. Generally, these rocks are dipping towards the east on the eastern flank and towards the west on the western flank conforming a broad anticline. Fault structures have been interpreted from geophysical data and from drill core and mine exposures (Crossing, 2004; Coming et al., 2006).

Stratigraphic Units: Comming et al. (2006) and James and Comming (2007) subdivided stratigraphic units and grouped volcanic facies exposed in the Chatree mine that occur at specific levels in the stratigraphy. They have been grouped into certain stratigraphic units based from composition, texture and position in the stratigraphy. There are 4 stratigraphic units which are mentioned below.

Unit 1: Lithic rich fiamme breccia with interbedded fine-grained fiamme rich sandstone and siltstone with thin layers of accretionary lapilli-rich siltstone and polymictic mud matrix breccias. This unit un-conformably overlies the lower units.

Unit 2: Fine-grained epiclastic and minor sedimentary facies including laminated siltstone, mudstone and carbonaceous to calcareous fossiliferous siltstone; quartz-rich fiamme breccia, polymictic and monomictic rhyolitic breccia facies.

Unit 3: Polymictic andesitic breccia, polymictic andesitic-basaltic breccia which is partly inter-bedded and overlain by volcanoclastic sandstones, laminated carbonaceous mudstones and minor calcareous siltstone. This unit also includes thin isolated intervals of monomictic andesitic breccia, plagioclase phytic andesite and hornblende phytic andesite.

Unit 4: This unit is the lowest intersected stratigraphic unit. It contains monomictic andesitic breccias, plagioclase phyric andesite, hornblende phyric andesite and some polymictic andesitic breccias with isolated small bodies of coherent dacite and rhyolite with associated thin zones of monomictic dacitic and rhyolitic breccia. Andesite, dacite and basalt dike cross cut the whole succession.



ศูนย์วิทยทรัพยากร
จุฬาลงกรณ์มหาวิทยาลัย

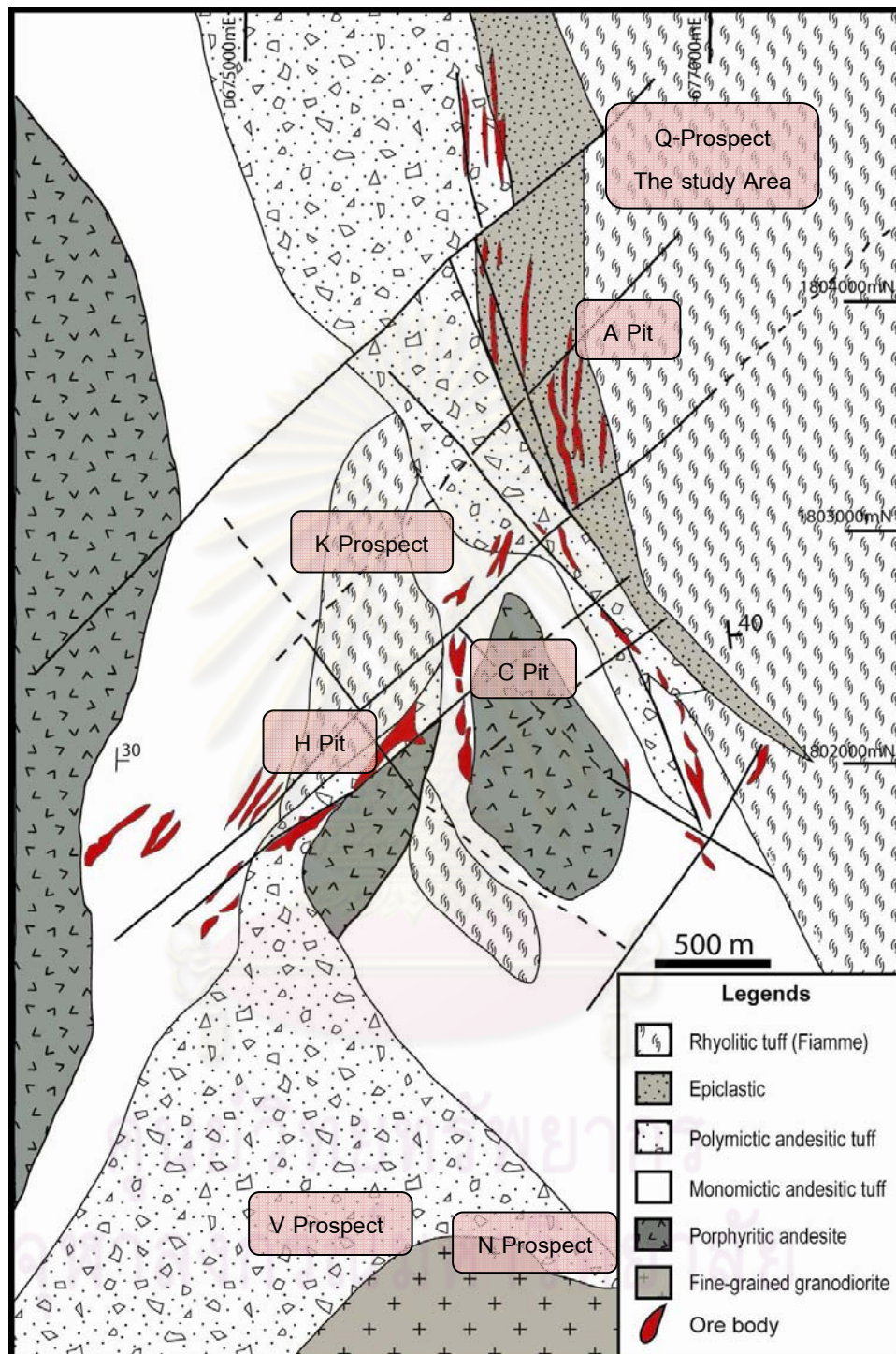


Figure 2.5 Surface and subsurface geologic map of the study and surrounding areas, Chatree gold deposit, boundary between Pichit and Phetchabun Provinces, north central Thailand (modified from Comming et al., 2006).

CHAPTER III

PETROGRAPHY

3.1 Introduction

In this chapter, macroscopic and microscopic descriptions of each rock type are described in detail. Based on geologic and stratigraphic data obtained from Comming (2006), Marhotorn (2008), Nakchaiya (2008) and this study, volcanic and related rocks in Chatree gold deposit can be subdivided into six units, i.e., porphyritic andesite, andesitic tuff, epiclastic sediments, rhyolitic tuff, granodiorite and andesite dike. Five of them (except granodiorite) are found in Q-prospect area, this study area. Granodiorite intruded into only the porphyritic andesite (Marhotorn, 2008), the lower volcanic layer whereas andesite dike appears to have cut into all volcanic rocks, pyroclastics and epiclastics (see Figure 3.1). However, only volcanic and pyroclastic rocks were under interest of this project. Therefore, forty three rock samples of these rock types, e.g., porphyritic andesite, andesitic tuff, rhyolitic tuff and andesite dike, were collected from fourteen drill-holes (see Figure 1.3). They include drill holes RD2270, RD2327, RD2686, RD2836, RD3039, RD3888, RD2884, RD2901, RD2937, RD7161, RD7151, RD7155, RD7162 and RD7157. All samples were slab cut prior to rough classification. Subsequently, thirty samples were selected and prepared as thin sections and polished thin sections. Petrographic description of all rock types are reported below.

3.2 Petrographic Description

3.2.1 Porphyritic Andesite

Porphyritic andesite samples, the lowest unit, are characterized by aphanitic rocks that have light to dark green groundmass with some white and black spots of phenocrysts (Figures 3.2). These phenocrysts contain mainly feldspars and

amphiboles. These rocks are sometimes cross cut by quartz-carbonate veins and calcite veins.

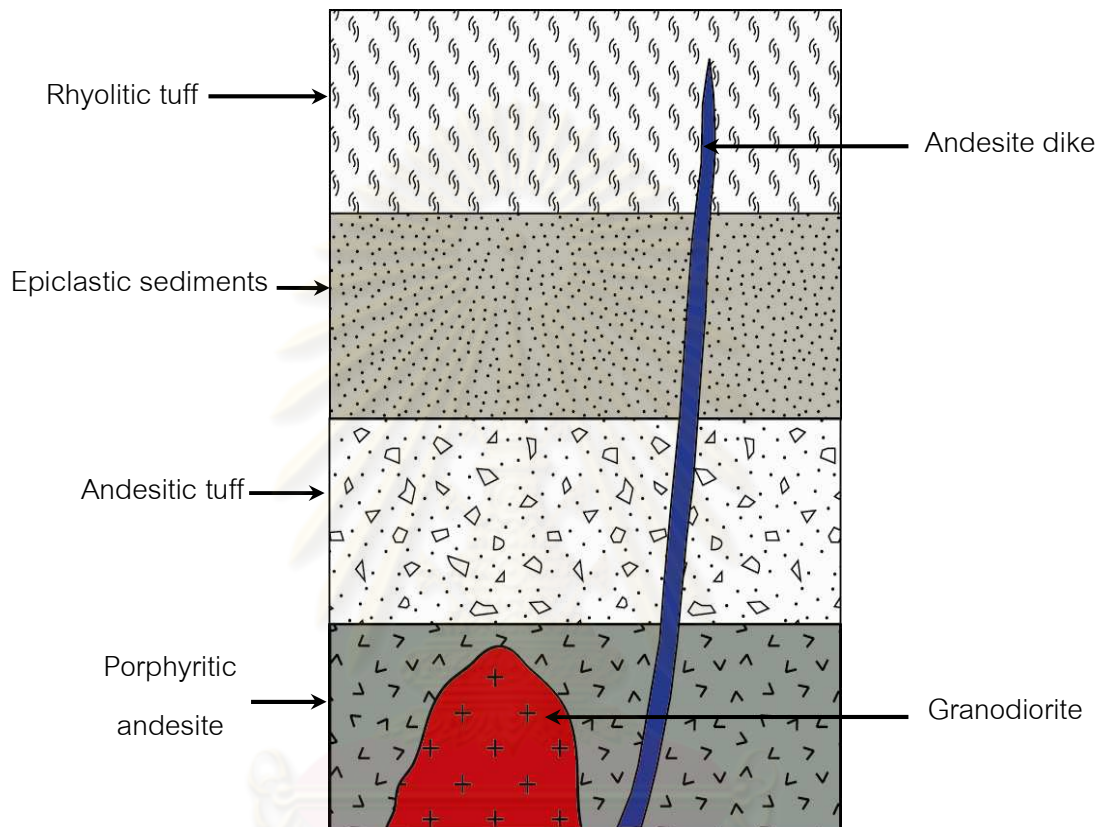


Figure 3.1 Simplified stratigraphic correlation of Chatree gold deposit, using geological survey and drill hole data (modified from Salam, 2008).

ศูนย์วิจัยทรัพยากร
จุฬาลงกรณ์มหาวิทยาลัย

Microscopically, porphyritic andesite is generally hypocristalline rock containing glass and crystals. Groundmass (~70%) is made up by mostly glassy materials and fine grains of quartz and K-feldspar. Subhedral to euhedral phenocrysts (~30%) set in the groundmass (Figure 3.3). The phenocrysts are mainly K-feldspar with subordinate plagioclase and minor relic amphibole (?). In general, mineral compositions consist of plagioclase, K-feldspar, quartz and relic amphibole. Moreover, secondary minerals are frequently found as chlorite, sericite, quartz and calcite replaced in those primary minerals (see Figures 3.3, 3.4, 3.5 and 3.6). Trachytic texture can also be found in some samples (Figure 3.6) that are usually indicated by flowing pattern of plagioclase microlites (less than 0.01 mm in sizes).

Plagioclase contains about 20 to 25% mode. It occurs significantly as phenocryst and partly in groundmass. Plagioclase phenocrysts always show subhedral to euhedral crystals and exhibit albite twins (Figure 3.3). An-content is estimated ranging from 35 to 43 that fall within andesine range. Size of plagioclase phenocrysts ranges from 0.5 to 2 mm. K-feldspar in groundmass always occurs as microlite with small subhedral crystal (Figure 3.6). K-feldspar commonly contains about 15 to 20% that occurs as both phenocryst and groundmass. It always shows subhedral to euhedral crystals (Figures 3.3, 3.4 and 3.6). K-feldspar groundmass is hardly identified under microscope. Size of phenocrystic K-feldspar ranges from 0.5 to 1 mm. Highly altered K-feldspar usually formed as replacements of sericite and chlorite along cleavage (Figure 3.4).

Relic hornblende (~5%) occurs as phenocryst ranging in size from 0.2 to 0.5 mm. These crystals show relic rhombohedral shape with two direction cleavage with intersection angles of 60 and 120 degrees (Figure 3.5). Hornblende phenocrysts are crucially replaced by sericite (Figure 3.5) and calcite (Figure 3.6).

Secondary minerals (up to 10 to 15% mode) are composed of chlorite, sericite and opaque minerals (probably pyrite). Rectangular opaque mineral with size smaller than 0.1 mm also disseminates in groundmass (Figures 3.4 and 3.5).

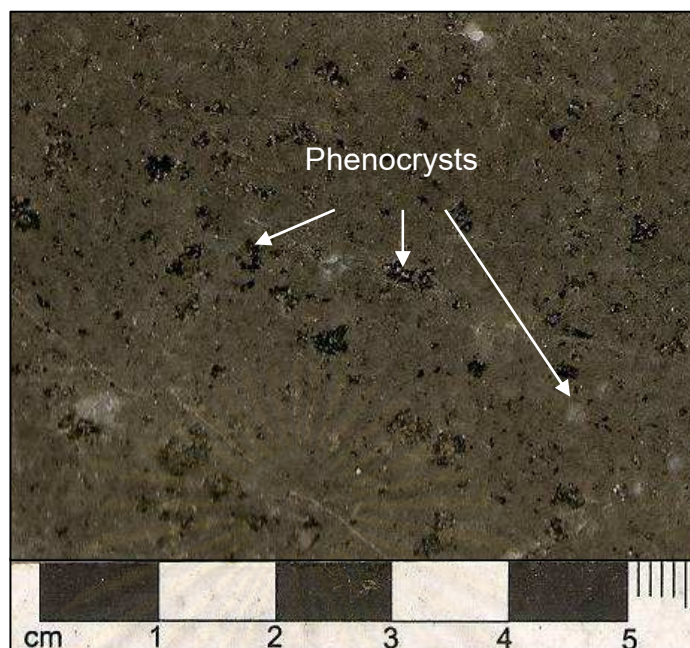


Figure 3.2 A slab specimen of porphyritic andesite (sample no.Q7 of RD2327) showing aphanitic rock with porphyritic texture. Black and white spots are phenocrysts, probably plagioclase, K-feldspar and relic hornblende.

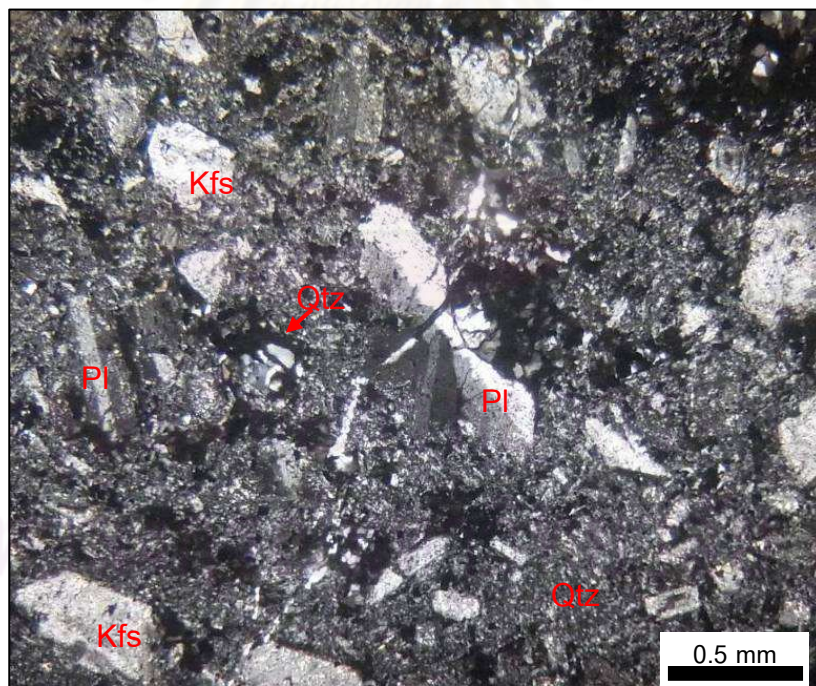


Figure 3.3 Photomicrograph (under cross-polarized light) of porphyritic andesite (sample no. Q1 of RD2270) showing porphyritic texture. The phenocrysts are subhedral to euhedral plagioclase (Pl) and K-feldspar (Kfs) sit in glass and fine-grained quartz (Qtz).

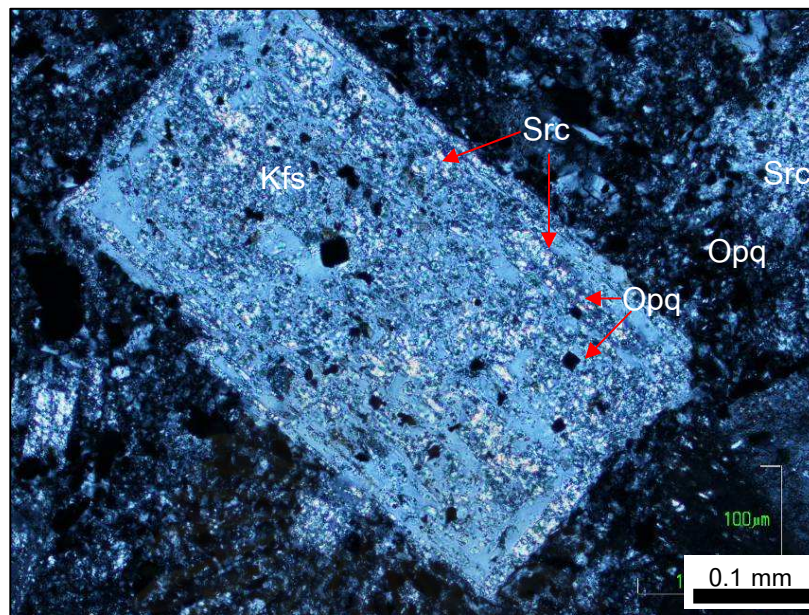


Figure 3.4 Photomicrograph (under cross-polarized light) of porphyritic andesite (sample no. Q1 of RD2270) showing euhedral K-feldspar (Kfs) phenocrysts with replacement of sericite (Src). Euhedral opaque (Opq) minerals (pyrite) disseminated in groundmass and in K-feldspar phenocryst.

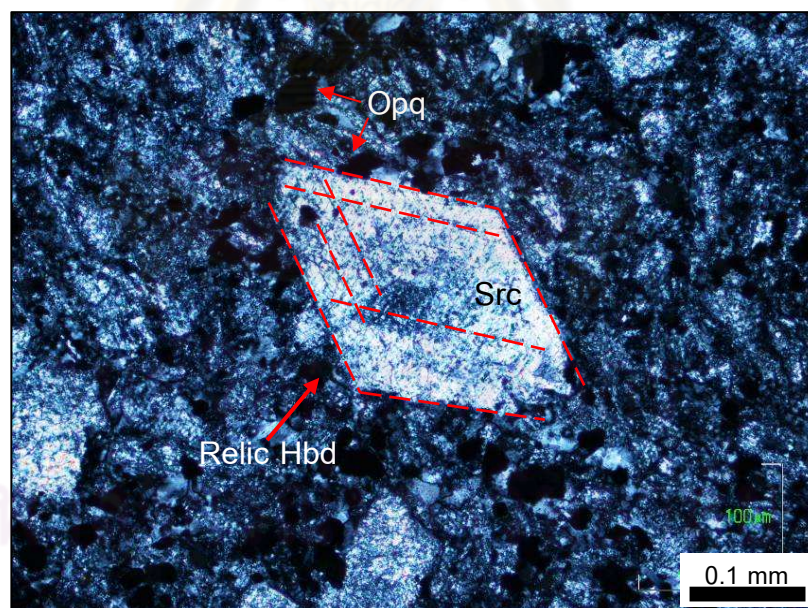


Figure 3.5 Photomicrograph (under cross-polarized light) of porphyritic andesite (sample no. Q1 of RD2270) showing relic hornblende (Hbd) grain fully replaced by sericite (Src). This relic hornblende shows rhombohedral shape with two-direction cleavages with intersection angle of 60 and 120 degree. Opaque (Opq) minerals are also found in groundmass.

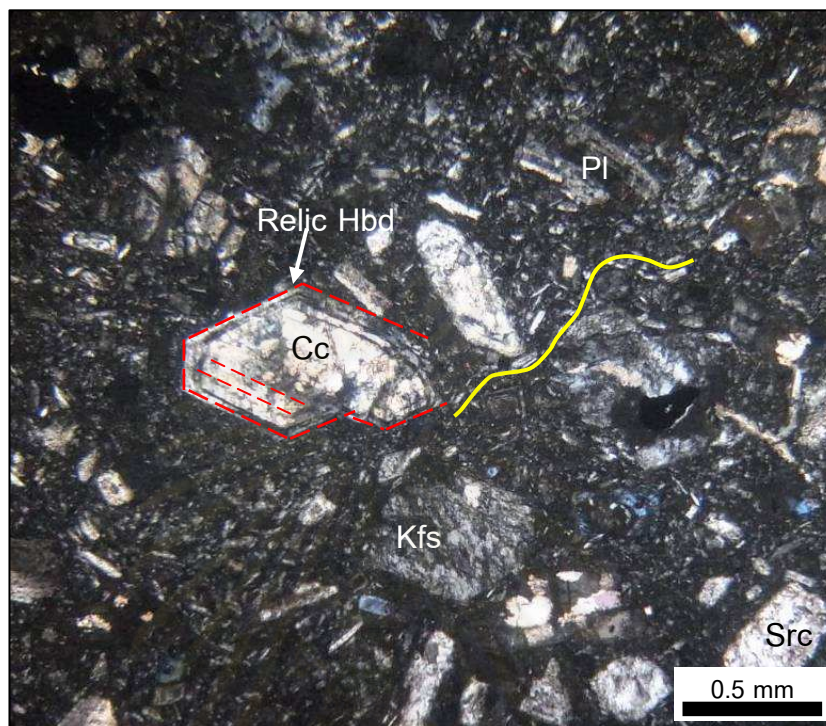


Figure 3.6 Photomicrograph (cross-polarized light) of porphyritic andesite (sample no. Q7 of RD2327) showing phenocrysts sit in microlite and glassy groundmass. Trachytic texture (see yellowed-lines) is also recognized. Plagioclase (PI) and K-feldspar (Kfs) phenocrysts are partly replaced by sericite. Relic hornblende (Hbd) altered fully to calcite (Cc).

ศูนย์วิทยทรัพยากร
จุฬาลงกรณ์มหาวิทยาลัย

3.2.2 Andesitic Tuff Unit

Pyroclastic rocks at Q-prospect are found overlying the porphyritic andesite. Based on classification diagram (Fisher, 1966; Figure 3.7) and mineral composition, these pyroclastic rocks can be classified as abundant andesitic tuff with a few andesitic lapilli-tuff.

Macroscopically, core samples of andesitic lapilli-tuff show clearly fragmental texture which is made up by coarse ash and volcanic lapilli with size up to 10 mm. Andesitic lapilli-tuff is commonly characterized by greenish grey to dark green rocks containing poorly sorted angular to subrounded clasts which may reach up to 30% mode (Figure 3.8). Clasts in these rock samples have different colors with common green and reddish brown. On the other hand, andesitic tuff is generally characterized by greenish grey rock that is composed mainly of ashes ranging in size from 0.5 to 2 mm.

Microscopically, these lithic clasts are mainly characterized by rhyolite and andesite and occasionally by sedimentary rocks (Figure 3.9). Plagioclase and K-feldspar are subhedral to anhedral with quantity of about 30% mode. K-feldspar and plagioclase appear to be fragmental crystals in these rocks. Quartz usually occurs as angular fragments with amount of about 10 to 25%.

Groundmass consists of quartz, microcrystalline plagioclase and glass. This rock type commonly shows patchy alteration to chlorite and sericite.

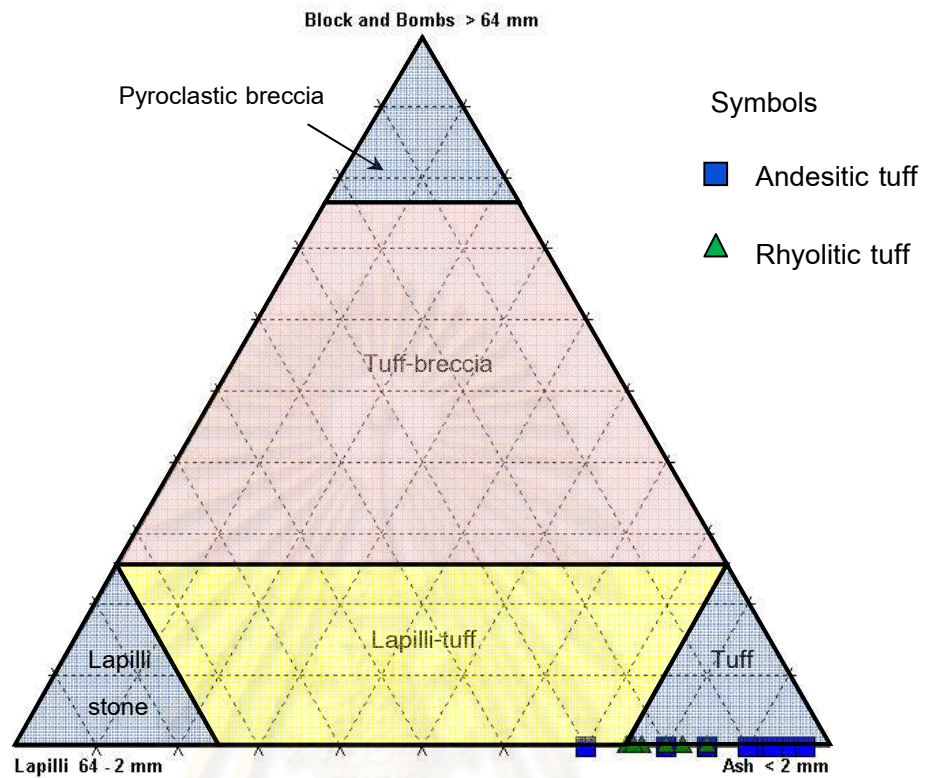


Figure 3.7 Classification diagram of pyroclastic rocks (Fisher, 1966) and compositional plots of andesitic tuff and rhyolitic tuff samples under this study.

ศูนย์วิทยทรัพยากร
จุฬาลงกรณ์มหาวิทยาลัย

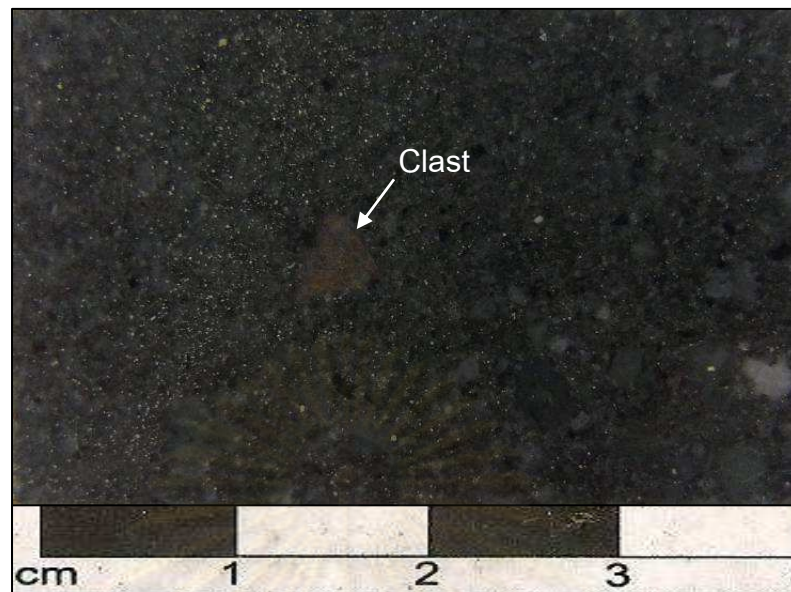


Figure 3.8 A slab specimen of andesitic tuff (sample no. A28 of RD7155) showing various sizes (mostly < 1 cm) of volcanic clasts.

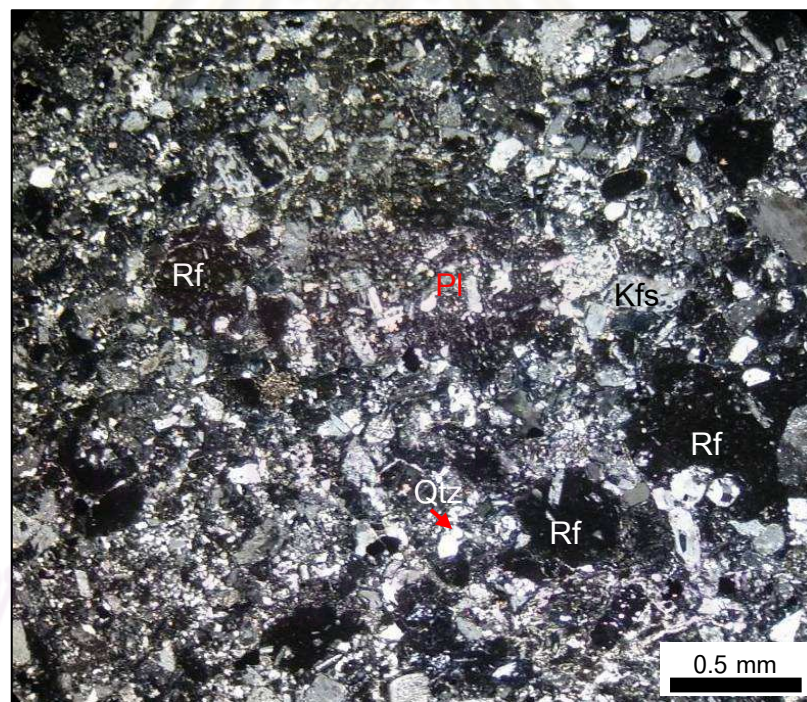


Figure 3.9 Photomicrograph (under cross-polarized light) of andesitic tuff (sample no. A28 of RD7155) showing quartz (Qtz), plagioclase (Pl), K-feldspar (Kfs) and rock fragments (Rf) ranging in size mostly < 0.5 mm of andesite consisting of plagioclase phenocryst surrounded by glassy material.

3.2.3 Rhyolitic Tuff Unit

Rhyolitic tuff is situated on the upper most units in Q-prospect (Figure 3.1). It widely distributes in the eastern area (Figure 2.5). Based on classification diagram (Fisher, 1966); these pyroclastic rocks can be classified as rhyolitic tuff (Figure 3.7).

Macroscopically, rhyolitic tuff has various colors usually white, pale pink and pale green. In general, their constituents are composed of about 40% quartz crystal, 40% ash and 20% lapilli. They appear to have been moderately to poorly sorted. Regarding to lapilli materials, they are mainly characterized by porphyritic andesite and rhyolite. These rocks always show fiamme texture containing lenticular phenocrysts and welded materials (Figure 3.10). This texture indicates that they were pressured, sheared or loaded during the eruption event. Rock samples of this group usually show local silicification.

Microscopically, rhyolitic tuff includes about 5-10% volcanic fragments and 10-20% anhedral quartz grains. Volcanic fragments are cemented abundantly by microcrystalline quartz and glassy material. These fragments are characterized mainly by rhyolite (Figures 3.11 and 3.12).

Quartz fragments are commonly subangular shape with rounded edge. Moreover, some of them have embayed outlines (Figure 3.11).

Secondary minerals are mainly composed of sericite, chlorite and calcite. Sericite and calcite occur as lenticular texture surrounded by chlorite (Figure 3.13).

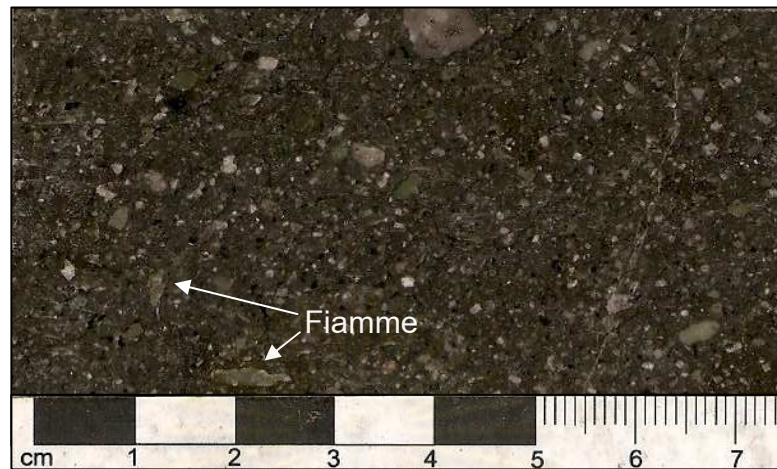


Figure 3.10 A slab specimen of rhyolitic tuff (sample no. Q17 of RD2884) showing volcanic fragments (maybe rhyolite) and angular quartz grains. Fiamme texture, lenticular chlorite and welded materials, is generally found.

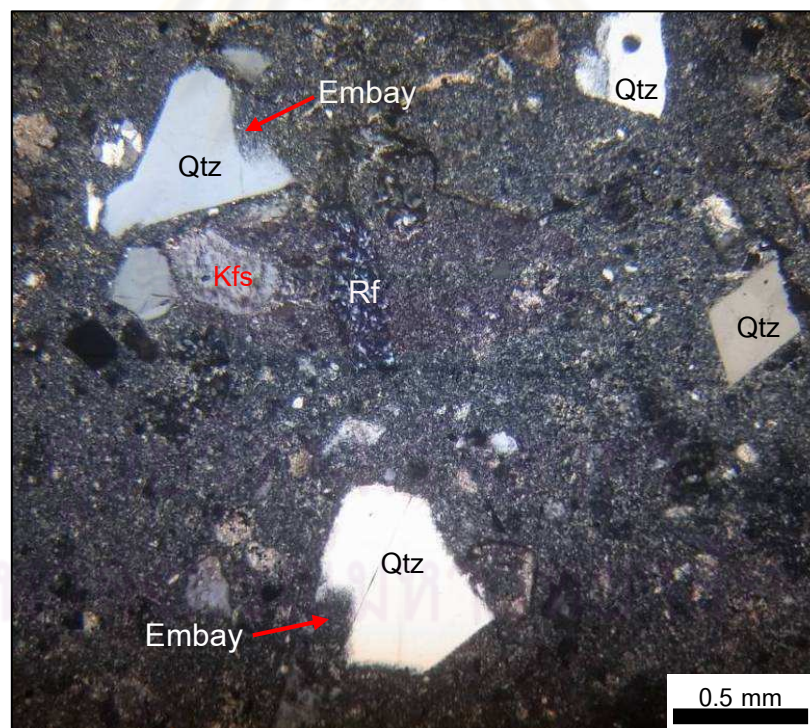


Figure 3.11 Photomicrograph (under cross-polarized light) of rhyolitic tuff (sample no. Q17 of RD2884) shows angular to subrounded quartz (Qtz) grains and rock fragments (Rf) set in fine-grained quartz. Some quartz grains show embay outline. The rock fragments are mostly rhyolite.

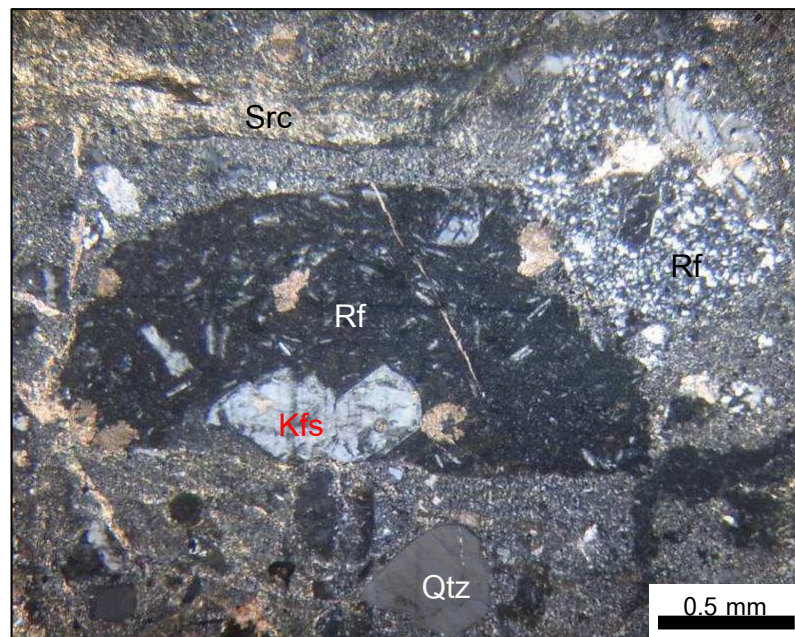


Figure 3.12 Photomicrograph (under cross-polarized light) of rhyolitic tuff (sample no. Q19 of RD2884) showing volcanic rock fragments (Rf) that appear to be porphyritic andesite with size of about 1 to 2 mm. K-feldspar (Kfs) and rounded quartz (Qtz) grains sit in groundmass. Sericite (Src) is generally found in this rock.

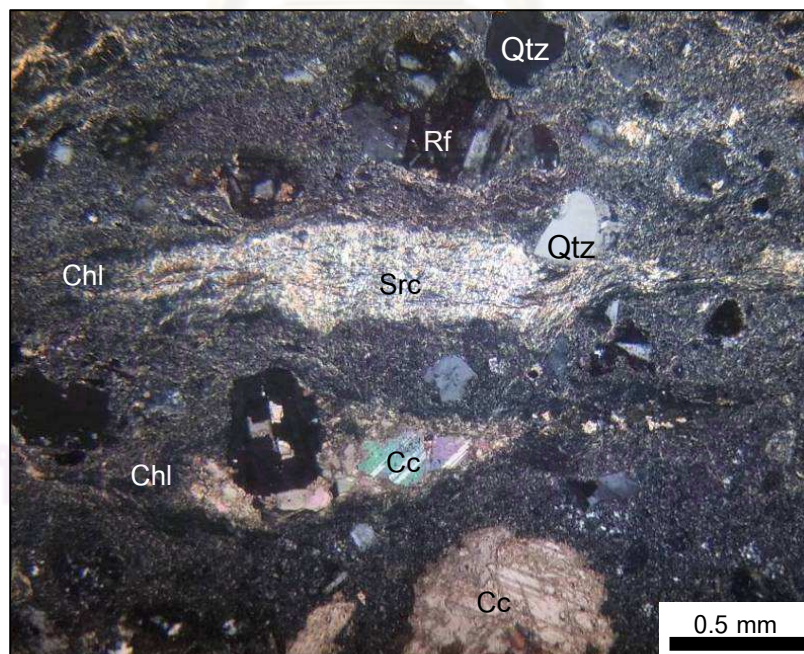


Figure 3.13 Photomicrograph (under cross-polarized light) of rhyolitic tuff (sample no. Q19 of RD2884) showing lenticular sericite (Src) surrounded by chlorite (Chl). Rock fragment (Rf), quartz (Qtz), calcite (Cc) is commonly found.

3.2.4 Andesite Dike

Andesite dike is the latest stage cutting through porphyritic andesite, andesitic tuff and rhyolitic tuff. This rock also shows magnetic property. These samples are normally aphanitic rocks that have green color with black and white spots of porphyritic texture (Figure 3.14).

Microscopically, these rocks show hypocrystalline texture and contain about 50% plagioclase, 20% clinopyroxene and 10% quartz. Moreover, it consists of small plagioclase phenocrysts enclosed partly by pyroxene crystals, called subophitic texture (Figure 3.15). Plagioclase lath generally ranges in size from 0.2 up to 0.5 mm. Pyroxene, mostly characterized by clinopyroxene (Figures 3.15 and 3.16) with size ranging from 0.1 to 1 mm. Epidote (10%) and chlorite (10%) are common secondary minerals that may be replacing plagioclase and pyroxene (Figure 3.16).



Figure 3.14 A slab specimen of andesite dike (sample no. Q6 of RD2327) shows aphanitic groundmass and porphyritic texture. Black and white spots indicate phenocrysts which may be plagioclase and pyroxene.

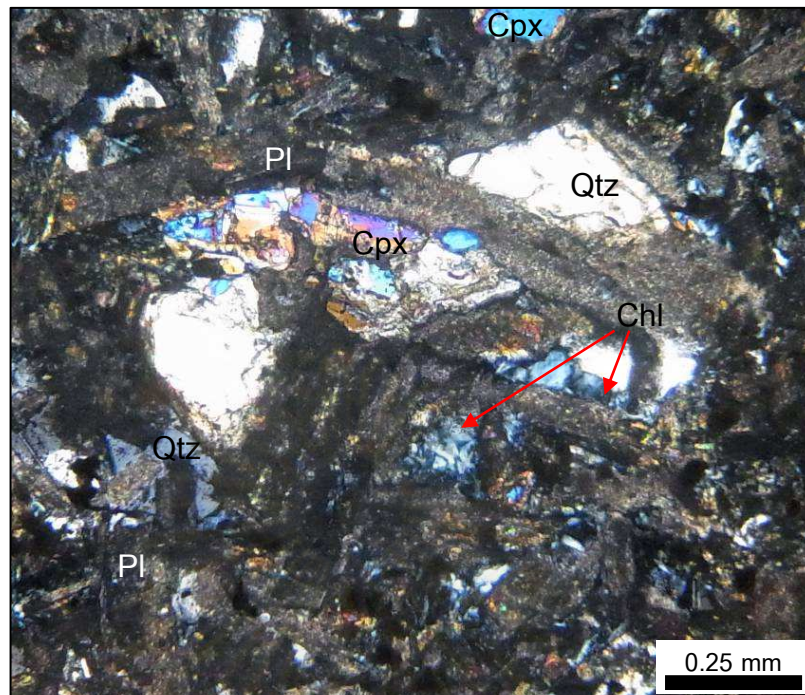


Figure 3.15 Photomicrograph (under cross-polarized light) of andesite dike (sample no. Q6 of RD2327) showing subophitic texture, euhedral plagioclase (Pl) enclosed partly by clinopyroxene (Cpx), quartz (Qtz) and chlorite (Chl) surrounded by glassy material and plagioclase.

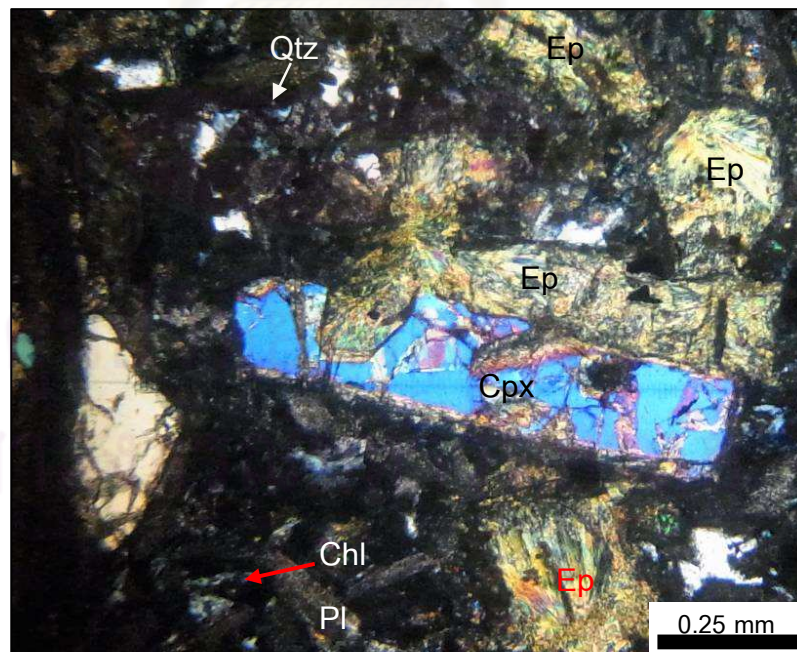


Figure 3.16 Photomicrograph (under cross-polarized light) of andesite dike (sample no. Q6 of RD2327) shows clinopyroxene (Cpx), plagioclase (Pl) and quartz (Qtz). Epidote (Ep) and chlorite (Chl) are also found in this rock.

CHAPTER IV

GEOCHEMISTRY

4.1 Introduction

Volcanic and pyroclastic rocks within the Q-prospect can be subdivided, based on petrographic feature, into four major rock units, including porphyritic andesite, andesitic tuff, rhyolitic tuff and andesite dike. In addition, alteration and weathering have been recognized in many samples that would affect significantly on their geochemistry. Twenty five less altered samples were selected and prepared for whole-rock analyses of major, trace and rare earth elements in order to geochemical investigation and interpretation of magmatic evolution and tectonic setting. Core samples were crushed using jaw crusher prior to hand pick for clean fragments to avoid weathered surfaces, veinlets and xenocrysts. All selected fragments were subsequently powdered using an agate mortar.

The powder samples were initially dried at 110°C for 12 hours in an oven and then were measured loss on ignition (LOI) by weight after heating at 900°C for 3 hours using TMF-200 electric furnace. Subsequently, the dried powder samples were weighted to 0.8 g and then mixed with 1.0 g of lithium metaborate (LiBO_2) and 3.0 g of lithium tetraborate ($\text{Li}_2\text{B}_4\text{O}_7$) in order to make glass beads for major- and some trace-element analyses which were carried out using a X-ray Fluorescence Spectrometer (XRF; model PW 2404).

Analyses of trace and rare earth elements were accomplished by an Inductively Coupled Plasma-Mass Spectrometer (ICP-MS; model Agilent technology 7500 series). Powder samples of 0.1000 g (± 0.0001 g) were dissolved in a mixed $\text{HF-HNO}_3\text{-HClO}_4$ acid within sealed Teflon beakers. Detection limits were estimated at 0.01% for major oxides, 0.01-1 ppm for trace elements and 0.01 ppm for rare earth elements. All

techniques applied to whole-rock analyses are based at Department of Earthscience and Technology, Faculty of Engineering and Resource Science, Akita University, Japan.

4.2 Geochemical Analysis

Twenty five rock samples including seven porphyritic andesite samples, five andesitic tuff samples, eleven rhyolitic tuff samples and two andesite dike samples were analyzed, accordingly. Representative analyses of chemical compositions are summarized in Table 4.1 whereas all the analyses are reported in Appendix C.

4.2.1 Major Compositions

Porphyritic andesitic rocks consist of samples Q-4, Q-7, Q-8, Q-13, Q-14, Q-24, A-34 and A-35. These rocks vary in composition between 43.77 - 54.82% SiO_2 (av. 49.78%), 0.39 - 0.63% TiO_2 (av. 0.51%), 14.84 - 18.69% Al_2O_3 (av. 16.74%), 7.10 - 10.33% FeO_t (av. 9.12%), 0.17 - 0.44% MnO (av. 0.30%), 4.50 - 9.26% MgO (av. 6.59%), 0.81 - 3.64% CaO (av. 2.41%), 0.19 - 1.61% Na_2O (av. 0.66%), 2.36 - 10.43% K_2O (av. 7.07%) and 0.03 - 0.15% P_2O_5 (av. 0.11%).

Andesitic tuffs (i.e., Q-9, Q-43, A-28, A-36 and A-38) are composed of 46.31 - 55.29% SiO_2 (av. 51.34%), 0.43 - 0.56% TiO_2 (av. 0.49%), 15.75 - 18.28% Al_2O_3 (av. 16.59%), 8.33 - 10.84% FeO_t (av. 9.15%), 0.28 - 0.48% MnO (av. 0.37%), 4.77 - 9.23% MgO (av. 6.68%), 0.23 - 3.19% CaO (av. 0.97%), 0.16 - 0.21% Na_2O (av. 0.18%), 6.98 - 10.12% K_2O (av. 8.37%), and 0.06 - 0.11% P_2O_5 (av. 0.09%). In general, andesitic tuff has the same major oxide ranging within the same composition range of porphyritic andesite.

Rhyolitic tuffs, including samples Q-14, Q-17, Q-22, Q-40, Q-41, Q-42, A-25, A-27, A-31, A-33 and A-39, have various compositions ranging from 67.10 to 80.02% SiO_2 (av. 72.76%), 0.13 to 0.32% TiO_2 (av. 0.24%), 5.71 to 14.43% Al_2O_3 (av. 10.46%), 2.15 to 5.25% FeO_t (av. 3.56%), 0.02 to 0.26% MnO (av. 0.11%), 0.76 to 3.33% MgO (av. 1.87%), 0.34 to 4.29% CaO (av. 1.51%), 0.12 to 2.26% Na_2O (av. 0.35%), 2.03

to 8.38% K_2O (av. 5.25%) and 0.04 to 0.10% P_2O_5 (av. 0.07%). They quite vary in chemical compositions which may have been effected by alteration processes.

Andesite dikes containing only two samples (Q-6 and A-26) are composed of 52.32 and 53.90% SiO_2 (av. 53.11%), 1.18 and 0.90% TiO_2 (av. 1.04%), 17.12 and 16.45% Al_2O_3 (av. 16.78%), 8.89 and 7.45% FeO_t (av. 8.17%), 0.14 and 0.15% MnO (av. 0.15%), 3.40 and 4.31% MgO (av. 3.86%), 6.76 and 7.48% CaO (av. 7.12%), 4.32 and 3.26% Na_2O (av. 3.79%), 1.52 and 1.51% K_2O (av. 1.52%), and 0.30 and 0.23% P_2O_5 (av. 0.26%), respectively. In addition, TiO_2 , CaO , Na_2O and P_2O_5 contents of these andesite dikes are obviously higher than other rock types. On the other hand, their MnO and K_2O contents are lower than porphyritic andesite and andesitic tuff. That shows quite different composition of this younger dike.

Harker-type diagrams show variation plots of other major oxides against wt% of SiO_2 (Figure 4.1). Negative correlation between SiO_2 and some major oxides particularly TiO_2 , Al_2O_3 , FeO_t , MnO and MgO are recognized whereas some elements (e.g., CaO , Na_2O , K_2O and P_2O_5) show unclearly correlation. Moreover, SiO_2 contents can be used to distinguish rhyolitic tuff from the other groups, due to their extremely high SiO_2 contents which appear to have been silicified by fluid of late stage hydrothermal activity. MgO plotted against the other oxides were also investigated as shown in Figure 4.2. This type of diagram is more appropriate for these rock series which contain variable MgO contents as suggested by Rollinson (1993). In general, MgO variation shows positive correlation against TiO_2 , Al_2O_3 , FeO_t , MnO and P_2O_5 and negative correlation against SiO_2 . However, these chemical variations may indicate important role of differentiation and fractional crystallization processes during the magmatic evolution of porphyritic andesite, and magma related to andesitic tuff and rhyolitic tuff. Consequently, they appear to have been originated from the same magma source. On the other hand, andesite dikes show clearly different compositional trend of major and minor oxides, particularly TiO_2 , CaO , Na_2O and P_2O_5 ; it would indicate different magma source from the former rocks.

Table 4.1 Major oxide (in wt. %), trace and rare earth elements (in ppm) for Q-prospect volcanic rocks

Rock	Porphyritic andesite			Andesitic tuff			Rhyolitic tuff			Andesite dike	
Sample	Q-7	Q-8	Q-13	Q-9	A-38	Q-43	Q-14	Q-17	A-31	Q-6	A-26
SiO ₂	48.53	47.62	51.07	48.55	52.92	53.61	67.10	67.18	67.88	52.32	53.90
TiO ₂	0.56	0.42	0.53	0.53	0.48	0.46	0.32	0.30	0.31	1.18	0.90
Al ₂ O ₃	18.69	15.71	17.07	16.27	16.41	18.28	11.16	14.43	11.54	17.12	16.45
FeOt	10.18	10.33	8.06	8.33	8.82	8.16	4.12	3.74	5.25	8.89	7.45
MnO	0.31	0.23	0.44	0.30	0.46	0.31	0.16	0.07	0.17	0.14	0.15
MgO	5.31	7.89	4.50	9.23	7.34	5.08	1.74	0.95	2.97	3.40	4.31
CaO	0.81	3.58	2.20	0.83	0.23	0.36	3.41	1.05	1.27	6.76	7.48
Na ₂ O	0.30	0.19	0.19	0.20	0.20	0.21	0.16	0.20	0.16	4.32	3.26
K ₂ O	9.45	6.50	10.43	8.55	8.06	10.19	6.47	8.38	7.41	1.52	1.51
P ₂ O ₅	0.12	0.03	0.12	0.11	0.06	0.09	0.10	0.06	0.07	0.30	0.23
LOI	5.19	6.76	4.40	6.12	4.40	3.64	4.06	3.22	2.60	2.24	3.83
Total	99.44	99.26	99.01	99.01	99.40	100.39	98.80	99.59	99.61	98.20	99.47
Sc	33.09	27.59	27.06	29.49	28.55	31.09	18.17	17.59	17.32	22.50	19.01
V	329.40	195.30	183.10	202.70	227.10	233.50	127.90	91.86	145.50	230.30	184.80
Cr	24.27	22.26	27.44	24.74	24.30	22.61	21.27	13.17	27.21	34.87	90.63
Co	26.75	32.05	21.06	28.79	22.15	17.96	11.68	6.31	12.00	23.33	23.41
Ni	11.42	10.95	13.99	13.78	11.96	7.79	8.00	5.66	10.59	18.44	39.42
Cu	83.71	62.95	177.30	46.60	50.79	112.00	18.41	27.53	48.07	100.90	79.61
Zn	44.01	49.01	67.42	57.51	151.90	56.41	24.51	114.40	58.69	40.53	76.80
Ga	18.35	16.99	19.54	17.36	20.07	20.33	12.67	14.32	12.92	21.22	19.81
Rb	148.10	89.63	140.90	108.90	83.64	153.40	94.00	124.50	96.70	22.80	20.71
Sr	138.70	77.21	172.80	95.79	120.00	938.70	62.68	122.40	39.43	638.40	392.20
Y	13.09	16.18	11.36	7.75	3.67	6.78	6.76	14.62	5.32	23.04	17.40
Zr*	37.92	46.93	56.12	25.36	24.24	48.58	30.27	88.38	28.21	151.34	127.33
Nb	0.87	0.88	1.19	0.55	0.58	0.88	0.64	1.76	0.58	4.31	3.17
Cs	1.28	0.18	0.63	0.64	0.33	0.46	0.74	1.50	0.15	0.10	0.13
Ba	5241	1979	1318	3138	5467	2170	941	575	1100	235	304
Hf	0.50	0.62	0.74	0.35	0.31	0.57	0.38	1.31	0.35	1.89	1.65
Ta	0.25	0.24	0.26	0.23	0.24	0.24	0.13	0.20	0.12	0.42	0.43
Pb	1.11	0.98	2.06	9.91	3.08	2.17	1.91	3.10	0.73	4.62	4.15
Th	0.34	0.50	0.53	0.17	0.15	0.42	0.26	1.13	0.24	1.36	1.15
U	0.10	0.12	0.16	0.08	0.06	0.16	0.13	0.71	0.07	0.52	0.42

Table 4.1 Cont'

Rock	Porphyritic andesite			Andesitic tuff			Rhyolitic tuff			Andesite dike	
Sample	Q-7	Q-8	Q-13	Q-9	A-38	Q-43	Q-14	Q-17	A-31	Q-6	A-26
La	3.09	2.93	2.91	1.29	0.73	1.23	3.15	3.57	1.40	12.96	10.91
Ce	7.47	7.41	7.20	3.59	2.01	3.06	7.44	8.67	3.41	31.23	25.95
Pr	1.11	1.12	1.05	0.56	0.32	0.44	1.07	1.18	0.53	4.41	3.61
Nd	5.47	5.69	5.01	3.00	1.62	2.25	5.09	5.49	2.65	20.04	16.06
Sm	1.71	1.92	1.55	1.04	0.54	0.75	1.36	1.56	0.85	4.99	3.84
Eu	1.20	0.89	0.80	1.09	0.74	0.56	0.58	0.43	0.44	1.43	1.17
Gd	2.19	2.47	1.86	1.37	0.68	0.96	1.50	1.88	0.97	5.45	3.94
Tb	0.36	0.42	0.31	0.22	0.11	0.18	0.21	0.35	0.16	0.77	0.58
Dy	2.32	2.79	2.07	1.46	0.79	1.22	1.29	2.60	1.03	4.47	3.34
Ho	0.50	0.60	0.44	0.29	0.17	0.27	0.26	0.60	0.21	0.89	0.65
Er	1.47	1.78	1.39	0.87	0.54	0.89	0.77	2.11	0.68	2.53	1.86
Tm	0.20	0.26	0.20	0.12	0.08	0.13	0.11	0.33	0.11	0.34	0.25
Yb	1.36	1.84	1.44	0.79	0.55	0.98	0.72	2.30	0.70	2.18	1.65
Lu	0.19	0.26	0.22	0.11	0.09	0.16	0.11	0.37	0.11	0.31	0.23

ศูนย์วิทยทรัพยากร
จุฬาลงกรณ์มหาวิทยาลัย

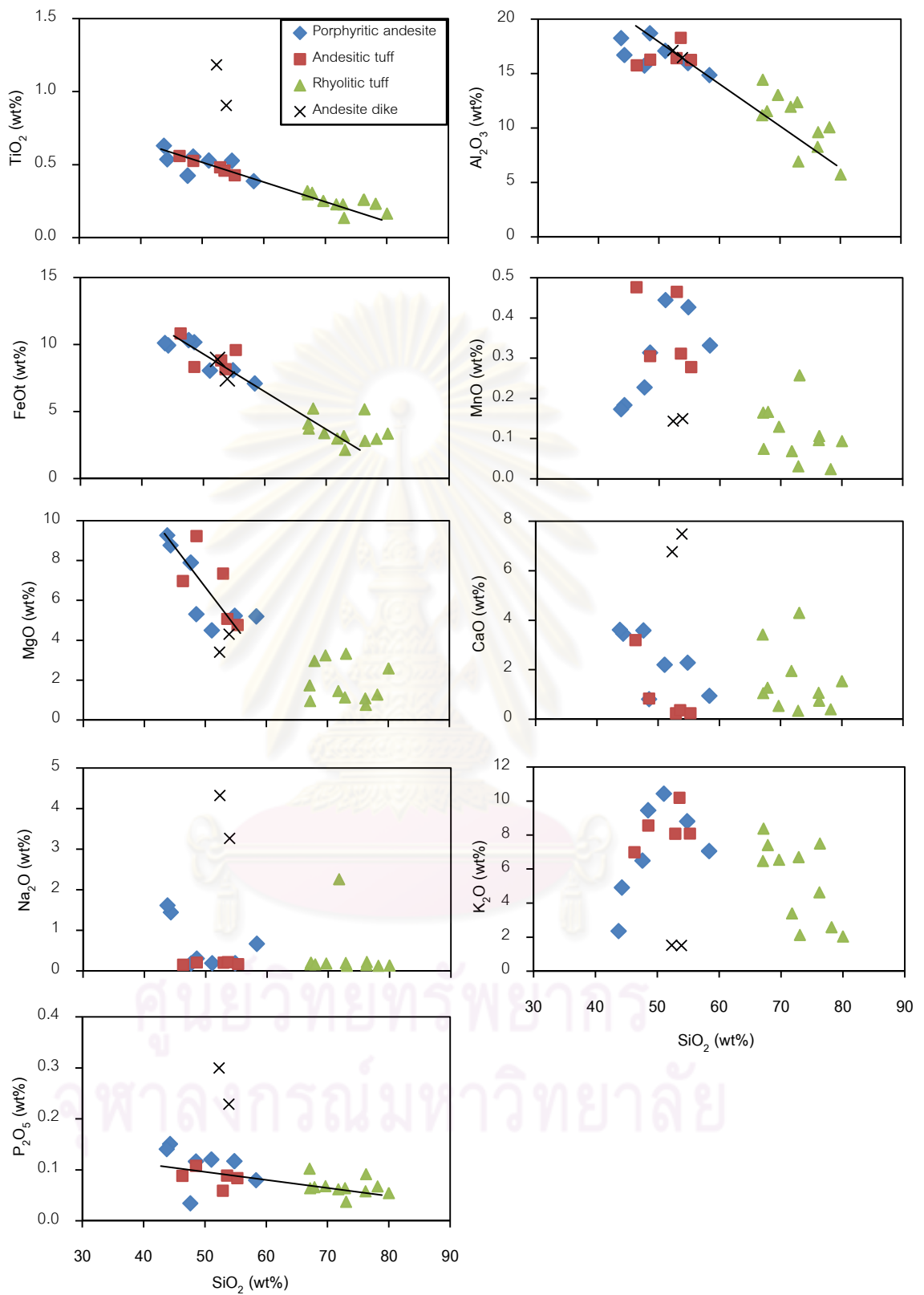


Figure 4.1 Harker-type variation diagrams of major and minor oxides (wt%) versus SiO_2 (wt%) of rock samples from Q-prospect.

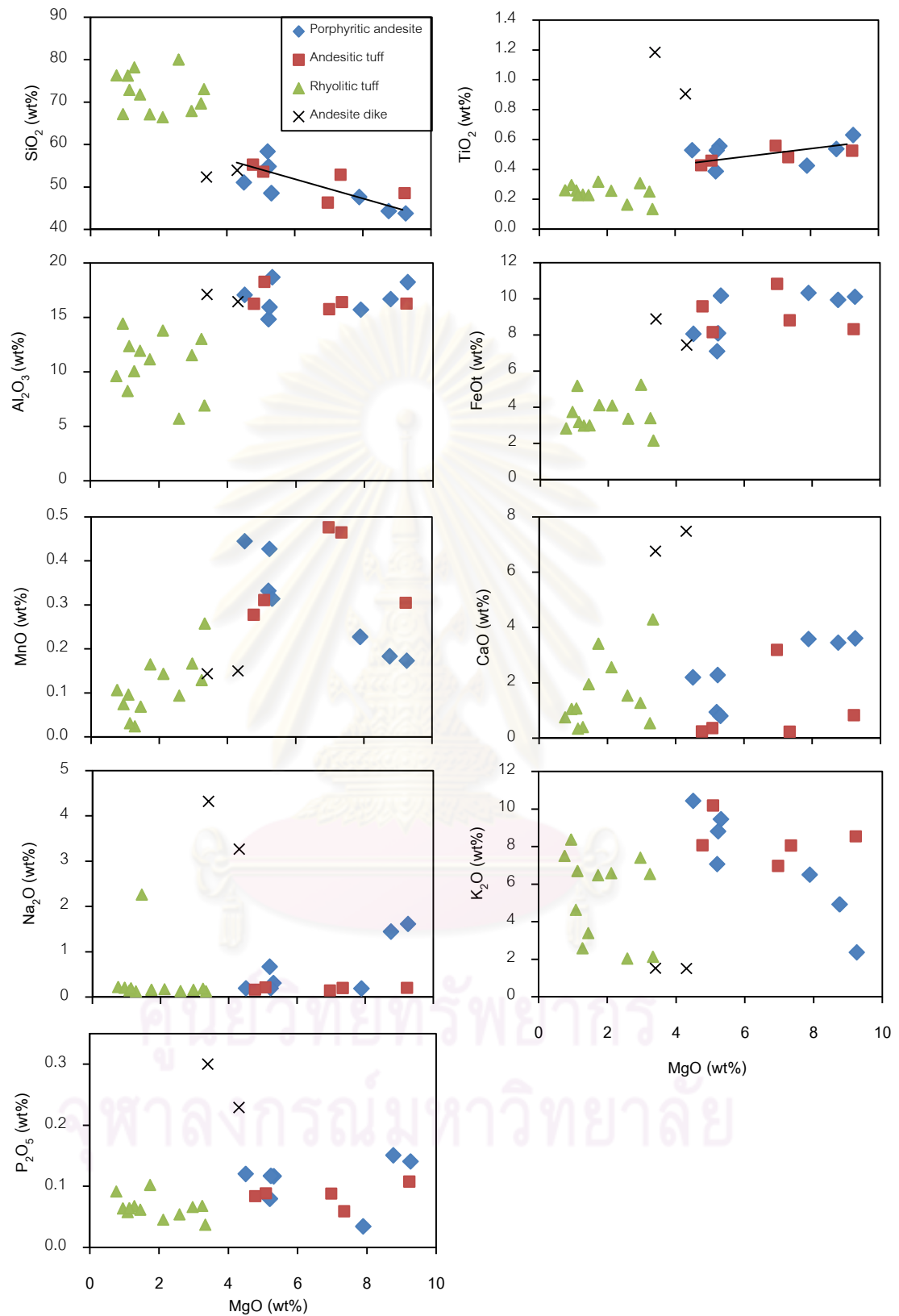


Figure 4.2 Harker-type variation diagrams of major oxides (wt%) versus MgO (wt%) of rock samples in the study area.

4.2.2 Trace Elements and Rare Earth Elements

Trace elements

Representative analyses of trace elements of volcanic samples from Q prospect, Chatree Gold Deposit are summarized in Table 4.1 and all analyses are collected in Appendix C. The detailed description of some crucial elements is given below.

Lithium (Li) values range from 13.56 to 39.68 ppm (av. 23.79 ppm) in porphyritic andesite, 11.27 to 23.66 ppm (av. 18.44 ppm) in andesitic tuff, 6.08 to 15.53 ppm (av. 10.68 ppm) in rhyolitic tuff, and 13.20 to 16.98 ppm (av. 15.09 ppm) in andesite dike.

Beryllium (Be) contents vary from 0.30 to 0.48 ppm (av. 0.39 ppm) in porphyritic andesite, 0.28 to 0.41 ppm (av. 0.33 ppm) in andesitic tuff, 0.14 to 0.43 ppm (av. 0.33 ppm) in rhyolitic tuffs and 0.67 to 1.03 ppm (av. 0.85 ppm) in andesite dike.

Scandium (Sc) ranges from 23.18 to 34.74 ppm (av. 29.12 ppm) in porphyritic andesite, 0.28 to 0.41 ppm (av. 31.53 ppm) in andesitic tuff, 5.31 to 18.69 ppm (av. 13.25 ppm) in rhyolitic tuff, and 19.01 to 22.50 ppm (av. 20.76 ppm) in andesite dike.

Vanadium (V) contents are from 183.10 to 329.40 ppm (av. 234.73 ppm) for porphyritic andesite, 202.70 to 323.80 ppm (av. 242.06 ppm) for andesitic tuff, 25.14 to 157.30 ppm (av. 88.96 ppm) for rhyolitic tuff and 184.80 to 230.30 ppm (av. 207.55 ppm) for andesite dike.

Chromium (Cr) contents range from 20.70 to 32.96 ppm (av. 25.14 ppm) in porphyritic andesites, 22.61 to 28.94 ppm (av. 25.33 ppm) in andesitic tuff, 4.72 to 29.38 ppm (av. 15.18 ppm) in rhyolitic tuff and 34.87 ppm and 90.63 ppm (av. 62.75 ppm) in andesite dike.

Cobalt (Co) values range from 21.06 to 32.05 ppm (av. 26.24 ppm) in porphyritic andesite, 17.96 to 29.71 ppm (av. 24.04 ppm) in andesitic tuff, 3.18 to 14.18 ppm (av. 8.27 ppm) in rhyolitic tuff, and 23.33 to 23.41 ppm (av. 23.37 ppm) in andesite dike.

Nickel (Ni) contents vary from 8.92 to 15.02 ppm (av. 12.63 ppm) in porphyritic andesite, 7.79 to 13.78 ppm (av. 10.67 ppm) in andesitic tuff, 1.70 to 10.59 ppm (av. 5.26 ppm) in rhyolitic tuff and 18.44 to 39.42 ppm (av. 28.93 ppm) in andesite dike.

Copper (Cu) values range from 35.42 to 228.60 ppm (av. 101.56 ppm) in porphyritic andesite, 29.35 to 112.00 ppm (av. 64.27 ppm) in andesitic tuff, 6.49 to 66.37 ppm (av. 29.63 ppm) in rhyolitic tuff, and 79.61 to 100.90 ppm (av. 90.26 ppm) in andesite dike.

Zinc (Zn) ranges from 30.32 to 109.70 ppm (av. 68.90 ppm) in porphyritic andesite, 57.51 to 166.90 ppm (av. 108.90 ppm) in andesitic tuff, 24.51 to 100.20 ppm (av. 52.50 ppm) in rhyolitic tuff, and 40.53 to 76.80 ppm (av. 58.67 ppm) in andesite dike.

Gallium (Ga) values range from 16.34 to 19.54 ppm (av. 17.86 ppm) in porphyritic andesite, 15.28 to 20.33 ppm (av. 18.16 ppm) in andesitic tuff, 7.65 to 14.32 ppm (av. 10.74 ppm) in rhyolitic tuff, and 19.81 to 21.22 ppm (av. 20.52 ppm) in andesite dike.

Rubidium (Rb) contents vary from 41.88 to 148.10 ppm (av. 100.56 ppm) for porphyritic andesite, 83.64 to 153.40 ppm (av. 110.44 ppm) for andesitic tuff, 21.23 to 124.50 ppm (av. 75.84 ppm) for rhyolitic tuff, and 20.71 to 22.80 ppm (av. 21.76 ppm) for andesite dike.

Strontium (Sr) values range from 77.21 to 224.60 ppm (av. 148.20 ppm) in porphyritic andesite, 78.43 to 938.70 ppm (av. 268.42 ppm) in andesitic tuff, 28.71 to 122.40 ppm (av. 67.61 ppm) in rhyolitic tuff, and 392.20 to 638.40 ppm (av. 515.30 ppm) in andesite dike.

Yttrium (Y) contents vary from 8.21 to 16.18 ppm (av. 11.38 ppm) in porphyritic andesite, 3.67 to 7.75 ppm (av. 6.18 ppm) in andesitic tuff, 3.84 to 14.62 ppm (av. 7.05 ppm) in rhyolitic tuff, and 17.40 to 23.04 ppm (av. 20.22 ppm) in andesite dike.

Zircon (Zr) contents range from 28.01 to 56.10 ppm (av. 41.88 ppm) for porphyritic andesite, 24.24 to 48.58 ppm (av. 31.37 ppm) for andesitic tuff, 22.04 to 88.38 ppm (av. 38.79 ppm) for rhyolitic tuff, and 127.33 to 151.34 ppm (av. 139.33 ppm) for andesite dike.

Niobium (Nb) contents are from 0.72 to 1.19 ppm (av. 0.89 ppm) for porphyritic andesite, 0.31 to 0.88 ppm (av. 0.55 ppm) for andesitic tuff, 0.04 to 1.76 ppm (av. 0.72 ppm) for rhyolitic tuff and 3.17 to 4.31 ppm (av. 3.74 ppm) for andesite dike.

Cesium (Cs) contents are from 0.21 to 3.06 ppm (av. 1.04 ppm) in porphyritic andesites, 0.33 to 1.08 ppm (av. 0.67 ppm) in andesitic tuff, 0.13 to 1.92 ppm (av. 0.77 ppm) in rhyolitic tuff and 0.10 ppm and 0.13 ppm (av. 0.12 ppm) in andesite dike.

Barium (Ba) contents range from 64.17 to 5241 ppm (av. 2347 ppm) for porphyritic andesite, 1911 to 6086 ppm (av. 3754 ppm) for andesitic tuff, 269.60 to 1400 ppm (av. 900.83 ppm) for rhyolitic tuff, and 235.30 to 304.20 ppm (av. 269.75 ppm) for andesite dike.

Hafnium (Hf) values range from 0.37 to 0.74 ppm (av. 0.55 ppm) in porphyritic andesite, 0.31 to 0.57 ppm (av. 0.38 ppm) in andesitic tuff, 0.21 to 1.31 ppm (av. 0.49 ppm) in rhyolitic tuff, and 1.65 to 1.89 ppm (av. 1.77 ppm) in andesite dike.

Tantalum (Ta) values narrow range from 0.20 to 0.29 ppm (av. 0.26 ppm) in porphyritic andesite, 0.21 to 0.24 ppm (av. 0.23 ppm) in andesitic tuff, 0.06 to 0.21 ppm (av. 0.13 ppm) in rhyolitic tuff, and 0.42 to 0.43 ppm (av. 0.43 ppm) in andesite dike.

Lead (Pb) contents are from 0.98 to 7.01 ppm (av. 2.37 ppm) for porphyritic andesite, 1.34 to 9.91 ppm (av. 3.72 ppm) for andesitic tuff, 0.73 to 6.09 ppm (av. 2.73 ppm) for rhyolitic tuff and 4.15 to 4.62 ppm (av. 4.38 ppm) for andesite dike.

Thorium (Th) contents range from 0.21 to 0.53 ppm (av. 0.40 ppm) in porphyritic andesites, 0.15 to 0.42 ppm (av. 0.25 ppm) in andesitic tuff, 0.18 to 1.13 ppm (av. 0.45 ppm) in rhyolitic tuff and 1.15 ppm and 1.36 ppm (av. 1.26 ppm) in andesite dikes.

Uranium (U) contents are from 0.09 to 0.23 ppm (av. 0.14 ppm) for porphyritic andesite, 0.06 to 0.31 ppm (av. 0.14 ppm) for andesitic tuff, 0.07 to 0.71 ppm (av. 0.29 ppm) for rhyolitic tuff and 0.42 to 0.52 ppm (av. 0.47 ppm) for andesite dike.



ศูนย์วิทยทรัพยากร
จุฬาลงกรณ์มหาวิทยาลัย

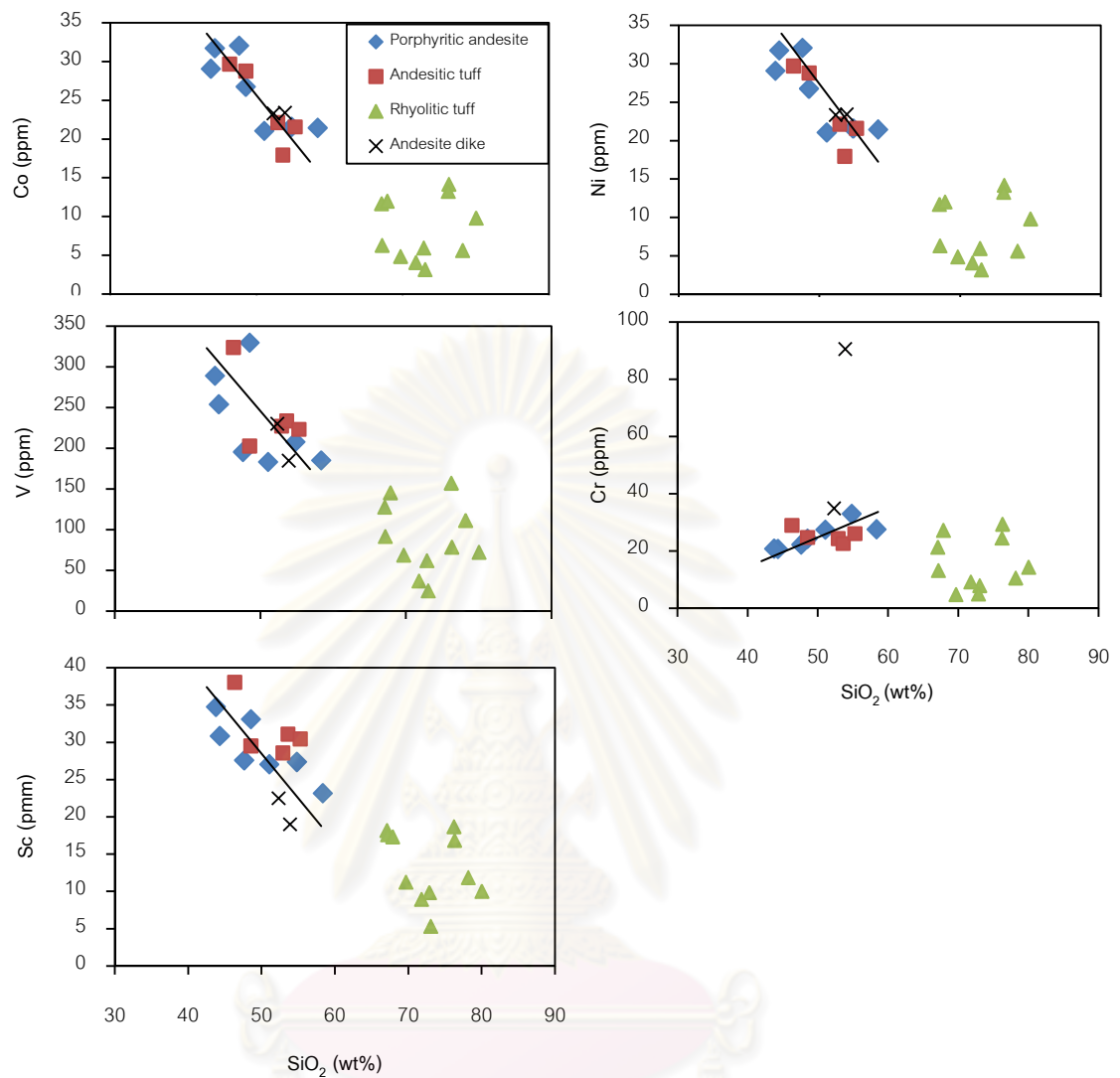


Figure 4.3 Variation diagrams plotting SiO_2 (wt. %) against some trace elements (ppm).

ศูนย์วิจัยทรัพยากรธรณี
จุฬาลงกรณ์มหาวิทยาลัย

Trace elements can be used to identify the geological processes. In general, they can be subdivided into incompatible and compatible elements. The incompatible elements are characterized by two main groups; the low field strength (LFS) group (e.g., Cs, Sr, K, Rb and Ba) are mobile; on the other hand, the high field strength (HFS) elements (e.g., REE, Sc, Y, Th, Zr, Hf, Ti, Nb, Ta and P) are immobile. Compatible elements also include immobile elements (e.g., Co, Ni, V and Cr) and mobile elements (e.g., Mn, Zn and Cu). Middlemost (1985) suggests that Sc, V, Cr, Co and Ni are usually concentrated in the ferromagnesian minerals instead of magma. Consequently, these elements are usually low concentrations in andesitic rocks which have been originated from differentiated magmas. In addition, the variation diagrams of SiO_2 versus trace elements can be used to investigate differentiation, fractional crystallization and other processes involved in the magmatic evolution (Figure 4.3). As a result, plots show negative correlation between SiO_2 versus Co, Ni, Sc and V. These elements appear to decrease in more felsic composition.

Figures 4.4 to 4.7 show MORB (Pearce, 1983) normalized incompatible element patterns of the Q-prospect volcanic, pyroclastic and dike rocks. These rocks are characterized by enrichments of LFS (e.g., Sr, K, Rb, Ba and Th) and depletion of HFS (e.g., Ta, Nb, Nb, Ce, P, Zr, Hf, Sm, Ti and Y) that indicated to island-arc environment (Pearce, 1982). Spider patterns between host rocks (e.g., prophyritic andesite, andesitic tuff and rhyolitic tuff) and andesite dike are obviously different; patterns of andesite dike show Ce, P and Sm enrichment related to calc-alkaline series whereas the host rocks are close to tholeiitic series (Hawkesworth and Powell, 1980 cited in Wilson, 1989).

The primitive mantle (composition by McDonough et al., 1992) normalized trace element patterns of the Q-prospect volcanic, pyroclastic and dike rocks are shown in Figures 4.8 to 4.11. These spider diagrams mark spikes clearly at Ba, K, Sr and slightly at U with a pronounced trough at Nb. These features may indicate that these rocks were formed by island-arc as suggested by Wilson (1989).

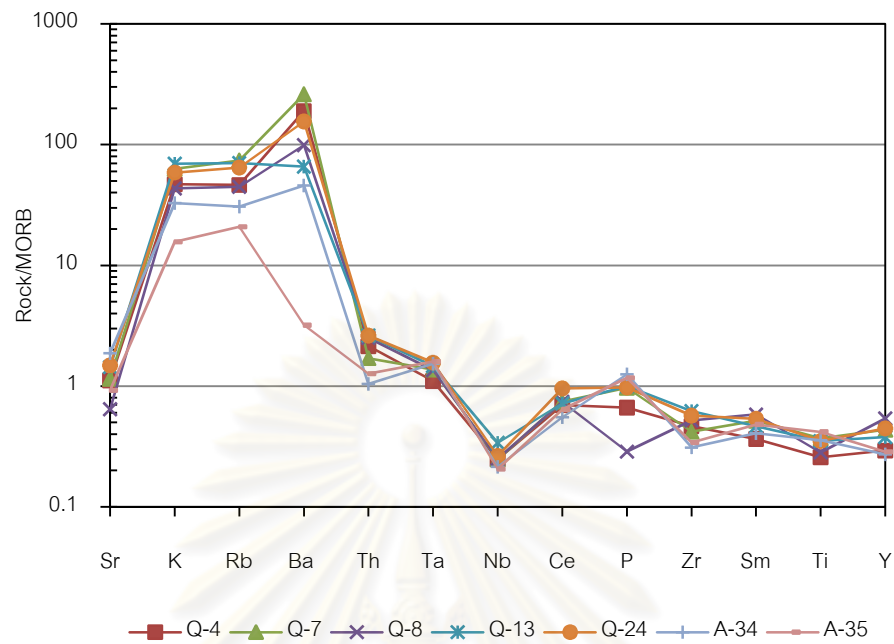


Figure 4.4 MORB normalized incompatible element patterns of porphyritic andesites from Q-prospect. The MORB values are from Pearce (1983).

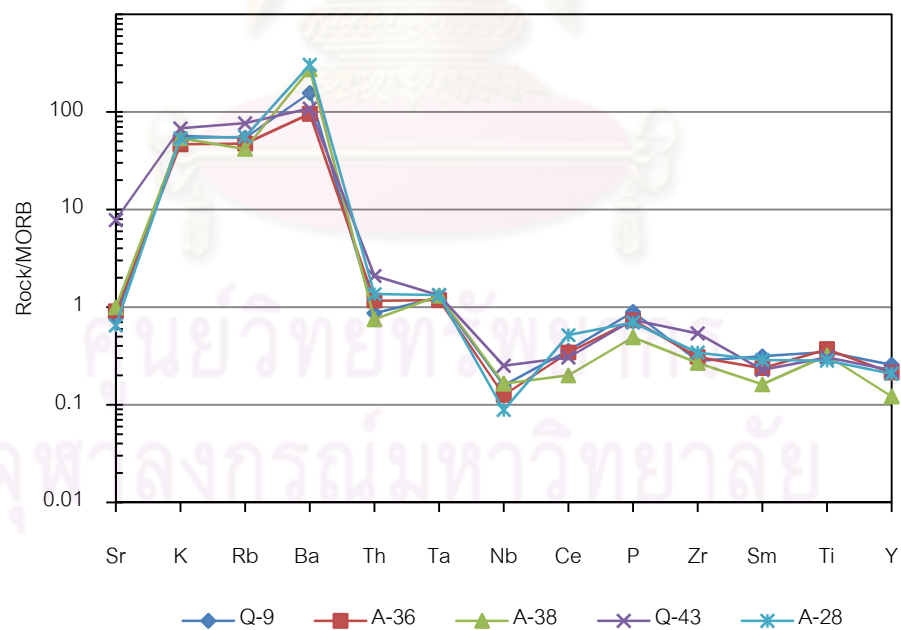


Figure 4.5 MORB normalized incompatible element patterns of andesitic tuffs from Q-prospect. The MORB values are from Pearce (1983).

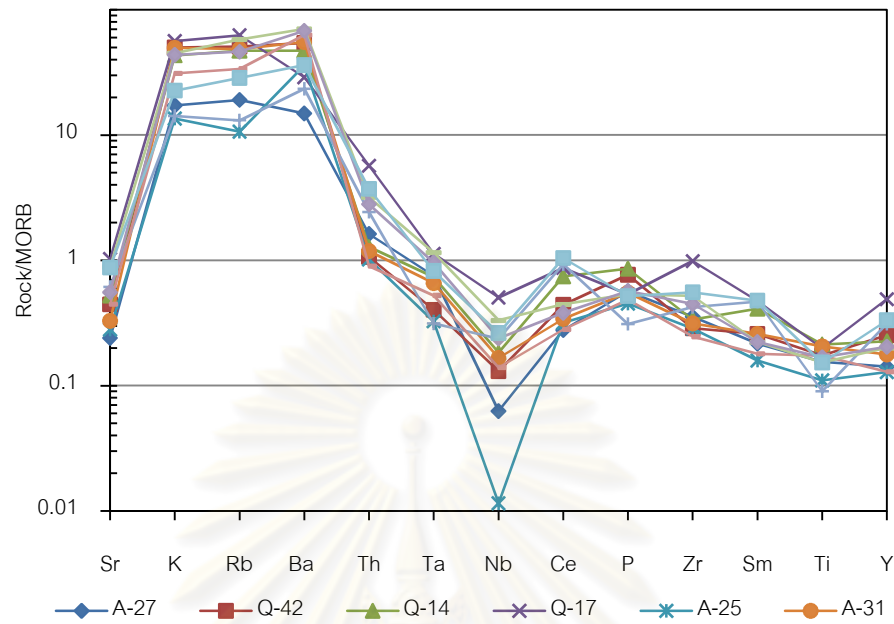


Figure 4.6 MORB normalized incompatible element patterns of rhyolitic tuffs from Q-prospect. The MORB values are from Pearce (1983).

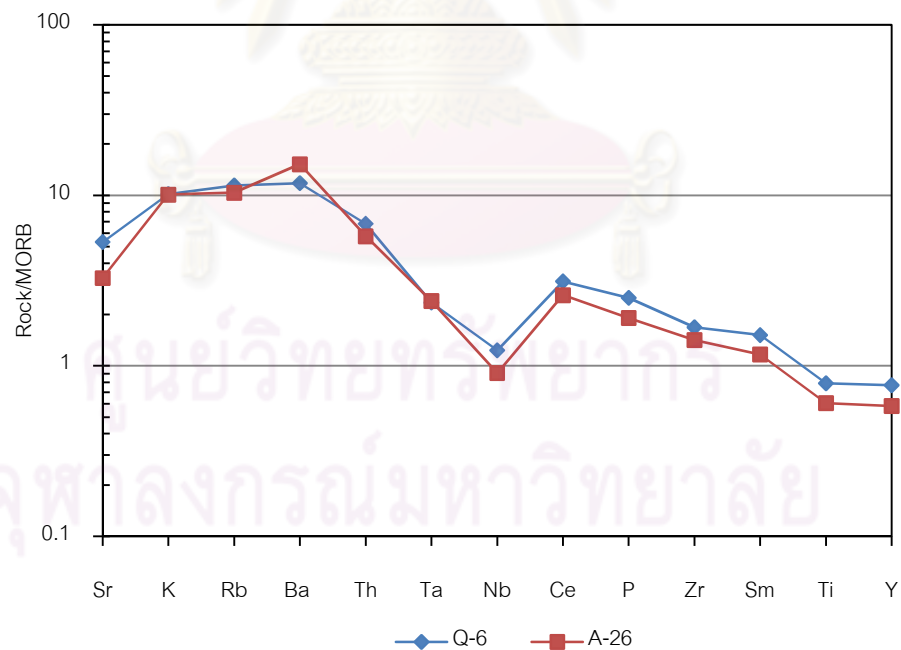


Figure 4.7 MORB normalized incompatible element patterns of andesite dikes from Q-prospect area. The MORB values are from Pearce (1983).

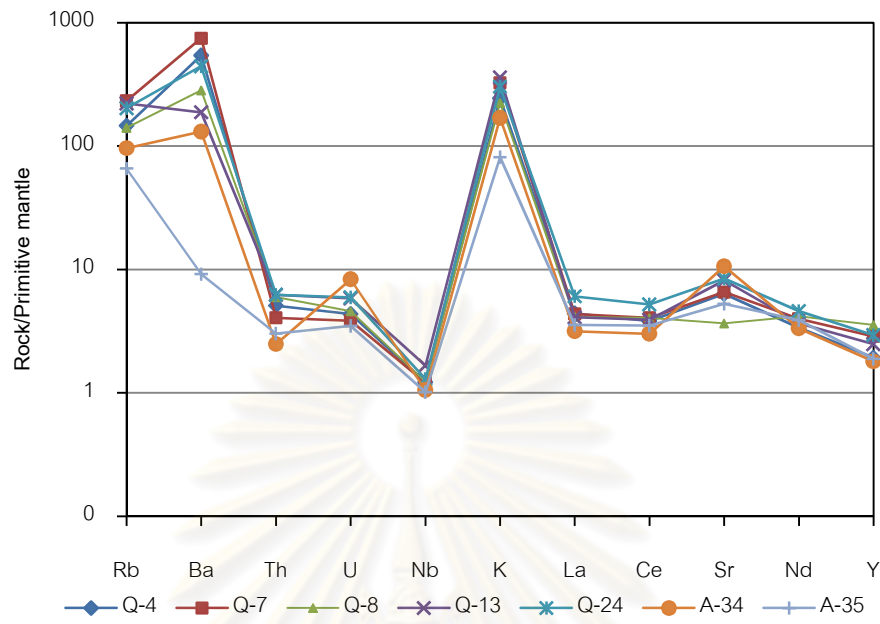


Figure 4.8 Primitive mantle (McDonough et al., 1992) normalized incompatible element patterns of porphyritic andesites from Q-prospect area.

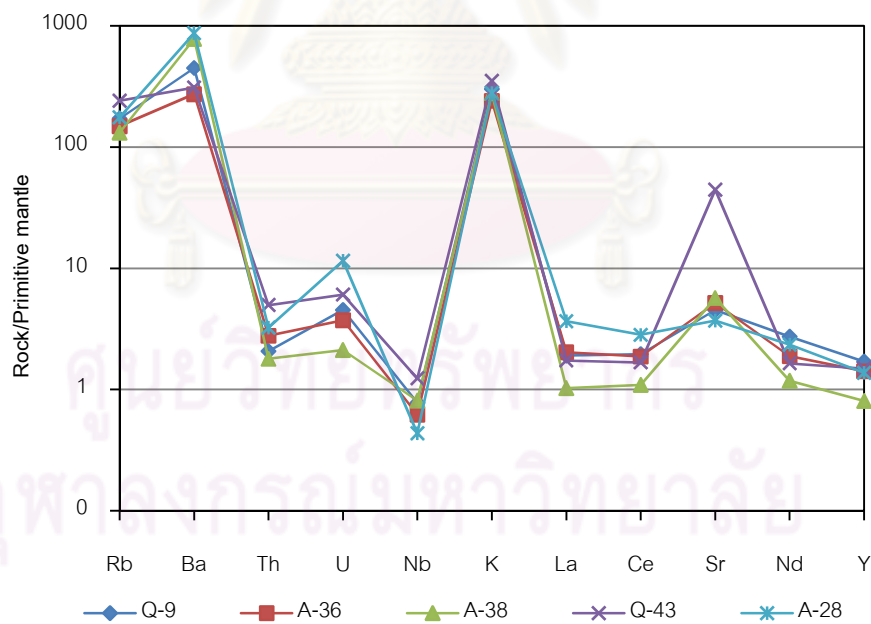


Figure 4.9 Primitive mantle (McDonough et al., 1992) normalized incompatible element patterns of andesitic tuff from Q-prospect area.

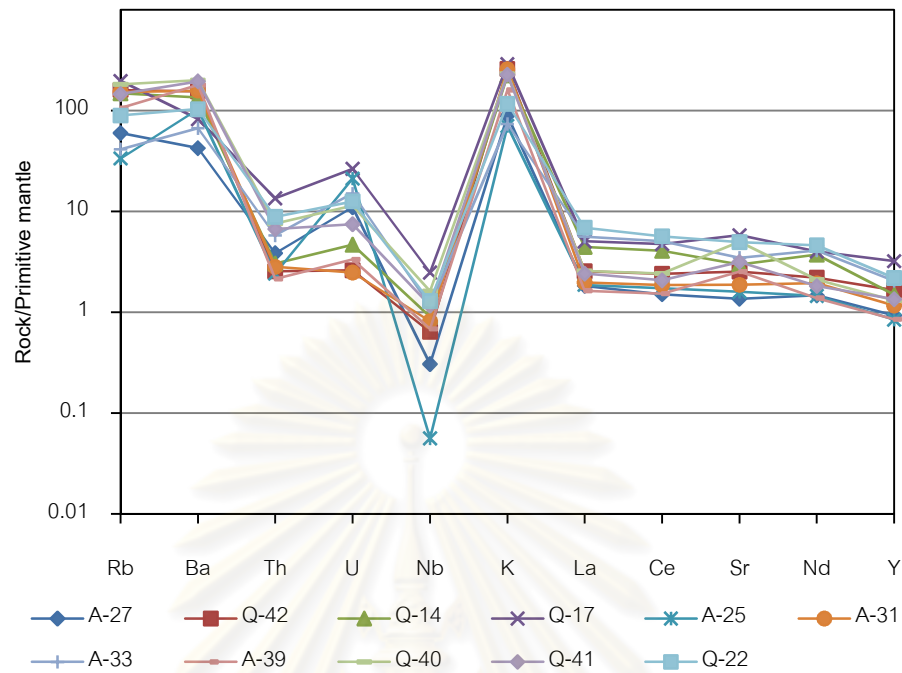


Figure 4.10 Primitive mantle (McDonough et al., 1992) normalized incompatible element patterns for rhyolitic tuff from Q-prospect area.

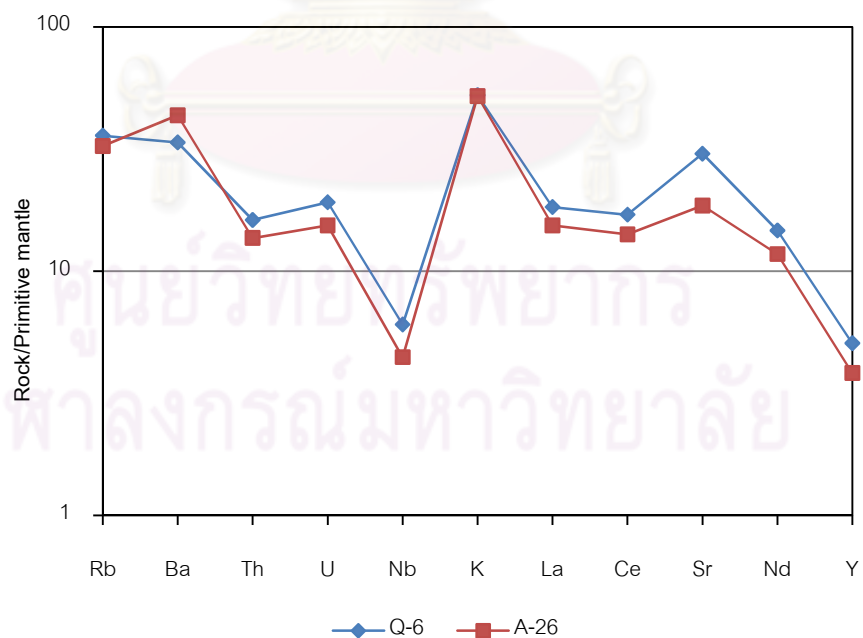


Figure 4.11 Primitive mantle (McDonough et al., 1992) normalized incompatible element patterns for andesite dike from Q-prospect area.

Rare earth elements

Rare earth elements (REE) of samples are selectively present in Table 4.1 and mostly collected in Appendix C. The detailed description of some elements is given below.

Lanthanum (La) values range from 2.25 to 4.31 ppm (av. 3.02 ppm) in porphyritic andesite, 0.73 to 2.60 ppm (av. 1.46 ppm) in andesitic tuff, 1.16 to 4.90 ppm (av. 2.37 ppm) in rhyolitic tuff, and 10.91 to 12.96 ppm (av. 11.94 ppm) in andesite dike.

Cerium (Ce) ranges from 5.54 to 9.58 ppm (av. 7.23 ppm) in porphyritic andesite, 2.01 to 5.19 ppm (av. 3.46 ppm) in andesitic tuff, 2.77 to 10.40 ppm (av. 5.50 ppm) in rhyolitic tuff, and 25.95 to 31.23 ppm (av. 28.59 ppm) in andesite dike.

Praseodymium (Pr) values range from 0.84 to 1.31 ppm (av. 1.06 ppm) in porphyritic andesite, 0.32 to 0.69 ppm (av. 0.50 ppm) in andesitic tuff, 0.38 to 1.40 ppm (av. 0.76 ppm) in rhyolitic tuff, and 3.61 to 4.41 ppm (av. 4.01 ppm) in andesite dike.

Neodymium (Nd) contents vary from 4.57 to 6.29 ppm (av. 5.28 ppm) for porphyritic andesite, 1.62 to 3.21 ppm (av. 2.53 ppm) for andesitic tuff, 1.89 to 6.31 ppm (av. 3.58 ppm) for rhyolitic tuff, and 16.06 to 20.04 ppm (av. 18.05 ppm) for andesite dike.

Samarium (Sm) values range from 1.21 to 1.92 ppm (av. 1.59 ppm) in porphyritic andesite, 0.54 to 1.04 ppm (av. 0.81 ppm) in andesitic tuff, 0.52 to 1.57 ppm (av. 1.00 ppm) in rhyolitic tuff, and 3.84 to 4.99 ppm (av. 4.41 ppm) in andesite dike.

Europium (Eu) contents range from 0.53 to 1.20 ppm (av. 0.85 ppm) in porphyritic andesites, 0.56 to 1.09 ppm (av. 0.79 ppm) in andesitic tuff, 0.27 to 0.61 ppm (av. 0.46 ppm) in rhyolitic tuff and 1.17 ppm and 1.43 ppm (av. 1.30 ppm) in andesite dikes.

Gadolinium (Gd) contents are from 1.43 to 2.47 ppm (av. 1.93 ppm) for porphyritic andesite, 0.68 to 1.37 ppm (av. 1.05 ppm) for andesitic tuff, 0.61 to 1.88 ppm (av. 1.16 ppm) for rhyolitic tuff and 3.94 to 5.45 ppm (av. 4.69 ppm) for andesite dike.

Terbium (Tb) values range from 0.23 to 0.42 ppm (av. 0.31 ppm) in porphyritic andesite, 0.11 to 0.22 ppm (av. 0.17 ppm) in andesitic tuff, 0.08 to 0.35 ppm (av. 0.18 ppm) in rhyolitic tuff, and 0.58 to 0.77 ppm (av. 0.68 ppm) in andesite dike.

Dysprosium (Dy) ranges from 1.50 to 2.79 ppm (av. 2.02 ppm) in porphyritic andesite, 0.79 to 1.46 ppm (av. 1.18 ppm) in andesitic tuff, 0.66 to 2.60 ppm (av. 1.24 ppm) in rhyolitic tuff, and 3.34 to 4.47 ppm (av. 3.90 ppm) in andesite dike.

Holmium (Ho) contents vary from 0.32 to 0.60 ppm (av. 0.43 ppm) for porphyritic andesite, 0.17 to 0.29 ppm (av. 0.25 ppm) for andesitic tuff, 0.14 to 0.60 ppm (av. 0.27 ppm) for rhyolitic tuff, and 0.65 to 0.89 ppm (av. 0.77 ppm) for andesite dike.

Erbium (Er) contents range from 0.95 to 1.78 ppm (av. 1.30 ppm) in porphyritic andesites, 0.54 to 0.89 ppm (av. 0.77 ppm) in andesitic tuff, 0.46 to 2.11 ppm (av. 0.88 ppm) in rhyolitic tuff and 1.86 ppm and 2.53 ppm (av. 2.20 ppm) in andesite dikes.

Thulium (Tm) values narrow range from 0.14 to 0.26 ppm (av. 0.19 ppm) in porphyritic andesite, 0.08 to 0.13 ppm (av. 0.11 ppm) in andesitic tuff, 0.06 to 0.33 ppm (av. 0.13 ppm) in rhyolitic tuff, and 0.25 to 0.34 ppm (av. 0.29 ppm) in andesite dike.

Ytterbium (Yb) contents are from 0.98 to 1.84 ppm (av. 1.32 ppm) for porphyritic andesite, 0.55 to 0.98 ppm (av. 0.78 ppm) for andesitic tuff, 0.44 to 2.30 ppm (av. 0.93 ppm) for rhyolitic tuff and 1.65 to 2.18 ppm (av. 1.92 ppm) for andesite dike.

Lutetium (Lu) values range from 0.16 to 0.26 ppm (av. 0.20 ppm) in porphyritic andesite, 0.09 to 0.16 ppm (av. 0.12 ppm) in andesitic tuff, 0.06 to 0.37 ppm (av. 0.14 ppm) in rhyolitic tuff, and 0.23 to 0.31 ppm (av. 0.27 ppm) in andesite dike.

The whole series of REE are relatively immobile during weathering, hydrothermal alteration and low-grade metamorphic (Rollinson, 1993). The REE analyses are normalized by composition of chondrite (reported by Boynton, 1984) prior to plotting. The chondrite-normalized REE patterns of all rock types are present in Figures 4.12 to 4.15. The patterns of porphyritic andesite and rhyolitic tuff show gentle

slopes that indicate high degrees of partial melting >20% (compared to those reported by Rollinson, 1993) and have LREE fractionated patterns with average $(La/Yb)_N$ ratios of about 1.58 and 1.79, respectively (Figures 4.12 and 4.14). The andesitic tuff presents almost flat patterns with an average $(La/Yb)_N$ ratio of 1.25 (Figure 4.13). In addition, most of the patterns show similarly high positive Eu anomalies (Figures 4.12 to 4.14). On the other hand, patterns of andesite dikes show significantly LREE enrichment, that may indicate low degree of partial melting (Rollinson, 1993), yielding an average $(La/Yb)_N$ ratio of about 4.23 with low negative Eu anomalies (Figure 4.15).

Moreover, the different magma series, based on REE patterns, are characterized by slope of REE patterns, such as; the tholeiitic basalts typically have light-REE depleted patterns, whereas the calc-alkaline basalts are light-REE enriched (Wilson, 1989). These characteristic suggest that the porphyric andesite, andesitic tuff and rhyolitic tuff may have been generated from tholeiitic magma series, whereas andesite dike was formed from calc-alkaline magma.

The Eu^{+2} compatible in feldspar (Rollinson, 1993) are liberated by hydrothermal alteration to sericite or chlorite whereas incompatible trivalent REE remain relatively immobile (Giffkins et. al, 2005). This information confirms different magma source of the late stage andesite dike. On the other hand, all previous volcanic and pyroclastic rocks seem to have similar magma source which appear to have undertaken fractionation crystallization and magma differentiation processes.

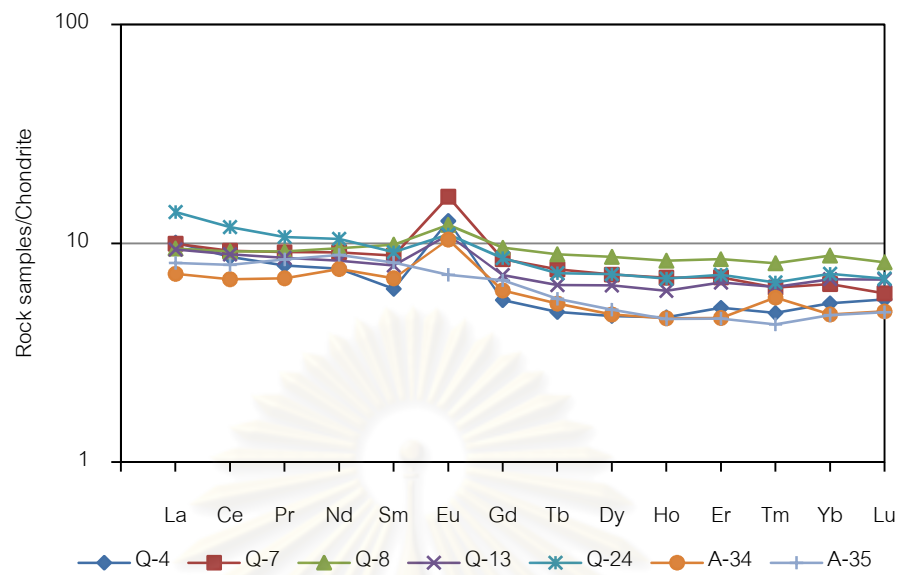


Figure 4.12 Chondrite normalized REE patterns of samples from porphyritic andesite rocks. The chondrite compositions are from Boynton (1984).

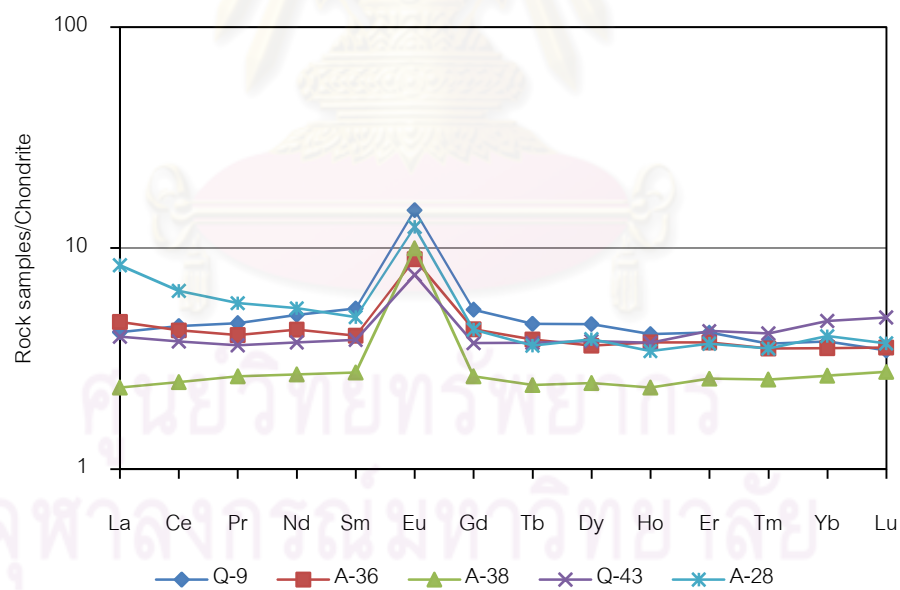


Figure 4.13 Chondrite normalized REE patterns of samples from andesitic tuff. The chondrite compositions are from Boynton (1984).

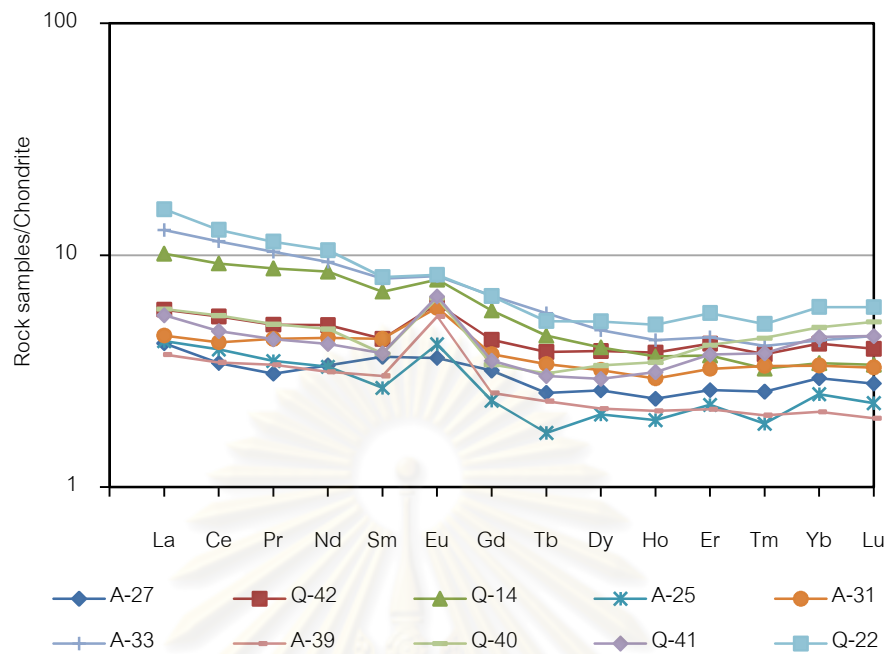


Figure 4.14 Chondrite normalized REE patterns of samples from rhyoritic tuff. The chondrite compositions are from Boynton (1984).

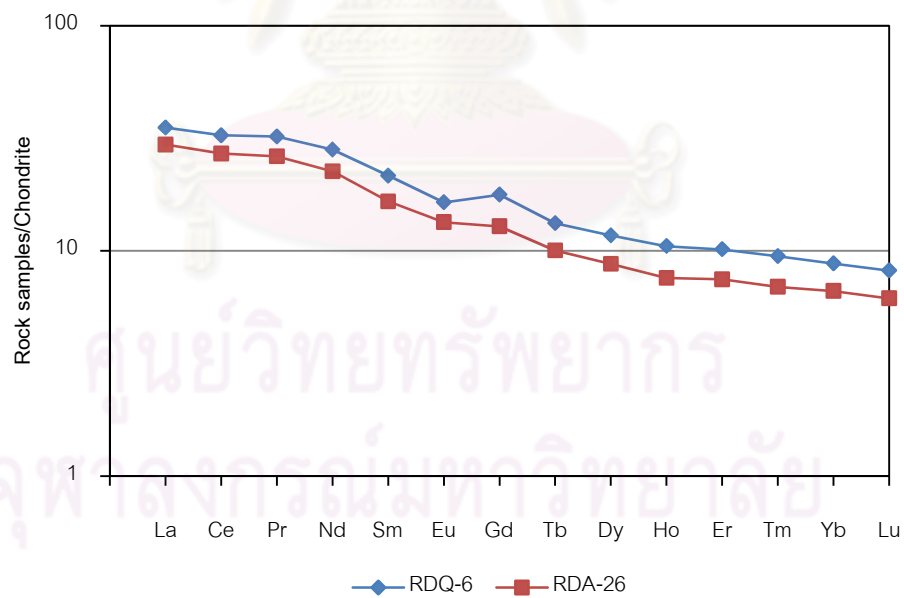


Figure 4.15 Chondrite normalized REE patterns of samples from andesite dike. The chondrite compositions are from Boynton (1984).

4.3 Rock Classification

Total alkali-silica diagram (TAS) is one of the most useful classification schemes available for volcanic rocks but the Chatree volcanic and pyroclastic rocks have very high K_2O contents (see Table 4.1) that would be a result of alteration. Figure 4.16 shows total alkalis-silica (TAS) diagram (Le Bas et al., 1986) which can yield unclearly nomenclature of these rock samples because the alkalis are likely to have been mobilized during weathering, alteration and metamorphism. Therefore, alternative diagram suggested by Winchester and Floyd (1977) is used; it is plotting between Zr/TiO_2 and SiO_2 (Figure 4.17). In this case, porphyritic andesites fall within andesite and sub-alkaline andesitic basalt (Sub-AB) fields; andesitic tuffs are classified as andesite and sub-alkaline andesitic basalt fields; rhyolitic tuffs are located within rhyolite and rhyodacite/dacite fields; late stage andesite dikes are classified as andesite and sub-alkaline andesitic basalt fields.

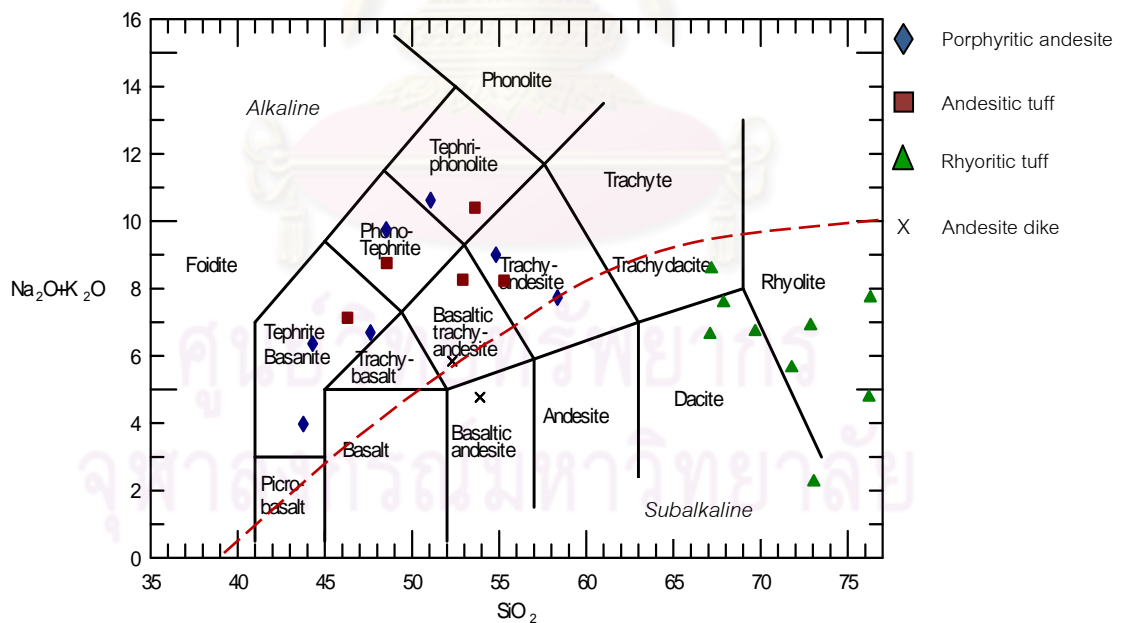


Figure 4.16 Total alkalis silica (TAS) diagram (Le Bas et al., 1986) for volcanic and pyroclastic rocks from Q-prospect area. The subdivision of volcanic rocks into alkaline and subalkaline (tholeiitic) was made from data of Irvine and Baragar (1971).

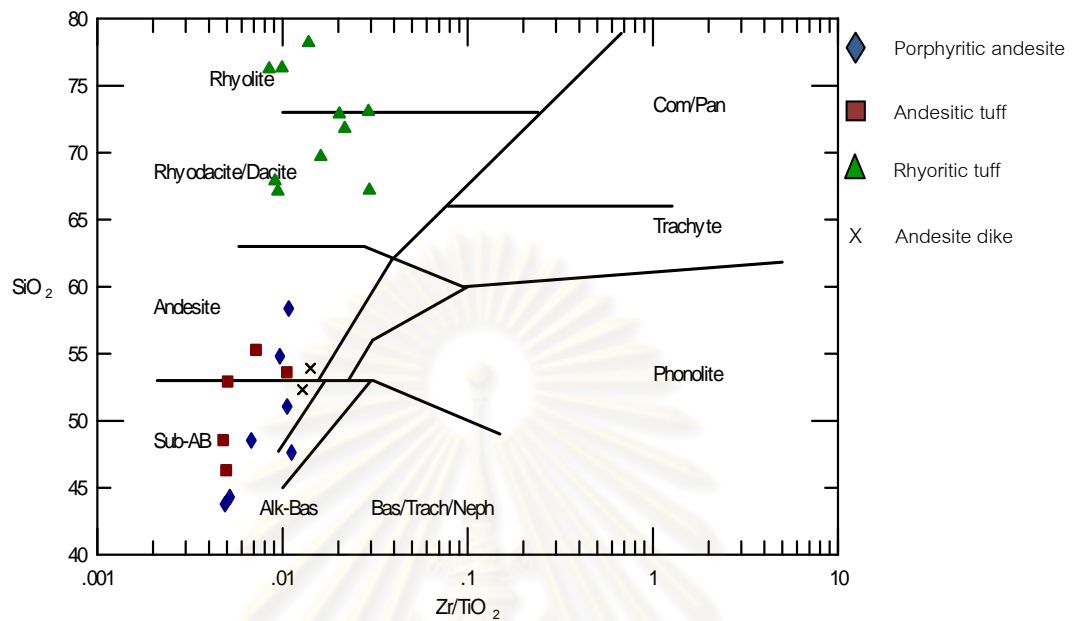


Figure 4.17 Rock classification plots of Zr/TiO_2 versus SiO_2 (Winchester and Floyd, 1977) for volcanic and pyroclastic rocks from Q-prospect.

ศูนย์วิทยทรัพยากร
จุฬาลงกรณ์มหาวิทยาลัย

CHAPTER V

DISCUSSIONS

Discussion will be focused into two main topics including (1) petrogenesis and (2) tectonic setting. Details of both aspects are described below.

5.1 Petrogenesis

Petrographic features indicate that the volcanic rocks in Q-prospect of the Chatree gold deposit are characterized by aphanitic and porphyritic textures which clearly indicate violent eruptions that may have been taken place more than one stage. On the other hand, late stage andesite dike is significantly characterized by plagioclase enclosing clinopyroxene crystals, called as subophitic texture which is a characteristic of shallow intrusive. These volcanic rocks can be distinguished, based on geochemistry, mostly as alkaline, except rhyolitic tuff is clearly related to sub-alkaline series using a diagram of Irvine and Baragar (1971) (Figure 4.16). Moreover, AFM diagram proposed by Irvine and Baragar (1971) is used additionally to differentiate these magma series. As the result, these volcanic rocks are mostly plotted on the calc-alkaline series (Figure 5.1). However, both diagrams are constructed from major oxides, particularly alkali contents which seem to have been modified by late alteration process.

Alternatively, Zr versus P_2O_5 diagram shows all the rock samples are plotted in the field of tholeiitic basalt (Figure 5.2). In addition, Y-Zr diagram (MacLean and Barrett, 1993) shows all samples of porphyritic andesite, andesitic tuff and rhyolitic tuff are related to tholeiitic magma series whereas samples of andesite dike are characterized by transitional and calc-alkaline magma series (Figure 5.3).

Low contents of Ni, Cr and Co indicate that these rocks appear to have originated from evolved derivative magma that is indirect from the primitive mantle

(Green, 1980). MORB-normalized trace elements (see Figures 4.4 to 4.7) and REE chondrite-normalized patterns (see Figures 4.12 to 4.15) show that all the studied samples are slightly depleted flat patterns. They suggest that the Q-prospect volcanic and related rocks may have derived from a similar source of a depleted mantle. However, LFS enrichment may be involved by metasomatic modification between the depleted mantle and subduction-derived fluids.

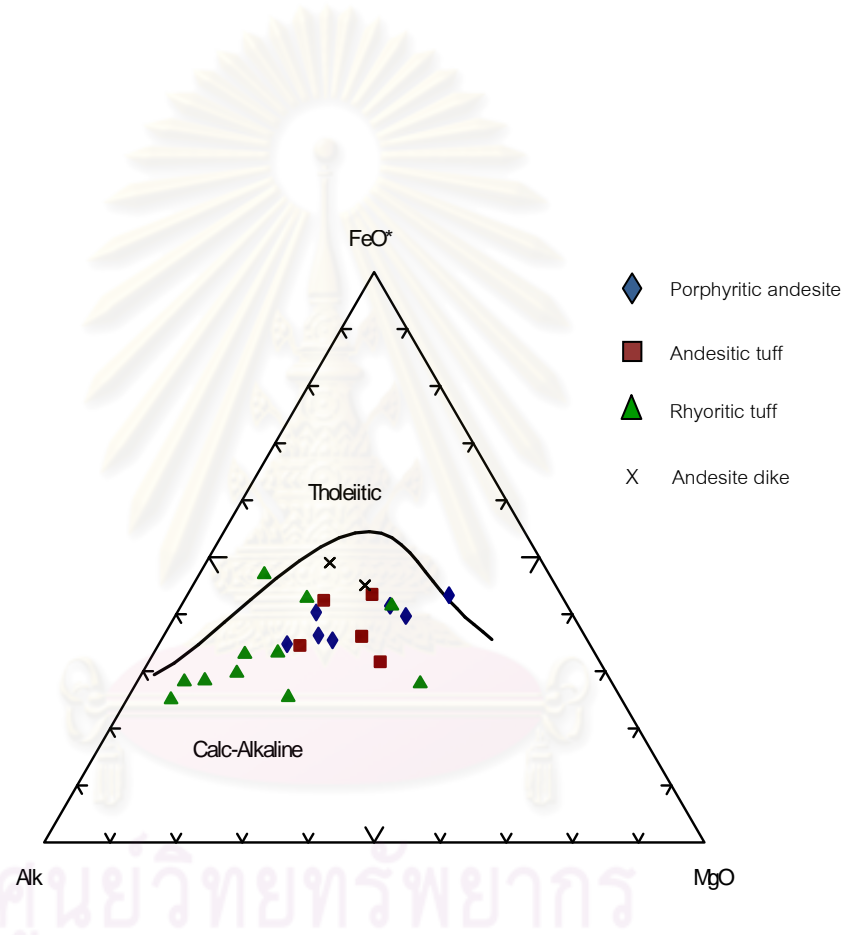


Figure 5.1 AFM diagram with a boundary line separating fields of tholeiitic and calc-alkaline (Irvine and Baragar, 1971). Most volcanic and related rocks from Q-prospect plots fall within the calc-alkaline field.

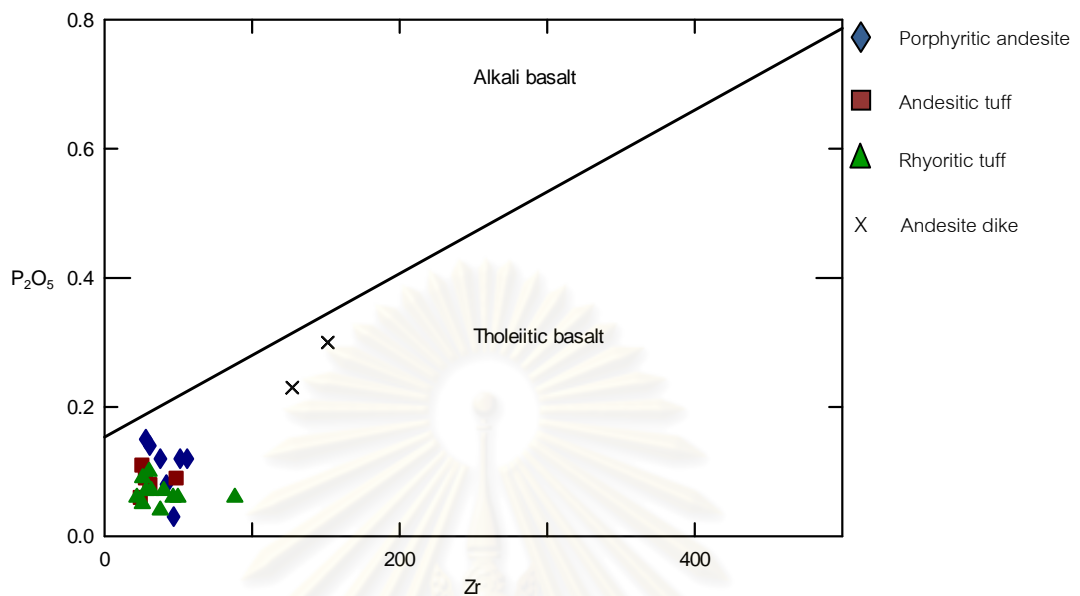


Figure 5.2 Zr versus P_2O_5 variation diagram after Winchester and Floyd (1976) for the discrimination between precursors of alkali basalt and tholeiitic character (sub-alkaline). All volcanic and related rocks of Q-prospect are plotted in tholeiitic basalt.

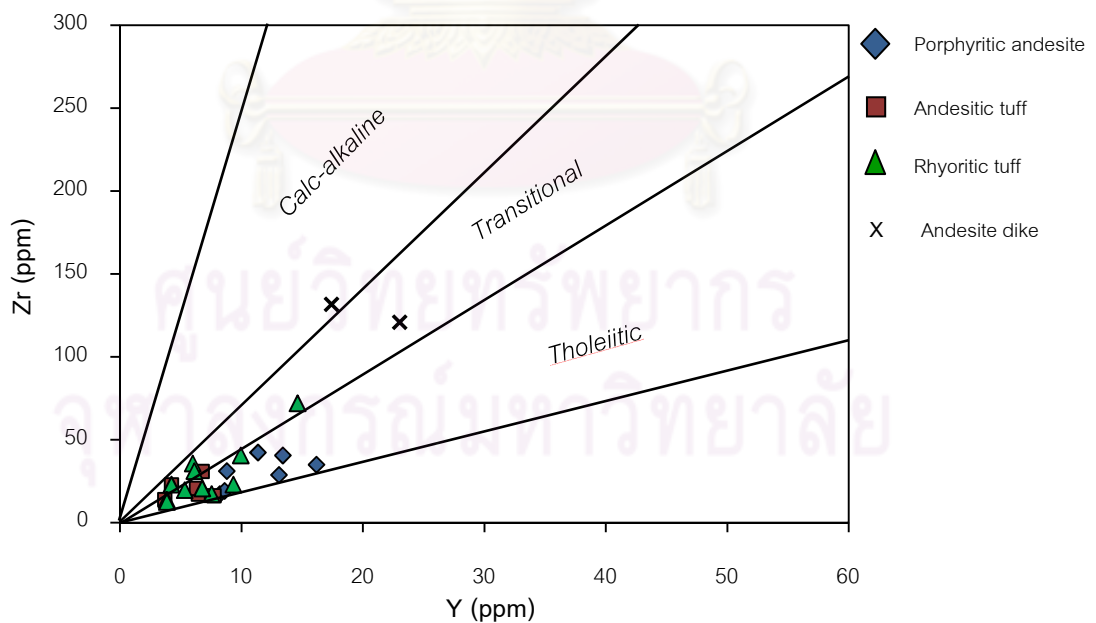


Figure 5.3 Y-Zr discrimination diagram showing volcanic and related rocks from Q-prospect falling within both areas of tholeiitic and calc-alkaline/transitional (fields after MacLean and Barrett, 1993).

5.2 Tectonic Setting

Many tectono-diagrams have been used for rock samples. Trace elements in particular are used to reconstruct the former tectonic environment. Th-Zr-Nb diagram (Wood, 1980), using immobile high field strength elements, is applied; consequently, Q-prospect rock samples as appear to be related to volcanic-arc basalt (Figure 5.4). Moreover, the La-Y-Nb triangular diagram (Cabanis and Lecolle, 1989; see Figure 5.5) and Ti-Zr variation diagram (after Pearce and Cann, 1973; see Figure 5.6) can also separate tectonic setting of these volcanic rocks as island-arc tholeiite for porphyritic andesite, andesitic tuff and rhyolitic tuff and as volcanic-arc calc-alkaline for andesite dike.

La/Yb versus Sc/Ni diagram which distinguishes different types of volcanic arc andesite (Bailey, 1981) indicates that these rocks occurred in oceanic-arc and continental-arc (Figure 5.7). Nb/Yb versus Th/Yb diagram (after Dunphy and Ludden, 1998) suggests that porphyritic andesite, andesitic tuff and rhyolitic tuff may have originated in oceanic island-arc environment whereas the andesite dikes may have originated in continental volcanic-arc (Figure 5.8).

All the results mentioned above clearly suggest that the Q-prospect volcanic and related rocks appear to have originated within a subduction environment. All the host rocks (i.e., porphyritic andesite, andesitic tuff and rhyolitic tuff) would erupt in an island-arc volcanism as a result of oceanic-oceanic convergence, whereas the late stage andesite dikes may have occurred in an arc volcanism.

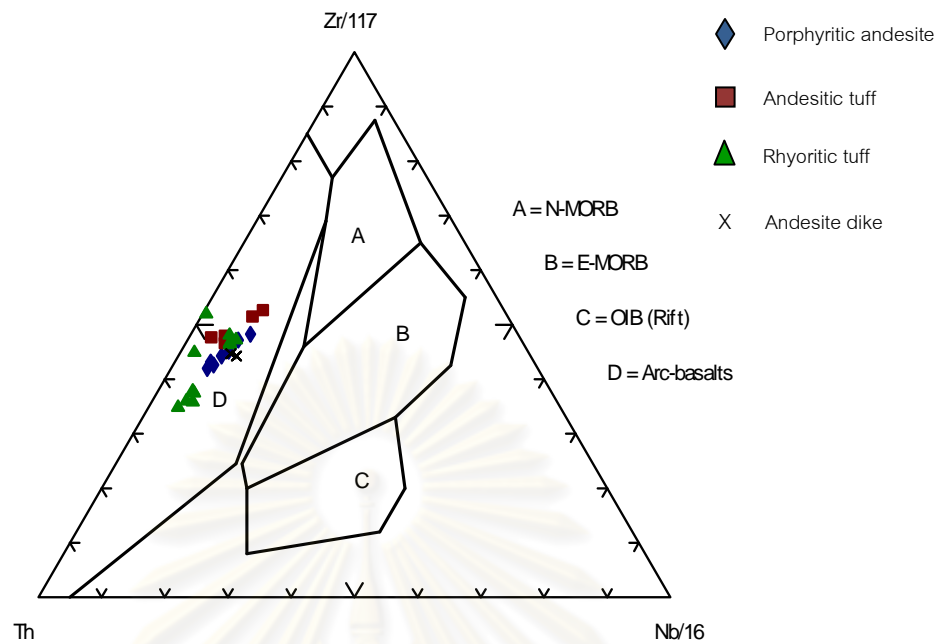


Figure 5.4 Plots of Th-Zr-Nb in triangular diagram (Wood 1980) for Q-prospect rock samples indicating volcanic arc basalts.

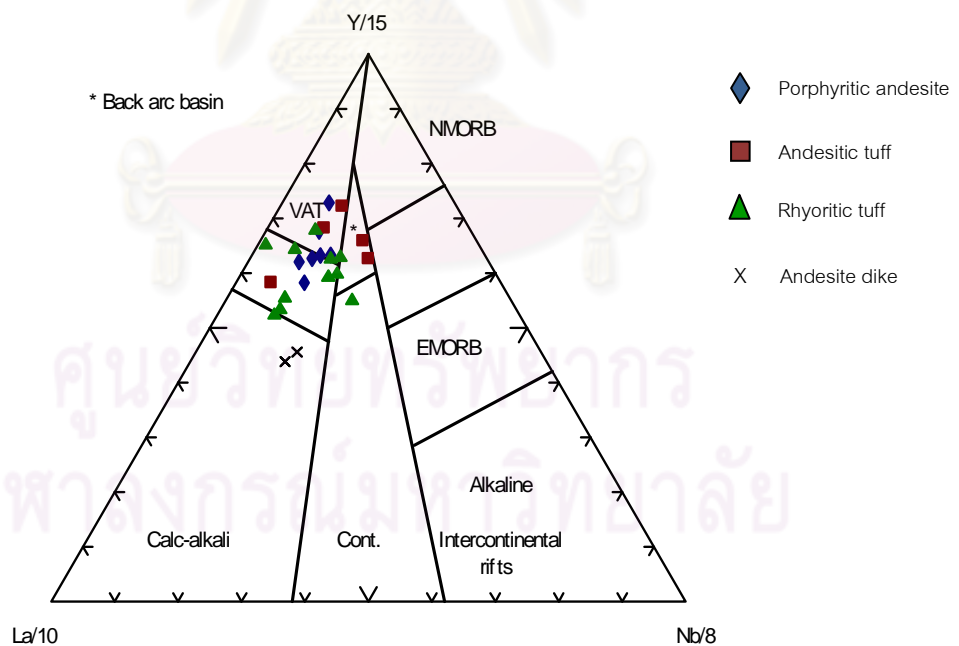


Figure 5.5 La-Y-Nb diagram (Cabanis and Lecolle, 1989) showing the porphyritic andesite, andesitic tuff and rhyolitic tuff plotted in volcanic arc tholeiite (VAT) and overlapping area of VAT and calc-alkali; andesite dikes are plotted in volcanic arc calc-alkali.

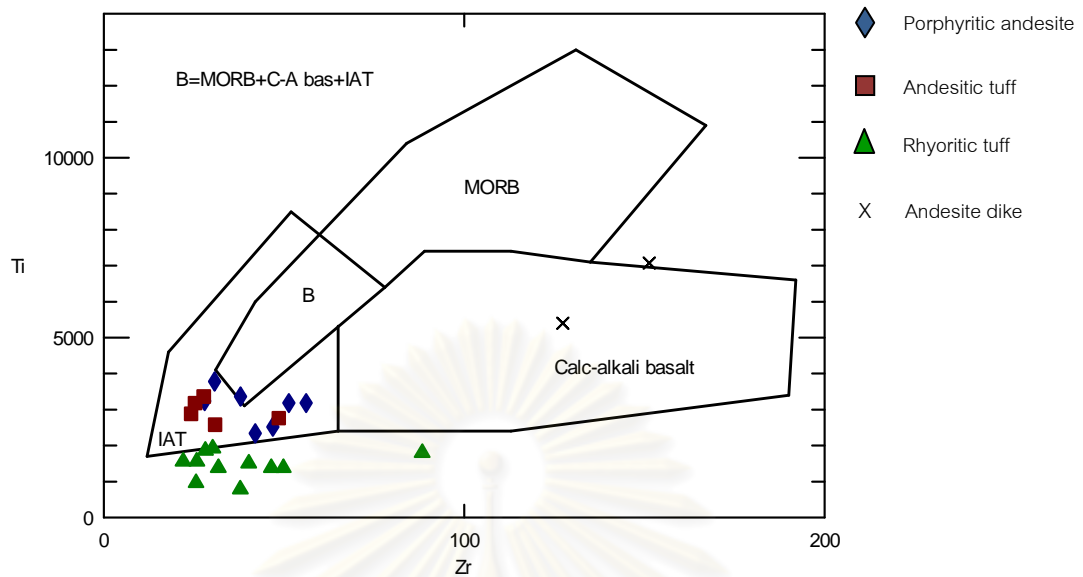


Figure 5.6 Ti-Zr variation diagram (Pearce and Cann, 1973) indicating Q-prospect rock samples are related to island-arc tholeiites and calc-alkali basalts.

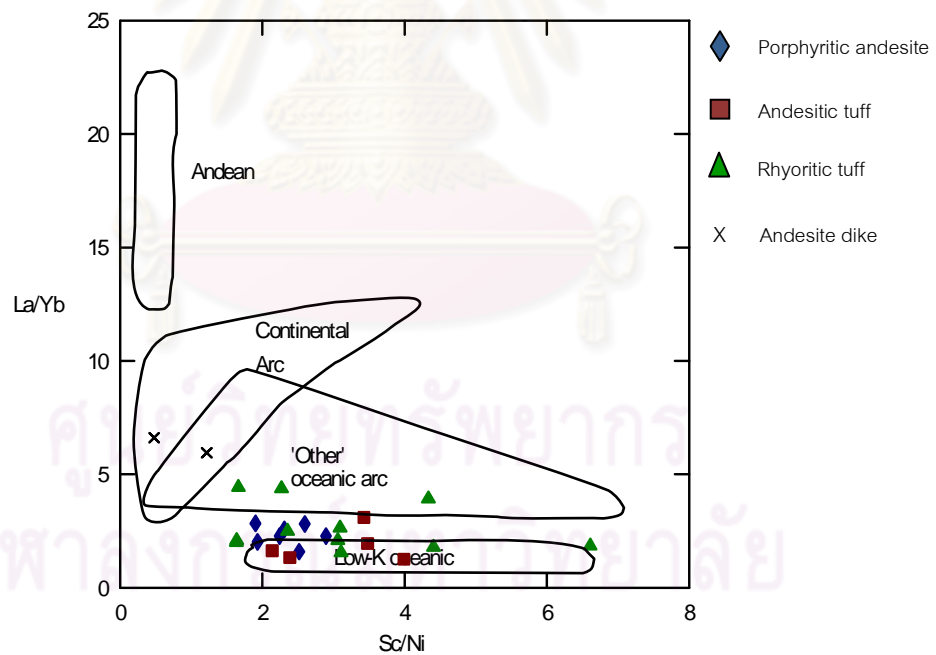


Figure 5.7 La/Yb versus Sc/Ni diagram distinguishing different types of volcanic arc andesite (Bailey, 1981) showing rock samples plotted mostly in oceanic arc except late stage andesite dike in continental arc.

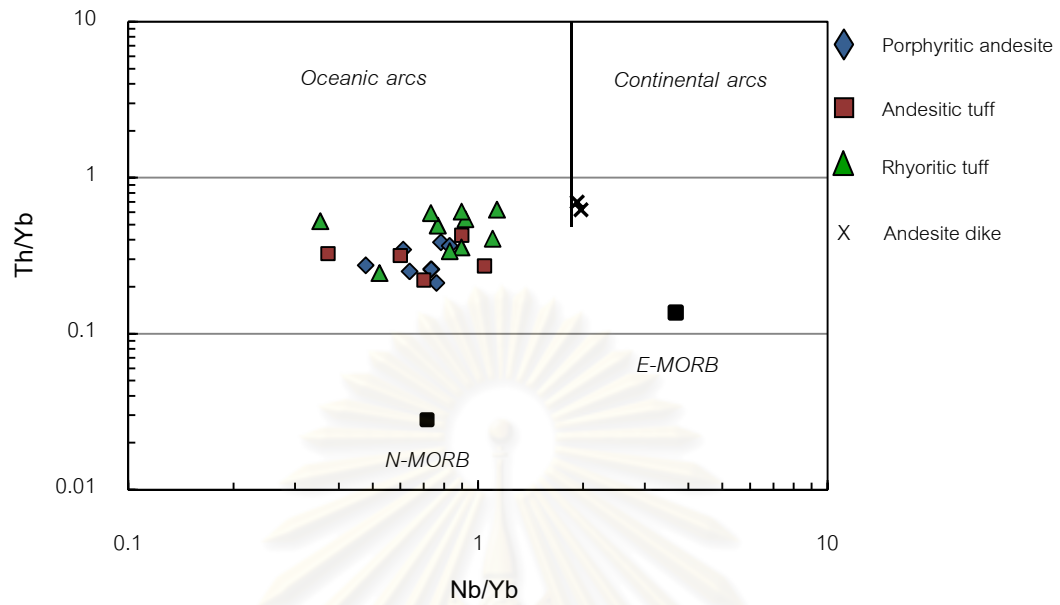


Figure 5.8 Th/Yb versus Nb/Yb diagram (Dunphy and Ludden, 1998) confirming most Q-prospect host rocks are related to oceanic arc whereas andesite dike is related to continental arc.

ศูนย์วิทยทรัพยากร
จุฬาลงกรณ์มหาวิทยาลัย

Primitive mantle (McDonough et al., 1992) normalized spider patterns (Figure 5.9) for selective samples of porphyritic andesite are compared to a pattern of recent volcanic rock of basaltic andesite (No. 347R4-1) from Yap Island arc, southern Philippine (Ohara et al., 2002); they show similar patterns. The primitive mantle normalized patterns (Figure 5.9), however, have high positive K anomaly that may have been effected by potassic alteration (see detail in Chapter III).

MORB (Preace, 1983) normalized trace elements (Figure 5.10) reveals that the porphyritic andesite has similar pattern with a recent volcanic rock of basaltic andesite (No. 347R4-1) from Yap Island arc, southern Philippine (Ohara et al., 2002). These patterns show enrichment of LFS (e.g., Sr, K, Rb, Ba and Th) and depletion of HFSE (e.g., Ta, Nb, Ce, P, Zr, Sm, Ti, Y and Yb) which is a signature of arc volcanism. It supports that the porphyritic andesitic rocks (representative of host rocks in this study) would occur in an island-arc subduction. Moreover, MORB normalized spidergrams of andesite dikes are similar to those of Eocene volcanic rocks (KG-1) from King George Island in the South Shetland arc, Antarctica (Machado et al., 2005) and Island-arc calc-alkaline (Sun, 1980); therefore, these andesite dikes may have erupted in an island arc (Figure 5.11).

The results from this study indicate that the volcanic and related rocks of Q-prospect, Chatree area, e.g., porphyritic andesite with age of 250 ± 6 Ma (James and Comming, 2007), andesitic tuff and rhyolitic tuff, appear to have originated within an island-arc volcanic environment. Tholeiitic magma should be initial source prior to magma differentiation taking place and yielding various compositions from andesitic to rhyolitic compositions. On the other hand, the younger andesite dike with age of 244 ± 7 Ma (James and Comming, 2007) may be a product of cal-alkaline island-arc volcanic rock. Model of tectonic evolution of Chatree volcanic rocks are shown in Figure 5.12.

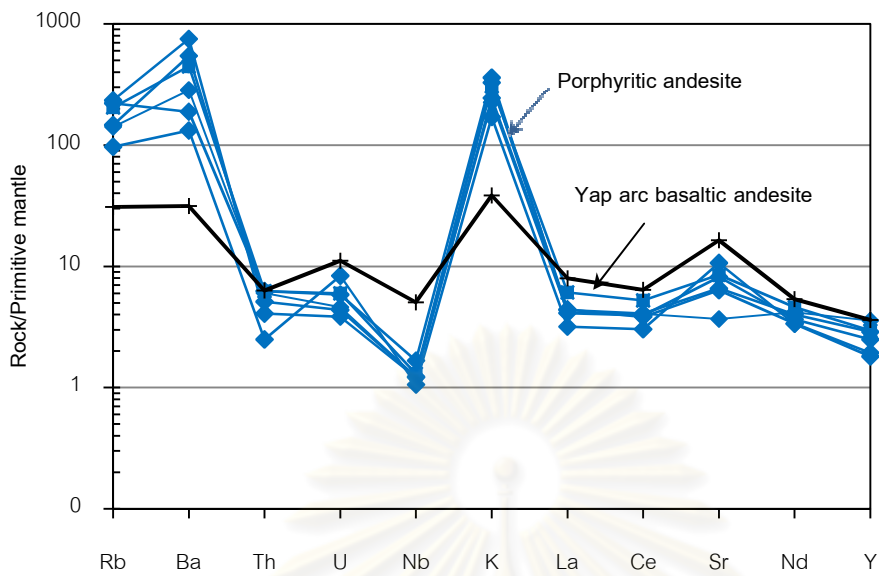


Figure 5.9 Primitive mantle (McDonough et al., 1992) normalized trace element patterns of selective porphyritic andesitic samples compared to that of 25 Ma basaltic andesite from Yap arc, southern Philippine (data from Ohara et al., 2002).

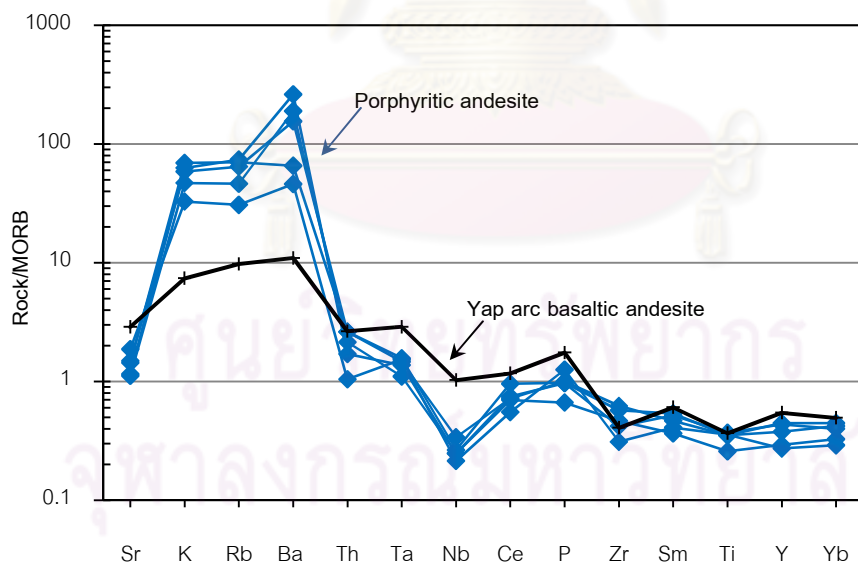


Figure 5.10 MORB (Preace, 1983) normalized trace element patterns of the selective porphyritic andesitic samples compared to that of 25 Ma basaltic andesite from Yap arc, southern Philippine (data from Ohara et al., 2002).

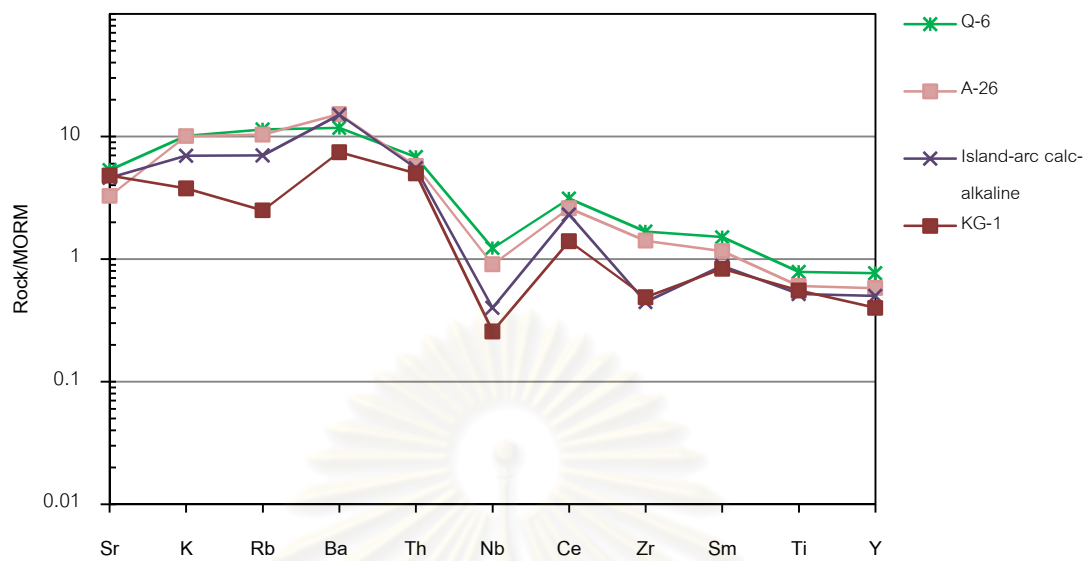


Figure 5.11 MORB (Preace, 1983) normalized spidergram of the andesite dikes (No. Q-6 and A-26) compared to those of Eocene volcanic rock (KG-1) from the South Shetland arc (Machado et al., 2005) and Island-arc calc-alkaline (Sun, 1980).

ศูนย์วิทยทรัพยากร
จุฬาลงกรณ์มหาวิทยาลัย

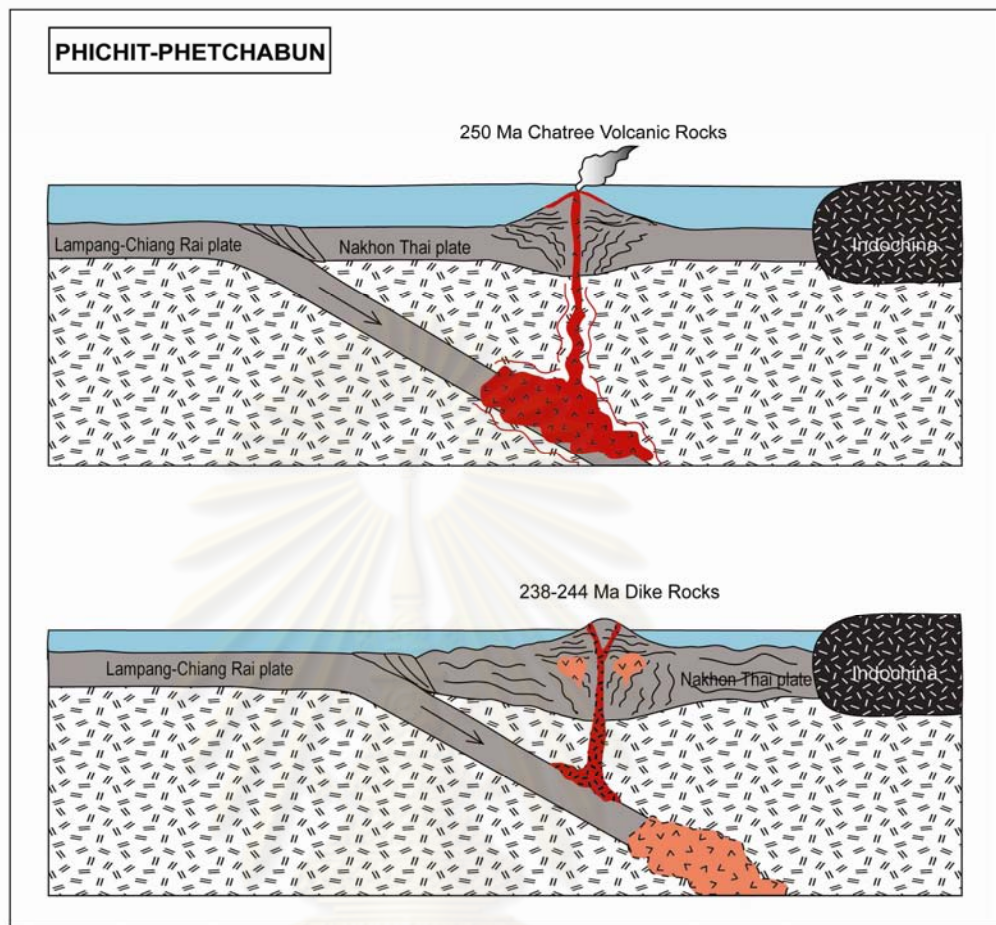


Figure 5.12 Evolution of tectonic setting of Chatree volcanic rocks, Phichit-Phetchabun Provinces.

ศูนย์วิทยทรัพยากร
จุฬาลงกรณ์มหาวิทยาลัย

The Permo-Triassic volcanic rocks along the Loei-Phetchabun-Nakorn Nayok volcanic belt can be subdivided into two sub-belts, i.e., Tha Li-Chon Daen (covering the study area)-Lop Buri (TCL) volcanic sub-belt (western part) and Loei-Phetchabun-Saraburi (LPS) volcanic sub-belt (eastern part) (see Figure 5.13). These volcanic sub-belts are separated based on their petrochemistry and mineralization data. The first sub-belt, Tha Li-Chon Daen-Lop Buri volcanic sub-belt, is located along Tha Li District, western Loei Province southward to Wang Sai Phun, Chon Daen Districts, Phichit Province to Lop Buri Provinces. The second sub-belt, Loei-Phetchabun-Saraburi volcanic sub-belt, is exposed in Loei Province southward to Phetchabun Province and Saraburi Province (Vivatpinyo et al., 2010). The volcanic rocks in both sub-belts had erupted in a subduction environment. The volcanic rocks in the first sub-belt were formed by island arc volcanism (Charusiri et al., 1995; Marhothorn, 2008; this study) and this belt is significantly associated with base metals (Cu, Pb and Zn), iron ore, barite, manganese, pyrite, silver and gold (Jungyusuk and Khositantont, 1992; Charusiri et al., 1995; Salam, 2006; James and Comming, 2007). On the other hand, the second sub-belt erupted in a continental volcanic arc (Kamvong et al., 2006; Vivatpinyo, 2006; Junplook, 2006; Vivatpinyo et al., 2010).

Regarding to tectonic model (Figure 5.14), these volcanisms would have been formed as a result of eastward subduction of the Lampang-Chiang Rai oceanic plate (or slab) beneath the Nakhon Thai oceanic plate during Permo-Triassic Period forming the Tha Li-Chon Daen-Lop Buri island-arc. During this period, high degree of partial melting of oceanic slab beneath the mantle wedge may have caused partial melting of the upper slab. Subsequently, mafic magma ascending and differentiation of melts eventually gave rise to arc andesite of the Q-prospect. This island arc had continuously become thick mature island arc or continental arc then yielding higher alkaline composition of calc-alkaline andesite dike. Moreover, heat source may have become decreasing and leading to lower degree of partial melting at shallower depth. Obvious different REE and spider trace element patterns (see Figures 4.4 to 4.15) of volcanic

hosts and younger dike indicate clearly different magmatic sources and degree of partial melting; however, they appear to be related to the same subduction zone.

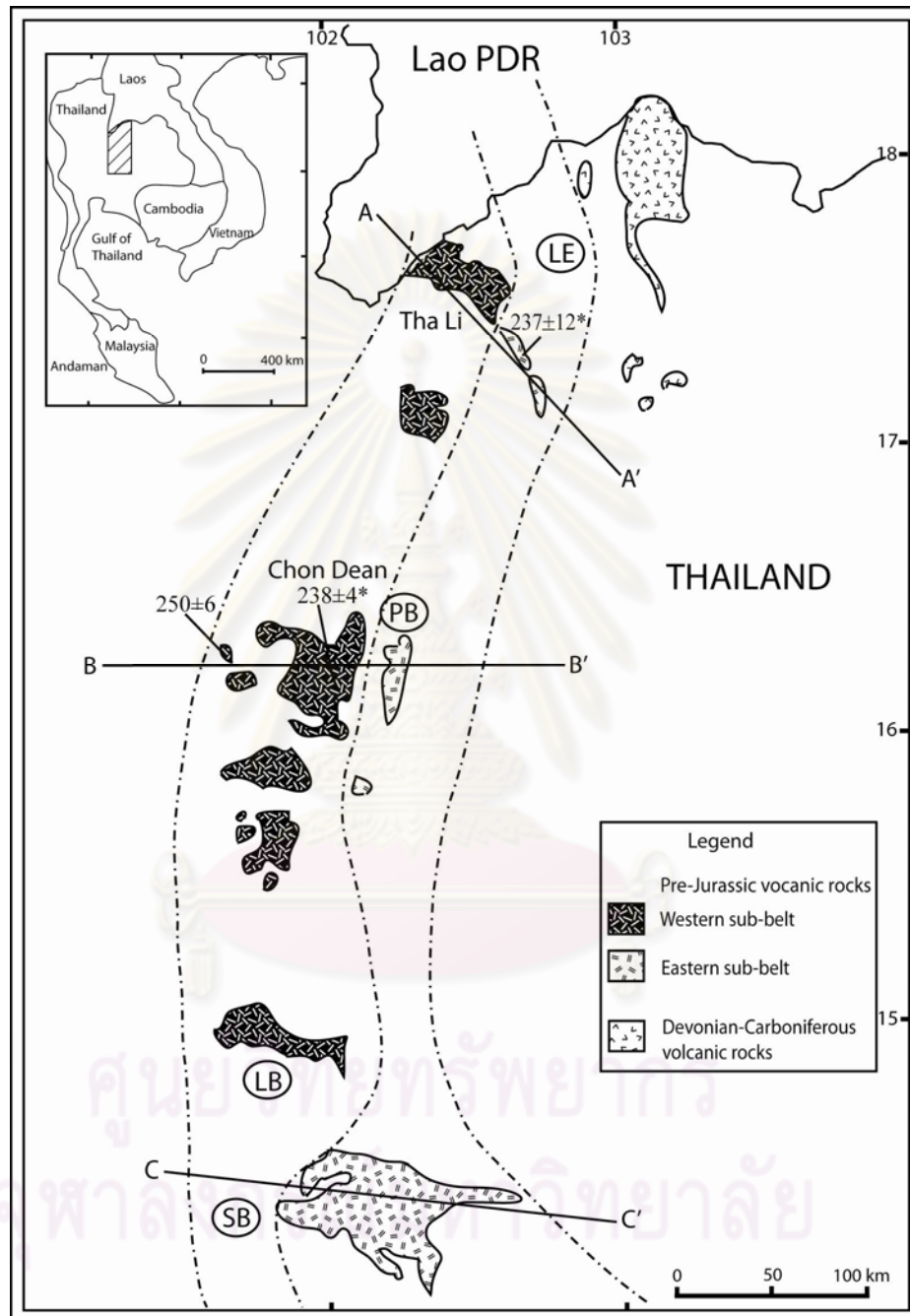


Figure 5.13 Subdivision of pre-Jurassic volcanic rocks along Eastern Volcanic belt; into Western sub-belt and Eastern sub-belt. Detail of cross section lines show in Figure 5.12. (LE = Loei Province, PB = Phetchabun Province, LB = Lop Buri Province, and SB = Saraburi Province)

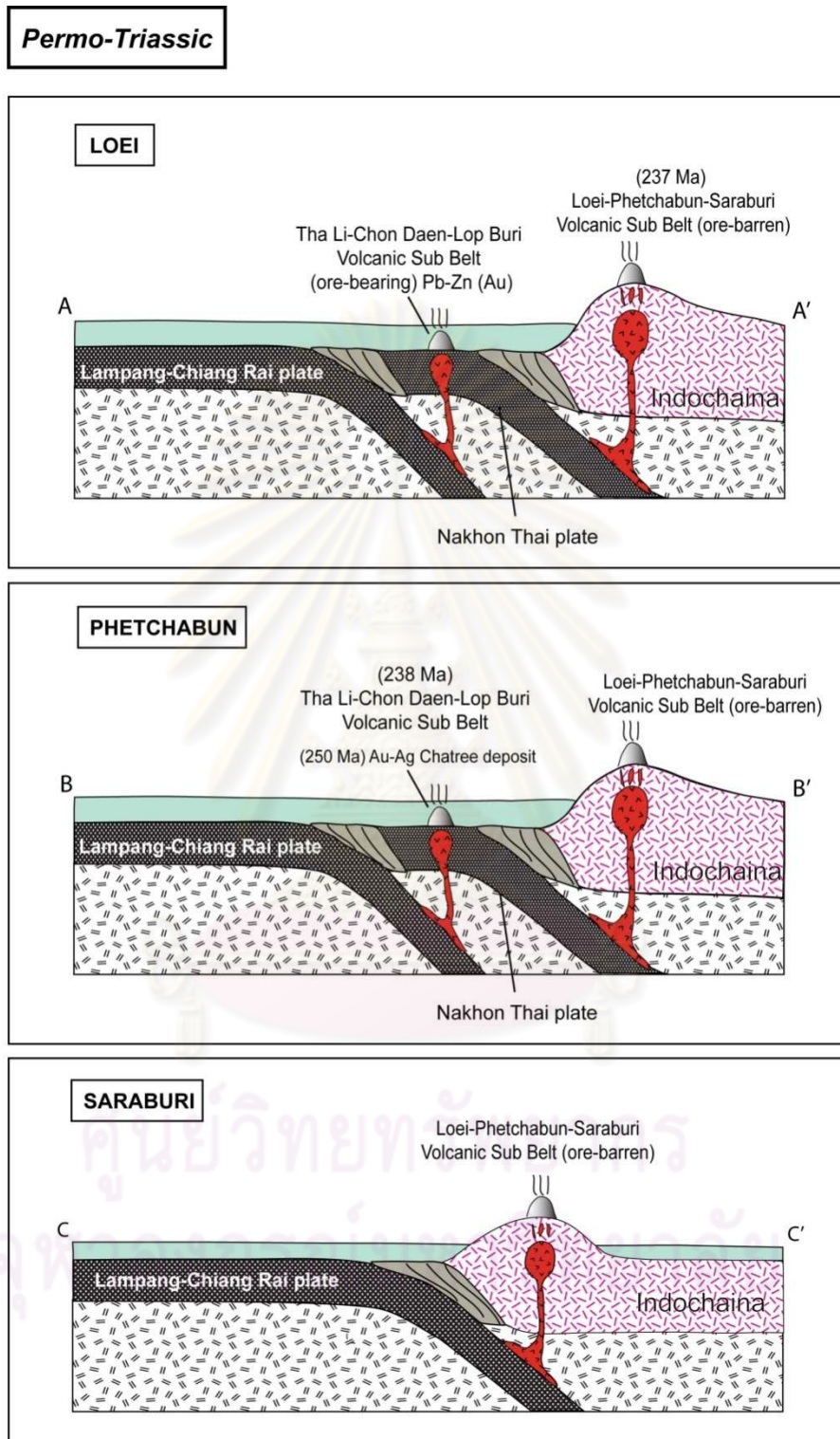


Figure 5.14 Tectonic model of Eastern Volcanic Belt of Thailand during Late Paleozoic to Early Mesozoic.

CHAPTER VI

CONCLUSIONS

Based on petrographic and geochemical investigations, the results of this study indicate that rocks at Q-prospect area are composed of coherent, pyroclastic rocks and late stage dike. Characteristics of these rocks are summarized below.

1) The volcanic and related rocks at Q-prospect consist of porphyritic andesite, andesitic tuff and rhyolitic tuff with late stage andesite dike.

2) Field study and previous works data on simplified stratigraphy indicate that the sequence of these volcanic rocks are ordered from older to younger as porphyritic andesite, andesitic tuff and rhyolitic tuff. These rocks are cross cut by andesite dike.

3) Geochemically, the porphyritic andesite, andesitic tuff and rhyolitic tuff appear to have originated from tholeiitic magma, whereas the younger andesite dike is a product of cal-alkaline magma. Tholeiitic magma should be initial source, evolved by process of high degree of partial melting prior to magma differentiation taking place and yielding various compositions from andesitic to rhyolitic compositions. Moreover, heat source may have become decreasing and led to lower degree of partial melting at shallower depth, and generated a new source of andesite dike.

4) These volcanisms would have been formed as a result of eastward subduction of the Lampang - Chiang Rai oceanic plate beneath the Nakhon Thai oceanic plate during Permo-Triassic Period forming an island-arc volcanic.

5) The Permo-Triassic volcanic rocks along the Loei-Phetchabun-Nakorn Nayok volcanic belt can be subdivide into two sub-belts, i.e., Tha Li - Chon Daen - Lop Buri (TCL) volcanic sub-belt (western part) and Loei - Phetchabun - Saraburi (LPS) volcanic sub-belt (eastern part).

REFERENCES

- Abbey, S. (1983). Studies in Standard Samples of silicate rocks and minerals 1969-1982. Canadian Geological Survey Paper 83-15, 114 pp.
- Bailey, J.C. (1981). Geochemical criteria for a refined tectonic discrimination of orogenic andesites. Chem. Geol. 32 (1-2): 139-154.
- Barr, S.M., Macdonald, A.S., Dunning, D.R., Ounchanum, P., and Yaowanoyothin, W. (2000). U–Pb (zircon) age and paleotectonic setting of the Lampang volcanic belt, northern Thailand. J. Geol. Soc. London. 157: 553–563.
- Barr, S.M., Tantisukrit, C., Yaowanoyothin, W., and Macdonald, A.J. (1990). Petrology and tectonic implications of Upper Palaeozoic volcanic rocks of the Chiang Mai belt, northern Thailand. J. Southeast Asian Earth Sci. 4: 37-47.
- Boynton, W.V. (1984). Geochemistry of the rare earth elements: meteorite studied. In Henderson P. (ed.), Rare earth element geochemistry. Elsevier, pp. 63-114.
- Bunopas, S. (1981). Paleographic history of western Thailand and adjacent parts of Southeast Asia-A plate tectonics interpretation. Doctoral dissertation. Victoria University of Wellington, New Zealand, 810 pp.
- Bunopas, S. (1992). Regional stratigraphic correlation in Thailand. In Piancharoen, C. (ed.), Proceedings of The National Conference on Geologic Resources of Thailand: Potential for future development. Bangkok, Thailand, pp. 2-24.
- Bunopas, S., and Villa, P. (1983). Tectonic and geologic evolution of Thailand. In Nutalaya, P. (ed.), Proceedings of the Workshop on Stratigraphic Correlation of Thailand and Malaysia, Had Yai, Thailand: 1. Geological Society of Thailand and Geological Society of Malaysia, pp. 212-232.
- Bunopas, S., and Vella, P. (1992). Geotectonics and geologic evolution of Thailand. National Conference on Geologic Resources of Thailand: Potential for Future Development, Bangkok, Thailand, pp. 209-228.

- Cabanis, B., and Lecolle, M. (1989). Le diagramme La/10-Y/15-Nb/8; un outil pour la discrimination des series volcaniques et la mise en evidence des processus de melange et/ou de contamination crustale. *Comptes Rendus de l'Academie des Sciences, Serie 2, Mecanique, Physique, Chimie, Sciences de l'Univers, Sciences de la Terre*. 309 (20): 2023-2029.
- Chairangsee, C., Ginze, C., Macharoensap, S., Nakornsri, N., Silpalit, M., and Sinpool Anunt, S. (1990). Geological map of Thailand 1:50,000 Exploration for sheet Amphoe Pak Chom 5345 I Ban Na Kho 5344 I, Ban Huai Khop 5445 III, King Amphoe Nam Som 5444 V. Thailand, pp. 1-109.
- Chaodumrong, P. (1992). Stratigraphy, sedimentology and tectonic setting of the Lampang Group, central North Thailand. Doctoral dissertation, University of Tasmania, Australia.
- Charusiri, P. (1989). Lithophile Metallogenetic Eepochs of Thailand: a Geological and Geochronological investigation. Doctoral dissertation, Department of Geology, Queen's University, Kingston, Canada.
- Charusiri, P., Daorerk, V., Archibald, D., Hisada, K., and Ampaiwan, T. (2002). Geotectonic Evolution of Thailand: A new Synthesis. Journal of the Geological Society of Thailand. 1: 1-20.
- Charusiri, P., Suwannachote, P., Nuchanong, T., Saengsil, S., and Yaemniyom, S. (1995). Alteration and Pb-Zn (Au) mineralization of the Phu Chang area, Changwat Loei, NE Thailand: Implication for a proposed genetic model. Proceeding of International Conference on Geology, Geotechnology and Mineral Resources of Indochina (Geo-Indo'95). Khon Kaen, Thailand, pp. 201-223.
- Chuaviroj S., Chaturongkawanich, S., and Sukawattananan, P. (1980). Geology of geothermal resources of northern Thailand (Part I, San Kamphaeng), Unpublished report of Geological Survey Division, Department of Mineral Resources, Bangkok, Thailand, 45 pp.
- Chonglakmani, C., and Satayalak, N. (1979). Geological map of Changwat Phetchabun, Thailand 1:250,000, Department of Mineral Resources, Bangkok, Thailand

- Corbett, G. (2004). Comments on controls to gold mineralization at gold prospects in the vicinity of the charee gold mine, Thailand. Corbett Geological Services, Australia, pp. 2-23. (Unpublished Manuscript)
- Crawford, A.J., and Panjasawatwong, Y. (1996). Ophiolite, ocean crust, and the Nan suture in SE Thailand. In Lee, T.Y. (ed), International Symposium on lithosphere dynamics of East Asia. Program and Extended Abstracts, Taipei, p. 38.
- Crossing, J. (2004). Geology of the Chatree region Thailand. Compass Geological. Australia. p 3. (Unpublished Manuscript)
- Crossing, J., (2006). Addition geological mapping of the Chatree regional Thailand, Company report, pp 1-15.
- Cumming, G., Lunwongsa, W., and Nuanlaong, S. (2006). The Geology and Mineralization at Chatree, Central Thailand. A report prepared for Kingsgate Consolidated Limited. Thailand. (Unpublished Manuscript)
- Diemar, M.G., and Diemar, V.G. (1999). Geology of the Chatree epithermal gold deposit, Thailand. Proceedings of Pacific Rim Conference 1999, Indonesia 10-13 October, 227-231.
- Diemar M.G., Diemar V.A., and Udornpornwirat S. (2000). The Chatree Epithermal Gold-Silver Deposit, Phichit-Petchabun Provinces, Thailand. In Symposium on Mineral, Energy, and Water Resource of Thailand. Bangkok, Thailand, pp. 423-427.
- Department of Mineral Resources. (1999). Geology of Thailand, Department of Mineral Resources. Thailand, Department of Mineral Resource, Thailand. (Unpublished Manuscript)
- Dunphy, J.M., and Ludden, J.N. (1998). Petrological and geochemical characteristics of a Paleoproterozoic magmatic arc (Narsajuaq terrane, Ungava Orogen, Canada) and comparisons to Superior Province granitoids. Precambrian Res. 91: 109-142.
- Fisher, R.V. (1966). Mechanism of deposition from pyroclastic flows. Amer. J. Sci. 264: 287-298.

- Gifkins, C., Herrmann, W., and Large, R. (2005). Altered volcanic rocks: a guide to description and interpretation. The Centre for Ore Deposit Research, University of Tasmania, Australia.
- Gladney, E.S., and Roelandts, I. (1988). 1987 Compilation of elemental concentration data for USGS BHVO-1, MAG-1, QLO-1, RGM-1, SCo-1, SDC-1, SGR-1, and STM-1, Geostandard Newslett. 12: 253-362.
- Govindaraju, K. (1994). 1994 Compilation of working values and descriptions for 383 Geostandards, Geostandard Newslett. 18: 1-158.
- Hada, S., Bunopas, S., Salyapongse, S., Thitisawan, V., Panjasawatwong, Y., Yaowanoyothin, W., Ishii, K., and Yoshikura, S. (1991). Terrane analysis and tectonics of the Nan-Chanthaburi suture zone, Abstracts of the Seventh Regional Conference on Geology, Mineral and Energy Resources of Southeast Asia, Bangkok, Thailand, November 1991. Geological Society of Thailand, pp. 40-41.
- Hada, S., Bunopas, S., Ishii, K., and Yoshikura, S. (1999). Rift-drift history and the amalgamation of Shan-Thai and Indochina/East Malaya blocks Gondwana Dispersion and Asian Accretion. In Metcalfe, I., Jishun, I., Charvet, J. and Hada, S. (eds.), Final Results Volume for IGCP Project 321. A.A. Balkema, Rotterdam, pp. 67-87.
- Hawkesworth, C.J., and Powell, M. (1980). Magma genesis in the Lesser Antilled island arc. Earth Planet. Sc. Lett. 51: 297-308.
- Hickey, R.L., Frey, F.A., and Gerlach, D.C. (1986). Multiple sources for basaltic arc rocks from the southern volcanic zone of the Andes (34-41°S): trace element and isotopic evidence for contributions from subducted oceanic crust, mantle and continental crust. J. Geophys. Res. 91: 5963-5983.
- Hinthong, C., Chuaviroj, S., Kaewyana, W., Srisukh, S., Pholprasit, C., and Pholachan, S. (1985). Geological map of Changwat Pranakorn Si Ayutthaya scale 1:250,000. Department of Mineral Resources, Bangkok, Thailand.
- Hughes, C.J. (1982). Igneous petrology (Developments in Petrology, 7). Elsevier Scientific Publishing Company, Amsterdam, 551 pp.

- Hutchison, C.S. (1973). Tectonic evolution of Sundaland, a Phanerozoic synthesis, Geol Soc. of Malaysia Bull. 6: 61-86.
- Hutchison, C.S. (1989). Geological Evolution of Southeast Asia. Oxford Monographs on Geology and Geophysics, No. 13, Oxford University Press, 368 pp.
- Intasopa, S. (1993). Petrology and geochronology of the volcanic rocks of the central Thailand volcanic belt. Doctoral dissertation. Department of Geology, University of New Brunswick, Canada, 242 pp.
- Intasopa, S., Dunn, T., and Lux, D.R. (1990). $^{40}\text{Ar}/^{39}\text{Ar}$ geochronology of the Central Thailand volcanic belt. Eos Trans. Am. Geophys. Union. 71: 1700.
- Intasopa, S., and Dunn, T. (1994). Petrology and Sr-Nd isotopic systems of the basalts and rhyolites, Loei, Thailand. J. Southeast Asian Earth Sci. 9: 167-180.
- Irvine, T. N., and Baragar, W.R. A. (1971). A guide to the chemical classification of the common volcanic rocks. Can. J. Earth Sci. 8: 523-548.
- Iwai, J., and Asama, K. (1964). Geology and paleontology of the Khorat Plateau and the plant-bearing Permian Formations, Report on the Stratigraphical and Palaeontological Reconnaissance in Thailand and Malaysia, Overseas technical Cooperation Agency, Tokyo, 1963-1964.
- James, R., and Cumming, G. (2007). Geology and mineralization of the Chatree epithermal Au-Ag deposit, Phetchabun province, central Thailand. Proceedings of GEOTHAI'07 International Conference on Geology of Thailand: Towards Sustainable Development and Sufficiency Economy. Bangkok, Thailand, pp. 378-390.
- Jungyusuk, N. (1985). Geology of Amphoe Chon Daen, Geological Survey report No. 0069. (in Thai), 49 p.
- Jungyusuk, N., and Sinsakul, S. (1989). Geology of Ban Na Chaliang, Amphoe Nong Phai and Amphoe Wichianburi. Geological Survey Report 127: 51-60.
- Jungyusuk, N., and Khositantont, S. (1992). Volcanic rocks and associated mineralization in Thailand. In Piancharoen, C. (ed.), Proceedings of The National Conference on Geologic Resources of Thailand: Potential for future development. Bangkok, pp. 528-532.

- Junplook, S. (2006). Petrochemistry of Volcanic rocks at Khao Champa area in Chulalongkorn University land development project, Amphoe Kaeng Khoi, Changwat Saraburi. Bachelor's Senior Project. Department of Geology, Faculty of Science. Chulalongkorn University.
- Kamvong, T. (2002). Petrography of igneous rocks from the eastern part of Amphoe Wang Pong, Changwat Phetchabun, north of central Thailand. Bachelor's Senior Project. Department of Geology, Faculty of Science. Chulalongkorn University.
- Kamvong, T., Charusiri, P., and Intasopa, S. (2006). Petrochemical Characteristics of igneous rocks from the Wang Pong Area, Phetchabun, North Central Thailand: Implications of tectonic setting. Journal of the Geological Society of Thailand. 1: 9-26.
- Khin Zaw, Burrett, C.F., Berry, R.F., and Bruce, E. (1999). Geological, tectonic and metallogenic relations of mineral deposits in SE Asia: Australian Mineral Industry Research Association (AMIRA) Final Report, (unpublished), University of Tasmania, 255 p.
- Kimura, J., Takkaku, Y., and Yoshida, T. (1995). Igneous rock analysis using ICP-MS with interna' standardization, isobaric Ion Overlap correction, and standard addition methods. Sci. Rep. Fukushima Univ. 56: 1-11.
- Kosuwan, S., Charusiri, P., Lumjuan, A. and Takashima, T. (1998). Active tectonics of the Mae Chan Fault, northern Thailand. Proceeding of the International Congress on GEOSEA, pp. 97-122.
- Kromkham, K., and Zaw, K. (2005). Geological Setting, Mineralogy and Alteration of the H Zone, the Chatree Deposit, central Thailand. Proceeding of the International Conference on Geology, Geotechnolgy and Mineral Resource of Indochina, Khon Kaen, Thailand, pp. 319-323.
- LeBas, M.J., LeMaitre, R.W., Streckeisen, A., and Zanettin, B. (1986). A chemical classification of volcanic rocks based on the total alkali silica diagram. J. Pet. 27: 745-750.

- Macdonald, A.S., and Barr, S.M. (1978). Tectonic significance of a Late Carboniferous volcanic arc in northern Thailand. In Nutalaya, P. (ed.), Proceedings of the Third Regional Conference on Geology and Mineral Resources of Southeast Asia, Geological Society of Thailand, Bangkok and Pattaya, Thailand, pp. 151–156.
- Machado, A., Lima, E.F., Chemale, F., Morate, Jr., Oteiza, O., Almeida, D.P.M., Figueiredo, A.M.G., Alexandre, F.M., and Urrutia, J.L. (2005). Geochemistry constraints of Mesozoic–Cenozoic calc-alkaline magmatism in the South Shetland arc, Antarctica. J. S. Am. Earth Sci. 18: 407-425.
- MacLean, W.H., and Barrett, T.J. (1993). Lithochemical techniques using immobile elements. J. Geochem. Explor. 48: 109–133.
- Marhotorn, K. (2002). Preliminary Fluid Inclusion Study of the Chatree Gold deposit, Changwat Pichit. Bachelor's Senior Project. Department of Geology. Faculty of Science. Chulalongkorn University.
- Marhothon, K. (2008). Petrochemistry of igneous rocks in the southern parts of the Chatree, Changwat Pichit. Master's Thesis. Department of Geology, Chulalongkorn University, Bangkok, Thailand, 162 pp.
- McBirney, A.R. (1993). Igneous petrology, 2nd edition. John and Bartlett Publishers, Boston, USA.
- McDonough, W. F., Sun, S.S., Ringwood, A.E., Jagoutz, E., and Hofmann, A.W. (1992). K, Rb and Cs in the Earth and Moon and the evolution of the Earth's mantle. Geochim. Cosmochim. Acta. 56: 1001-1012.
- Metcalfe, I. (1995). Gondwana dispersion and Asian accretion. Proceedings of the IGCP symposium of Geology of SE Asia, Hanoi, Vietnam, pp. 223-266.
- Metcalfe, I. (1997). The Paleo-Tethys and Paleozoic-Mesozoic Tectonic evolution of SE Asia. In Dheeradilok, P. et al. (eds.), Proceedings of the International Conference on Stratigraphy and tectonic Evolution of SE Asia and the South Pacific, Department of Mineral Resources, Bangkok, pp. 414-420.
- Metcalfe, I. (2002). Permian tectonic framework and paleogeography of SE Asia. J. Asian Earth Sci. 20: 551-566.

- Middlemost, Eric A. K. (1985). Magma and magmatic rocks: an introduction to igneous petrology. Longman Inc. New York, 266 pp.
- Nakchaiya, T. (2008). Stratigraphy, geochemistry and petrography of volcanic rocks in the Chatree gold mine, Changwat Pichit. Master's Thesis. Department of Geology, Chulalongkorn University, Bangkok, Thailand. 148 pp.
- Ohara, Y., Fujioka, K., Ishizuka, O., and Ishii, T. (2002). Peridotites and volcanics from the Yap arc system: implications for tectonics of the southern Philippine Sea Plate. Chem. Geol. 189: 35–53
- Panjasawatwong, Y. (1991). Petrology, geochemistry and tectonic implications of the igneous rocks in the Nan suture, Thailand, and an empirical study of the effects of Ca/Na, Al/Si and H₂O on plagioclase melt equilibria at 5-10 kb pressure. Doctoral dissertation, University of Tasmania. 239 p.
- Panjasawatwong, Y., Kanpeng, K., and Ruangvatanasirikul, K. (1995). Basalts in Li basin, northern Thailand. In Thanvarachorn, S., Hokjaroen, S. and Youngme, W. (eds.), Proceedings of the International Conference on Geology, Geotechnology and Mineral Resources of Indochina, Khon Kaen University, Khon Kaen, Thailand, pp. 225-234.
- Panjasawatwong, Y., Chantaramee, S., Limtrakun, P., and Pirarai, K. (1997). Geochemistry and tectonic setting of eruption of central Loei volcanic in the Pak Chom area Loei, northeast Thailand. Dheeradilok, P. et al., (eds.), Proceedings of the International Conference on Stratigraphy and Tectonic Evolution of Southeast Asia and the South Pacific, Bangkok, pp. 225–234.
- Panjasawatwong, Y. (1999). Petrology and tectonic setting of eruption of basaltic rocks penetrated in well GTE-1, San Kam Phaeng geothermal field, Chiang Mai, northern Thailand. In Ratanasthein, B., Rieb, S.L. (eds.), Proceedings of the International Symposium on Shallow Tethys (ST) 5. Department of Geological Sciences, Chiang Mai University, Chiang Mai, Thailand, pp. 242-264.
- Panjasawatwong, Y., Phajuy, B., and Hada, S. (2003). Tectonic setting of the Permo-Triassic Chiang Khong volcanic rocks, northern Thailand based on petrochemical characteristics. Gondwana Res. 6: 743–755.

- Panjasawatwong, Y., Khin Zaw, Chantaramee, S., Limtrakun, P., and Pirarai, K. (2006). Geochemistry and tectonic setting of the Central Loei volcanic rocks, Pak Chom area, Loei, northeastern Thailand. J. Asian Earth Sci. 26: 77-90.
- Pearce, J.A. (1982). Trace element characteristics of lavas from destructive plate margins. In Andesites: Orogenic andesites and related rocks, Thorpe, R.S. (ed.), 525-548. Chichester: Wiley.
- Pearce, J.A. (1983). The role of subcontinental lithosphere in magma genesis at destructive plate margins. In Continental basalts and mantle xenoliths, Hawksworth, C.J. and Norry, M.J. (eds.), 230-249. Nantwich: Shiva.
- Pearce, J.A., and Cann, J.R. (1973). Tectonic setting of basic volcanic rocks determined using trace element analysis. Earth Planet. Sc. Lett. 24: 290-300.
- Phajuy, B., Panjasawatwong, Y., and Osataporn, P. (2005). Preliminary geochemical study of volcanic rocks in the Pang Mayao area, Phrao, Chiang Mai, northern Thailand: tectonic setting of formation. J. Asian Earth Sci. 24: 756-776.
- Ponprasit, C., Prasomsap, T., and Ponwannapa, S. (1988). Geology of Phetchabun Province (sheet 5241 IV) and Ban Wang Pong (sheet 5141 I). Department of Mineral Resource. (In Thai)
- Potirat, S. (1996). Gold exploration and mining opportunity in Thailand. Mineral Resources Development Division Document (unpublished), No. 3/96, Department of Mineral Resources, Bangkok, 17 pp.
- Rodmanee, T. (1992). Report on semi-detailed Mineral Exploration at Chon Daen-Thab Khlo Selected Area, Changwat Phetchabun, Phichit, and Phisanulok. Mineral Exploration and Evaluation Section, Mineral Resources and Development Project, Department of Mineral Resource, Bangkok, 88 pp.
- Rollinson, H.R. (1993). Using geochemical data: evaluation, presentation and interpretation. Longman Scientific and Technical Ltd., Harlow, UK. 352 pp.

- Salam, A. (2006). A geological, geochemical and metallogenic study of the northern Chatree area, Phetchabun province, Loei Fold Belt, central Thailand – progress report. In: Geochronology, Metallogenesis and Deposit Styles of Loei Fold Belt in Thailand and Laos PDR, CODES: ARC Linkage Project, unpublished volume, CODES Centre of Excellence in Ore deposit Research, University of Tasmania.
- Salam, A. (2008). Geological setting, mineralization and geochronology of Chatree epithermal gold-silver deposit, Phetchabun Province, central Thailand, Australian Earth Sciences Convention, Perth, Australia.
- Sangsiri, P., and Pisutha-Arnond, V. (2008). Host Rock Alteration at the A Prospect of the Chatree Gold Deposits, Phichit Province, central Thailand: A Preliminary Re-Evaluation. Proceedings of the International Symposia on Geoscience Resources and Environments of Asian Terranes (GREAT 2008), 4th IGCP 516, and 5th APSEG, Bangkok, Thailand, pp. 258-261
- Sangsomphong, A. (2011). Analysis and modelling airborne geophysical data in the Phetchabun volcanic belt northern part of central Thailand. Master's Thesis. Department of Geology, Chulalongkorn University, Bangkok, Thailand, (in preparation).
- Singharajwarapan, S. (1994). Deformation and metamorphism of the Sukhothai Fold Belt, northern Thailand. Doctoral dissertation, University of Tasmania, Hobart, Tasmania, Australia. 385 pp.
- Singharajwarapan, S., Berry, R., and Panjasawatwong, Y. (2000). Geochemical characteristics and tectonic significance of the Permo-Triassic Pak Pat volcanic, Uttaradit, northern Thailand. Journal of Geological Society of Thailand 1: 1-7.
- Sun, S.S. (1980). Lead isotopic study of young volcanic rocks from mid-oceanic ridges, ocean islands and island arcs. Phil. Trans R. Soc. Lond. A297: 409-445.
- Sutthirat, C. (2009). Origin of Mafic and Ultramafic Rocks and Relation to Geological Sutures in Thailand. (A Final Research Report of Thailand Research Fund). Chulalongkorn University.

- Tangwattananugul, L. (2006). Geology and petrography of dike rocks in C-H pits at Akara mining, Changwat Pichit. Bachelor's Senior Project. Department of Geology, Faculty of Science. Chulalongkorn University, 52 pp.
- Tangwattananukul, L., Lunwongsa, W., Mitsuta, T., Ishiyama, H., Takashima I., Won-In, K., and Charusiri, P. (2008). Geology and Petrochemistry of Dike Rocks in the Chatree Gold Mine, Central Thailand: Implication for Tectonic Setting, Proceedings of the International Symposia on Geoscience Resources and Environments of Asian Terranes (GREAT 2008), 4th IGCP 516, and 5th APSEG; November 24-26, 2008, Bangkok, Thailand: 299-301.
- Ueno, K., Miyahigashi, A., Kamata, Y., Kato, M., Charoentitirat, T., and Limruk, S. (2010). Triassic shallow-marine limestone in the Central Plain of Thailand: its foraminiferal age and geotectonic implications. Proceeding 6th symposium of the International Geological Correlation Programme Project 516 (IGCP516): Geological Anatomy of East and South Asia. Kuala Lumpur, Malaysia: 37-39.
- Vivatpinyo, J. (2006). Petrochemistry of volcanic rocks at Khao Tham Sua area in Chulalongkorn University land development project, Amphoe Kaeng Khoi, Changwat Saraburi. Bachelor's Senior Project. Department of Geology, Faculty of Science. Chulalongkorn University, 52 pp.
- Vivatpinyo, J., Junplook, S., Charusiri, P., and Sutthirat, C. (2010). Petrochemistry of volcanic rocks in Saraburi area, Central Thailand: Implication for the Late Paleozoic tectonic setting. Proceeding 6th symposium of the International Geological Correlation Programme Project 516 (IGCP516): Geological Anatomy of East and South Asia. Kuala Lumpur, Malaysia: pp. 82.
- Winchester, J.A., and Floyd, P.A. (1976). Geochemical magma type discrimination; application to altered and metamorphosed basic igneous rocks. Earth Planet. Sc. Lett. 28: 459-469.
- Winchester, J.A., and Floyd, P.A. (1977). Geochemical discrimination of different magma series and their differentiation products using immobile elements. Chem. Geol. 20: 325-343.

- Wilson, M. (1989). Igneous petrogenesis: a global tectonic approach. Unwin Hyman, Winchester. 466 pp.
- Wood, D.A. (1980). The application of a Th-Hf-Ta diagram to problems of tectonomagmatic classification and to establishing the nature of crustal contamination of basaltic lavas of the British Tertiary volcanic province. Earth Planet. Sc. Lett. 50 (1): 11-30.
- Yang, K. (1998). A plate tectonic reconstruction of the eastern Tethyan Orogen in southwestern China. In Flower, F.J., Chung, S., Lo, C. and Lee, T. (eds.), Mantle dynamics and plate interactions in East Asia - Geodynamics 27, pp. 269-287.
- Yang, K., Mo, X., and Zhu, Q. (1994) Tectono-volcanic belts and late Paleozoic–early Mesozoic evolution of southwestern Yunnan, China. J. Southeast Asian Earth Sci. 10: 245-262.
- Yoshikura, S. (1990). Geology of the Nan-Chanthaburi suture zone (II) - Petrology of basaltic rocks. Abstracts of the Technical Conference on Development of Geology for Thailand into the Year 2000, Department of Geology, Chulalongkorn, Bangkok, Thailand, pp. 11-13.
- Kingsgate Consolidated Limited website. Available from:
<http://www.kingsgate.com.au/company/chatree-gold-mine.htm> [2010, August 20]
- Siamanswer website. Available from: <http://siamanswer.com/media> [2011, January 15]



APPENDICES

ศูนย์วิทยทรัพยากร
จุฬาลงกรณ์มหาวิทยาลัย

APPENDIX A

No.	Core No.	Sample No.	Apparent depth (m)	Rock name
1	RD2270	Q-1	81.80 - 81.90	Silicified andesite
2	"	Q-2	86.90 - 87.00	Silicified andesite
3	"	Q-3	106.33 - 106.43	Qtz-carb-pyrite vein
4	"	Q-4	129.40 - 129.50	Porphyritic andesite
5	"	Q-5	148.30 - 148.40	Silicified mudstone
6	RD2327	Q-6	86.91 - 87.00	Andesite dike
7	"	Q-7	107.20 - 107.30	Porphyritic andesite
8	"	Q-8	113.20 - 113.30	Porphyritic andesite
9	RD2686	Q-9	52.44 - 52.54	Andesitic tuff
10	"	Q-10	64.12 - 64.22	Qtz-carb-chlorite crustiform
11	"	Q-11	115.68 - 115.78	Silicified siltstone
12	RD2836	Q-12	65.40 - 65.50	Andesitic tuff
13	"	Q-13	74.00 - 74.10	Porphyritic andesite
14	"	Q-14	83.70 - 83.80	Andesitic tuff
15	"	Q-15	89.30 - 89.40	Andesitic tuff
16	RD2884	Q-16	37.60 - 37.70	Lithic rich rhyolitic tuff
17	"	Q-17	69.46 - 69.56	Lithic rich rhyolitic tuff
18	"	Q-18	74.02 - 74.12	Lithic rich rhyolitic tuff
19	"	Q-19	80.60 - 80.70	Lithic rich rhyolitic tuff
20	"	Q-20	115.18 - 115.28	Rhyolitic tuff
21	RD2901	Q-21	99.90 - 100.00	Quartz rich rhyolitic tuff
22	"	Q-22	100.30 - 100.40	Quartz rich rhyolitic tuff
23	"	Q-23	129.42 - 129.52	Andesite dike
24	RD3039	Q-24	92.40 - 92.50	Porphyritic andesite
25	RD7152	A-25	191.33-191.45	Rhyolitic tuff
26	"	A-26	316.07 - 316.22	Andesite dike
27	RD7155	A-27	203.44-203.54	Rhyolitic tuff
28	"	A-28	217.10 - 217.20	Andesitic tuff
29	"	A-29	218.75-218.85	Silicified siltstone

APPENDIX A (Cont.)

No.	Core No.	Sample No.	Apparent depth (m)	Rock name
30	RD7155	A-30	219.10 – 219.20	Silicified siltstone
31	RD7157	A-31	132.00-132.10	Rhyolitic tuff
32	"	A-32	132.25-132.35	Rhyolitic tuff
33	"	A-33	266.50 - 266.60	Rhyolitic tuff
34	"	A-34	287.40 - 287.50	Porphyritic andesite
35	"	A-35	290.90-291.00	Porphyritic andesite
36	RD7161	A-36	162.40 - 162.50	Andesite
37	"	A-37	172.60-172.70	Rhyolitic tuff
38	"	A-38	312.10 - 312.20	Andesitic tuff
39	RD7162	A-39	149.30-149.40	Rhyolitic tuff
40	RD7165	Q-40	198.63-198.73	Fiamme rhyolitic tuff
41	"	Q-41	205.75 - 205.95	Rhyolitic tuff
42	RD3888	A-42	112.52-112.62	Rhyolitic tuff
43	"	A-43	206.65 - 206.75	Andesitic tuff

ศูนย์วิทยทรัพยากร
จุฬาลงกรณ์มหาวิทยาลัย

APPENDIX B

Analytical Techniques

Determination of Major and Some Trace Elements

Powdered rock samples were prepared for X-ray fluorescence (XRF) technique. The main procedure is presented as following:

1. 1.0 g of each sample was roasted at 110 °C about 12 hrs for calculating H_2O^- content that was determined by loss on weight.
2. These samples were burned at 900 °C about 3 hrs for calculating H_2O^+ which had still determined by loss on weight.
3. Mixing 0.8 g of these samples with 3.0 g of $\text{Li}_2\text{B}_4\text{O}_7$ and 1.0 g of LiBO_4 .
4. These mixtures were fused at about 1,040 °C for 2 minutes.
5. The homogeneous bead samples and standard are prepared and has always stored in the desiccator before X-ray fluorescence analysis.
6. X-ray spectrometer of Philips (model PW 2404) with Rh tube was used to analyse major and some trace elements by wave range dispersive method.
7. The data were determined by the detector and relatively computerized by the computer system. The final data are reported after these processing.

Determination of Trace and Rare Earth Elements

Inductively Coupled Plasma-Mass (ICP-MS) technique was used to determined trace and rare earth elements. The ordinal ICP-MS system requires solution samples because the samples are nebulized for introduction to argon plasma. Powdered rock samples, therefore, need to be decomposed using acid digestion. The procedure of this analysis in an orderly sequence is shown below.

1. Samples of 0.1000 g (± 0.0001 g) were weighed accurately by electric balance. Each sample powders were put into PTFE beakers and then add 0.4 ml of 60% HClO_4 and 0.4 ml of 45% HF into same beakers.

2. The mixtures of powders and acids were kept at 135 °C for 30 hrs.
3. The samples were evaporated to dryness at 135 °C for 12 hrs.
4. After cooling down, add 1 ml of 60% HNO₃ into beakers and covered it, these beakers were kept at 75 °C for a half hour.
5. At room temperature, 6 ml of di-ionized water were added into PTFE beakers and boiled at 90 °C about 3-4 hours.
6. After cooling down, sample solutions were diluted to 100 ml in volumetric flasks by adding di-ionized water. The dilution factor became 1000 times.
7. These samples were kept in polyethylene bottles and prepared for “standard addition method”.

Standard addition method

The digested samples were diluted immediately before ICP-MS analysis.

- 1) Two splits of 1 ml samples were separated from the 1000 time sample solutions and pipetted into 50 ml polyethylene test bottles.
- 2) 2.5 ml of 60% HNO₃ and 0.5 ml of 100 ppb Re (rhenium) internal standard solution were also added to each of the test bottles.
- 3) Additionally, 0.5 ml of 100 ppb mixed standard solutions was pipetted into one of the test bottles.
- 4) Both the tubes were diluted to 50 ml by adding the remaining micro liters of di-ionized water. The total dilution factor became 5000 times that of powdered rock samples.
- 5) Using the same procedure, a sample blank solution was prepared.
- 6) The sample blank solutions, X5000 sample solutions, X5000 standard addition solutions were used for acquisition and analyzed by ICP-MS.

APPENDIX C

Geochemical data of volcanic rocks from Q-propect

Rock	Porphyritic andesite				Andesitic tuff		Rhyolitic tuff							
Sample	Q-4	Q-24	A-34	A-35	A-36	A-28	A-27	Q-42	A-25	A-33	A-39	Q-40	Q-41	Q-22
SiO ₂	58.36	54.82	44.30	43.77	46.31	55.29	78.19	76.30	80.02	73.06	76.22	72.87	69.69	71.79
TiO ₂	0.39	0.53	0.54	0.63	0.56	0.43	0.23	0.26	0.16	0.13	0.26	0.23	0.25	0.23
Al ₂ O ₃	14.84	15.94	16.68	18.24	15.75	16.25	10.06	9.61	5.71	6.92	8.26	12.37	13.02	11.94
FeOt	7.10	8.10	9.94	10.12	10.84	9.59	2.98	2.83	3.36	2.15	5.19	3.18	3.40	2.99
MnO	0.33	0.43	0.18	0.17	0.48	0.28	0.02	0.11	0.09	0.26	0.10	0.03	0.13	0.07
MgO	5.20	5.23	8.76	9.26	6.97	4.77	1.28	0.76	2.59	3.33	1.09	1.14	3.24	1.45
CaO	0.94	2.28	3.45	3.61	3.19	0.24	0.40	0.75	1.53	4.29	1.07	0.34	0.54	1.95
Na ₂ O	0.67	0.19	1.44	1.61	0.15	0.16	0.12	0.22	0.13	0.12	0.14	0.19	0.18	2.26
K ₂ O	7.06	8.81	4.92	2.36	6.98	8.07	2.58	7.50	2.03	2.13	4.63	6.70	6.54	3.38
P ₂ O ₅	0.08	0.12	0.15	0.14	0.09	0.08	0.07	0.09	0.05	0.04	0.06	0.06	0.07	0.06
LOI	3.78	3.22	7.29	9.74	7.06	4.58	3.25	1.42	3.22	7.00	1.81	2.71	2.80	3.22
Total	98.75	99.66	97.66	99.64	98.37	99.75	99.18	99.84	98.91	99.42	98.82	99.82	99.85	99.35
Sc	23.2	27.4	30.8	34.7	38.1	30.5	11.9	16.9	10.0	5.3	18.7	9.8	11.2	8.9
V	185.0	207.7	253.8	288.8	323.8	223.2	111.3	78.8	72.4	25.1	157.3	62.2	69.1	37.1
Cr	27.6	33.0	20.7	20.8	28.9	26.1	10.5	29.4	14.3	7.9	24.5	4.9	4.7	9.2
Co	21.4	21.6	31.7	29.1	29.7	21.6	5.6	14.2	9.8	3.2	13.3	6.0	4.9	4.1
Ni	8.9	14.4	13.8	15.0	10.9	8.9	3.9	10.3	4.2	3.2	6.0	2.2	1.7	2.1
Cu	35.4	228.6	75.7	47.3	82.6	29.4	17.7	50.3	66.4	12.4	36.3	12.6	6.5	29.8
Zn	30.3	76.0	105.8	109.7	111.8	166.9	54.6	41.2	49.3	38.5	35.2	27.7	100.2	33.2
Ga	16.5	19.3	16.3	18.0	17.7	15.3	8.6	7.6	7.9	8.1	8.1	13.9	13.3	10.7
Rb	92.9	129.2	61.3	41.9	94.6	111.7	38.0	101.7	21.2	26.1	67.3	115.6	92.3	56.9
Sr	134.1	178.9	224.6	111.1	109.2	78.4	28.7	53.3	33.6	73.3	53.3	105.8	66.6	104.6
Y	8.8	13.4	8.2	8.6	6.4	6.3	4.2	7.5	3.8	9.3	3.9	6.0	6.1	9.9
Zr*	42.1	51.4	28.0	30.8	27.8	30.9	31.8	25.8	25.6	37.9	22.0	46.5	40.3	49.9
Nb	0.9	0.9	0.8	0.7	0.4	0.3	0.2	0.5	0.0	0.8	0.5	1.2	0.8	0.9
Cs	0.2	0.5	1.4	3.1	1.1	0.8	0.8	0.2	0.1	0.6	0.6	1.9	0.9	0.8
Ba	3797	3111	919	64	1911	6086	296	1085	717	466	1251	1400	1356	720
Hf	0.5	0.6	0.4	0.4	0.3	0.4	0.3	0.3	0.2	0.4	0.2	0.7	0.5	0.7
Ta	0.2	0.3	0.3	0.3	0.2	0.2	0.1	0.1	0.1	0.1	0.1	0.2	0.2	0.1
Pb	1.2	1.7	7.0	2.5	1.3	2.1	1.6	1.4	5.1	2.8	3.4	6.1	1.2	2.7
Th	0.4	0.5	0.2	0.3	0.2	0.3	0.3	0.2	0.2	0.5	0.2	0.6	0.6	0.7
U	0.1	0.2	0.2	0.1	0.1	0.3	0.3	0.1	0.6	0.4	0.1	0.3	0.2	0.3

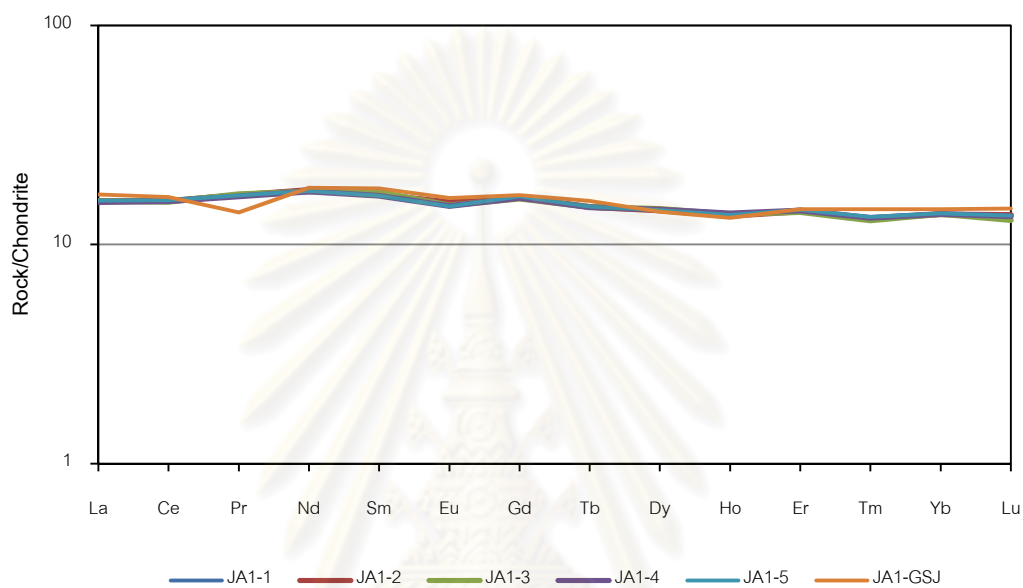
APPENDIX C (Cont.)

Rock	Porphyritic andesite				Andesitic tuff		Rhyolitic tuff							
Sample	Q-4	Q-24	A-34	A-35	A-36	A-28	A-27	Q-42	A-25	A-33	A-39	Q-40	Q-41	Q-22
La	3.1	4.3	2.2	2.5	1.4	2.6	1.3	1.8	1.3	4.0	1.2	1.8	1.7	4.9
Ce	7.0	9.6	5.5	6.4	3.4	5.2	2.8	4.4	3.2	9.3	2.8	4.4	3.8	10.4
Pr	1.0	1.3	0.8	1.0	0.5	0.7	0.4	0.6	0.4	1.3	0.4	0.6	0.5	1.4
Nd	4.6	6.3	4.6	5.3	2.6	3.2	2.0	3.0	2.0	5.6	1.9	2.9	2.5	6.3
Sm	1.2	1.8	1.4	1.6	0.8	1.0	0.7	0.8	0.5	1.5	0.6	0.7	0.7	1.6
Eu	0.9	0.8	0.8	0.5	0.7	0.9	0.3	0.5	0.3	0.6	0.4	0.5	0.5	0.6
Gd	1.4	2.2	1.6	1.8	1.1	1.1	0.8	1.1	0.6	1.7	0.7	0.9	0.9	1.7
Tb	0.2	0.3	0.3	0.3	0.2	0.2	0.1	0.2	0.1	0.3	0.1	0.1	0.1	0.2
Dy	1.5	2.3	1.5	1.6	1.2	1.3	0.8	1.2	0.7	1.5	0.7	1.1	0.9	1.7
Ho	0.3	0.5	0.3	0.3	0.3	0.2	0.2	0.3	0.1	0.3	0.2	0.2	0.2	0.4
Er	1.1	1.5	1.0	1.0	0.8	0.8	0.5	0.9	0.5	0.9	0.5	0.9	0.8	1.2
Tm	0.2	0.2	0.2	0.1	0.1	0.1	0.1	0.1	0.1	0.1	0.1	0.1	0.1	0.2
Yb	1.1	1.5	1.0	1.0	0.7	0.8	0.6	0.9	0.5	0.9	0.4	1.0	0.9	1.3
Lu	0.2	0.2	0.2	0.2	0.1	0.1	0.1	0.1	0.1	0.1	0.1	0.2	0.1	0.2

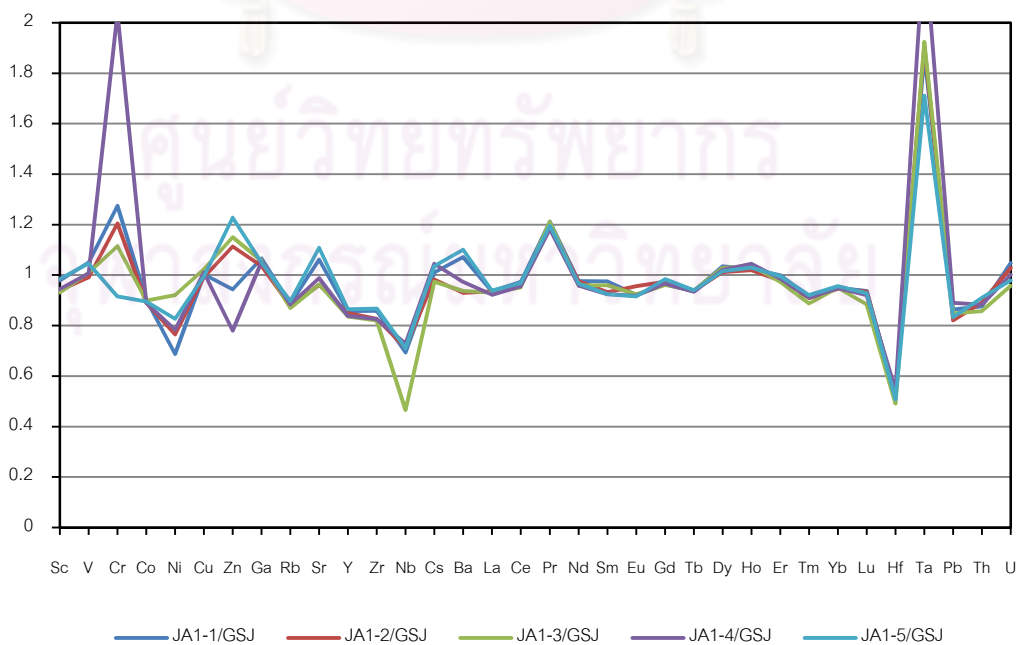
ศูนย์วิทยทรัพยากร
จุฬาลงกรณ์มหาวิทยาลัย

APPENDIX D

Chondrite normalized patterns for my rock standard analyzed in five time (e.g., JA1-1, JA1-2, JA1-3, JA1-4 and JA1-5) compare with rock standard data supplied from Geological Survey of Japan (GSJ) analyzed by ICP-MS.



Ratio between data of standard rocks (e.g., JA1-1, JA1-2, JA1-3, JA1-4 and JA1-5) that provided from this study and data of standard rock provided from GSJ



BIOGRAPHY

Miss Jensarin Vivatpinyo was born in Samutsongkram, central part of Thailand, on November 27, 1984. After finishing the high school from the Satthasamut School, Samutsongkram in 2003; she was chosen to study in Chulalongkorn University, where she acquired the B.Sc. degree in Geology from the Department of Geology, Faculty of Science, Chulalongkorn University in 2007. She has received the Science Excellent Education Scholarship from Commission on Higher Education, Ministry of Education Thailand since 2003. After graduation, she continued her studied the M.Sc. program in geology at Graduate School, Chulalongkorn University, in 2007. The research work has been focused on igneous rocks and tectonic setting. In 2007, she was an exchange research student at University of Tsukuba, Japan, which funded supported by Japan Student Service Organization (JASSO) for one year. She has received the Science Excellent Education Scholarship from Commission on Higher Education, Ministry of Education Thailand for her Master and Doctoral programs since 2008.



ศูนย์วิทยทรัพยากร
จุฬาลงกรณ์มหาวิทยาลัย